



TÉCNICO
LISBOA

**APPLICATIONS OF IONIC LIQUIDS IN
ELECTROCHEMICAL AND CATALYTIC STUDIES**

Robbe Vervecken

Thesis to obtain the Master of Science Degree in

Chemical Engineering

Supervisor: Prof. Luísa Margarida Dias Ribeiro de Sousa Martins

Prof. Tom Breugelmans

Jury

Chairperson: Prof. Benilde de Jesus Vieira Saramago

Supervisor: Prof. Luísa Margarida Dias Ribeiro de Sousa Martins

Members of the committee: Prof. Maria Matilde Soares Duarte Marques

Dr. Ana Paula da Costa Ribeiro

June 2015

Acknowledgements

First and foremost I would like to thank my supervisor, Professor Luísa Margarida Martins for introducing me to the topic of electrochemistry, the production of a poster for iFEQB and the support along the way. A special thank you for the corrections and alteration at the end, when the challenging deadline was approaching is in place. These fast adjustment made it possible to finish on time.

Professor Armando J.L. Pombeiro is to be thanked for accepting me in the research group and the interest shown in my work. The help and support of professor Tom Breugelmans on both the search for a topic as the support throughout the internship are greatly appreciated.

Professor Ângela Santos is to be thanked for the tutoring, when it comes to the usage of the density meter. Dmytro Nesterov and Rogério Chay deserve an acknowledgement for the brief explanation of some techniques used.

I would like to thank all my colleagues for their contribution in making this an interesting yet amusing learning process. Herein my gratefulness goes out to Ana Paula Ribeiro, Marta Mendes, Jiawei Wang, Elisa Spada, Anbu Sellamuthu, Anup Paul and Gonçalo Tiago.

Last but not least I would like to thank Romy Beaucage, Hilde Kemland and Dean Dudha for the mental support.

Abstract

Since the foundation of 'green chemistry' new ways are being searched to reduce waste generation and minimize the hazards in manufacturing processes. Ionic liquids fit perfectly in this ideology, making them a big field of interest. Their high thermal stability, absence of vapor pressure, relatively undemanding manufacture etc. makes them an excellent replacement for molecular solvents in many cases.

In this work, several ionic liquids were investigated regarding their electrochemical and catalytic properties as well as their ability to extract and oxidize different pigments.

Seven room-temperature ionic liquids formed from a combination of cations 1-alkyl-3-methylimidazolium (alkyl = butyl, hexyl or octyl, $[C_n\text{mim}]^+$, $n = 4, 6$ or 8), trihexyl(tetradecyl)phosphonium ($[P_{6,6,6,14}]^+$) or *N*-methyl-*N,N,N*-trioctyloctan-1-ammonium, and anions bis(trifluoromethylsulfonyl)imide ($[(CF_3SO_2)_2N]^-$), $[NTf_2]^-$), dicyanamide ($[DCA]^-$) or chloride, were investigated by cyclic voltammetry. The usable potential range of the said ionic liquids as well as the effect of their water content and the behavior of ferrocene in those media were investigated.

The applicability of trihexyl(tetradecyl)phosphonium dicyanamide, $[P_{6,6,6,14}][DCA]$, to the selective oxidation of cyclohexane to the cyclohexanol and cyclohexanone mixture catalysed by ferrocene, under mild conditions, was explored for the first time.

Moreover, liquid-liquid extraction of eight pigments by $[P_{6,6,6,14}][DCA]$ and the effectiveness of the extraction was examined in several conditions, such as exposure to the sun and in the presence of 30% hydrogen peroxide.

Keywords: Ionic liquids, electrochemistry, catalytic oxidation, cyclohexane, pigments, liquid-liquid extraction

Resumo

Desde o aparecimento da "química verde" estão a ser investigadas novas metodologias para reduzir a geração de resíduos e minimizar os riscos nos processos de fabrico. Os líquidos iónicos encaixam-se perfeitamente nesta ideologia, tendo-se tornado numa área de grande interesse. A sua elevada estabilidade térmica, ausência de pressão de vapor, fabrico relativamente pouco exigente, etc., torna-os frequentemente excelentes substitutos de solventes moleculares.

No presente trabalho foram investigadas as propriedades electroquímicas e catalíticas de vários líquidos iónicos bem como a sua capacidade para extrair e oxidar diferentes pigmentos.

O comportamento electroquímico de sete líquidos iónicos à temperatura ambiente, formados pela combinação dos cátions 1-alkil-3-metimidazólio (alkil = butil, hexil ou octil, $[C_n\text{mim}]^+$, $n = 4, 6$ ou 8), trihexil(tetradecil)fosfónio ($[P_{6,6,6,14}]^+$) ou *N*-metil-*N,N,N*-trioctiloctan-1-amónio, e aniões bis(trifluorometilsulfonil)imida ($[(CF_3SO_2)_2N]^-$, $[NTf_2]^-$), dicianamida ($[DCA]^-$) ou cloreto, foi investigado por voltametria cíclica. Foi determinada a gama de potencial útil dos referidos líquidos iónicos, bem como o efeito do teor de água nessa gama de potencial e o comportamento electroquímico do ferroceno nesses meios.

Foi também explorada, pela primeira vez, a aplicabilidade da dicianamida de trihexil(tetradecil)fosfónio, $[P_{6,6,6,14}][DCA]$, na oxidação seletiva de ciclohexano à mistura de ciclohexanol e ciclohexanona catalisada pelo ferroceno, sob condições moderadas.

Foi ainda examinada a eficiência da dicianamida de trihexil(tetradecil)fosfónio, $[P_{6,6,6,14}][DCA]$, para a extração líquido-líquido de oito pigmentos em diferentes condições operatórias, tais como a exposição ao sol e na presença de peróxido de hidrogénio.

Table of contents

CHAPTER 1: INTRODUCTION	1
1.1 Ionic liquids	1
1.1.1 Structure	1
1.1.2 Physicochemical properties	4
1.1.3 Electrochemical behavior	7
1.1.4 Catalytic application for the oxidation of cycloalkanes	11
1.1.5 Possible ecological effects	12
1.2 Pigments	13
1.2.1 Hazards	13
1.2.2 Treatment of wastewater	14
1.2.3 Characterization of dyes	15
1.2.4 Extraction of dyes from aqueous solution with ionic liquids	17
1.2.5 Effect of physical properties on the LLE of dyes	18
CHAPTER 2: EXPERIMENTAL PROCEDURE	19
2.1 Material	19
2.2 Equipment	19
2.3 Procedure	22
2.3.1 Density	22
2.3.2 Cyclic voltammetry	22
2.3.3 Peroxidative oxidation of cyclohexane	23
2.3.4 Pigments	24
2.3.5 Synthesis C_6mimBF_4	26
CHAPTER 3: RESULTS AND DISCUSSION	28
3.1 Density	28
3.2 Electrochemical behaviour of ionic liquids	29
3.3 Peroxidative oxidation of cyclohexane	38
3.4 Pigments	41
3.4.2 Amaranth C.I. 16185	45
3.4.3 Rhodamine 6G C.I. 45160	48
3.4.4 Chrysoidine C.I. 11270	51
3.4.5 Indigo C.I. 73015 A	53
3.4.6 Tartrazine C.I. 19140	56
3.4.7 Malachite green C.I. 42000	59
3.4.8 Methyl violet C.I. 42535	62
3.4.9 Methylene blue C.I. 52015	65
3.4.10 Rate of reaction	68
3.5 Discussion	69
3.5.1 Density	69
3.5.1 Electrochemical behaviour of ionic liquids	69
3.5.2 Peroxidative oxidation of cyclohexane	70
3.5.3 Pigments	70

CHAPTER 4: CONCLUSIONS AND FUTURE WORK..... 72

REFERENCE..... 74

ANNEX 83

Annex 1..... 83

Annex 2..... 84

Glossary

Alliquat 336	<i>N</i> -methyl- <i>N,N,N</i> -trioctyl-octan-1-ammonium chloride
AOP	advanced oxidation processes
BOD	biochemical oxygen demand
[C ₂ mim]	1-ethyl-3-methylimidazolium
[C ₃ mpyr]	1-methyl-1-propyl-pyrrolidinium
[C ₄ mim]	1-butyl-3-methylimidazolium
[C ₄ mpyr]	1-methyl-1-butyl-pyrrolidinium
[C ₆ mim]	1-hexyl-3-methylimidazolium
[C ₈ mim]	1-octyl-3-methylimidazolium
[C _{<i>n</i>} mim]	1-alkyl-3-methylimidazolium
C.I.	color index
CNT	carbon nanotubes
COD	chemical oxygen demand
CV	cyclic voltammetry
D	distribution ratio
[DCA]	dicyanamide
[DPyAM]BR ₂ .2HBr	<i>N,N'</i> -bis-2-aminoethyl-4,4'-bipyridinium dibromide dihydrobromide
Fc [°]	ferrocene
Fc ⁺	ferrocenium
GC	gas chromatograph
[Gmim][Cl]	1-glycyl-3-methyl imidazolium chloride
IL	ionic liquid
IL105	trihexyl(tetradecyl)phosphonium
LLE	liquid-liquid extraction
MV	methyl violet
[OMA]	trioctyl(methyl)ammonium
[PCA]	pyrazine carboxylic acid
[NTf ₂]	bis(trifluoromethylsulfonyl)imide
[N _{4.1.1.1}]	butyltrimethylammonium
[N _{8.8.8.1}]	<i>N</i> -methyl- <i>N,N,N</i> -trioctyl-octan-1-ammonium
[P _{6.6.6.14}]	trihexyl(tetradecyl)phosphonium
QRE	quasi-reference electrode
SS	suspended solids
TBHP	tert-butyl hydroperoxide
TOC	total organic carbon
TOF	turnover frequency

TON
TS-1
VOC
VTF

turnover number
titanium containing zeolite
volatile organic compounds
Vogel-Tamman-Fulcher

List of figures

Figure 1.1 A comparison of electrical conductivity versus temperature for ionic liquids with 1-butyl-3-methylimidazolium ([C ₄ mim] ⁺) as the cation and several anions, namely bis(trifluoromethyl)sulfonylimide ([NTf ₂] ⁻), hexafluorophosphate ([PF ₆] ⁻) and tetrafluoroborate ([BF ₄] ⁻).....	4
Figure 1.2 A comparison of density versus temperature for ionic liquids with [P6.6.6.14] ⁺ as the cation and several anions with a mentioning of the water content in percentages; [DCA] ⁻ (0.01 %), [Cl] ⁻ (0.03 %), [NTf ₂] ⁻ (0.04 %) and [Br] ⁻ (0.02 %).....	5
Figure 1.3 A comparison of density versus time for ionic liquids with [DCA] ⁻ as the anion and several cations with a mentioning of the water content in percentages; [C ₄ mim] ⁺ (0.00 %), [C ₄ mpyr] ⁺ (<0.15 %), [P _{6.6.6.14}] ⁺ (0.01 %) and [C ₂ mim] ⁺ (0.17 %).....	6
Figure 1.4 Viscosity versus time for ionic liquids with a mentioning of the water content in percentages; [P _{6.6.6.14}][DCA] (0.01 %), [N _{4.1.1.1}][NTf ₂] (0.01 %), [OMA][NTf ₂] (0.05 %), [C ₂ mim][NTf ₂] (0.05 %), [C ₂ mim][DCA] (0.19 %) and [C ₂ mim][EtSO ₄] (0.01 %-0.04 %).....	7
Figure 1.5 Absorption of water from atmospheric air at ambient temperature and moisture, with constant stirring as a function of exposure. (Δ) corresponds to [C ₈ mim][NO ₃], (*) to [C ₈ mim]Cl, (o) to [C ₄ mim][BF ₄] and (□) to [C ₄ mim][PF ₆]. [51].....	9
Figure 1.6 Peroxidative oxidation of cyclohexane to cyclohexanol and cyclohexanone.	11
Figure 1.7 The structure of Indigo and the presence of auxochromes (blue) and chromophores (red).	13
Figure 1.8 Structure and designation of the considered dyes.....	16
Figure 2.1 The DSA 5000 M Anthon Paar densitymeter.....	19
Figure 2.2 Nitrogen bottle, with a valve connected to a three electrode electrolyses cell, connected to the Potentiostat/galvanostat Model 273 A by EG&G Princeton Applied Research	20
Figure 2.3 A three electrode system with a Silver pseudo-reference electrode and a Platinum auxiliary- and working electrode.	20
Figure 2.4 Oil bath on a heating plate.....	21
Figure 2.5 Vacuum line.....	21
Figure 2.6 Karl Fischer 831 Coulometer.....	22
Figure 2.7 Biphasic mixture of IL105 and H ₂ O.....	24
Figure 2.8 The byphasic solution generated at the synthesis of [C ₆ mim][BF ₄]	26
Figure 3.1 Density plotted against the temperature; a comparison between literature results by Klomfar <i>et al.</i> [139], Diogo <i>et al.</i> [140], <i>Tariq et al.</i> [141], Neves <i>et al.</i> [142] and measurements using the DSA 5000M Anthon Paar density meter.	28
Figure 3.2 Cyclic voltammograms of [C ₄ mim][NTf ₂] (blue) and [C ₈ mim][NTf ₂] (red), at a platinum disk working electrode; v, 200 mVs ⁻¹ . Potentials are vs. an Ag quasi-reference electrode (QRE).	32
Figure 3.3 Cyclic voltammogram of [P6.6.6.14][DCA] (0.19 % water) at a platinum disk working electrode; v, 200 mVs ⁻¹ . Potentials are vs. an Ag quasi-reference electrode (QRE)......	33
Figure 3.4 Cyclic voltammograms of [C ₄ mim][NTf ₂] for different water contents; 1.00 % (red), 1.50 % (green), 3.12 % (purple), 4.95 % (light-blue) and 6.34 % (dark-blue) at a platinum disk working electrode; v, 200 mVs ⁻¹ . Potentials are vs. an Ag quasi-reference electrode.	33
Figure 3.5 Potential window available in [C ₄ mim][NTf ₂], [C ₆ mim][NTf ₂] and [C ₈ mim][NTf ₂] for different water contents at a platinum disk working electrode; v, 200 mVs ⁻¹ . Potentials are vs. an Ag quasi-reference electrode (QRE).	34
Figure 3.6 Potential window available in ILs consisting of [Cl] ⁻ as an anion and [P6.6.6.14], [N1.8.8.8] (in Aliquat 336) and [C ₆ mim] ⁺ as a cation for different water contents at a platinum disk working electrode; v, 200 mVs ⁻¹ . Potentials are vs. an Ag quasi-reference electrode	35
Figure 3.7 Potential window available in ILs consisting of [P6.6.6.14] ⁺ as a cation and [Cl] ⁻ and [DCA] ⁻ as an anion for different water contents at a platinum disk working electrode; v, 200 mVs ⁻¹ . Potentials are vs. an Ag quasi-reference electrode (QRE).....	35

Figure 3.8 Potential window available in ILs consisting of [C6mim] ⁺ as a cation and [Cl] ⁻ and [NTf2] ⁻ as an anion for different water contents at a platinum disk working electrode; v, 200 mVs ⁻¹ . Potentials are vs. an Ag quasi-reference electrode (QRE).....	36
Figure 3.9 Cyclic voltammograms of ferrocene in [C6mim][NTf2] at a platinum disk working electrode; v, 200 mVs ⁻¹ . Potentials are vs. an Ag quasi-reference electrode (QRE).	37
Figure 3.10 Proposed mechanism for cyclohexane oxidation via free-radical reaction pathway over ferrocene as catalyst, making use of TBHP as oxidant. [104]	40
Figure 3.11 The evolution of the liquid-liquid extraction of amaranth by IL105 in time at pH's of 2, 7 and 12	46
Figure 3.12 The evolution of the absorbance of Amaranth in time when influenced by 30 % H ₂ O ₂ at pH=7, Right corner: The Napierian logarithm of the ratio of absorbance and the initial absorbance of Amaranth vs. time	47
Figure 3.13 The evolution of the liquid-liquid extraction of Rhodamine 6G by IL105 in time and pH.	49
Figure 3.14 The evolution of the absorbance of Rhodamine 6G in time when influenced by 30 % H ₂ O ₂ at pH=7, Right corner: The Napierian logarithm of the ratio of absorbance and the initial absorbance of Rhodamine 6G vs. time.....	50
Figure 3.15 The evolution of the liquid-liquid extraction of chrysoidine by IL105 in time	51
Figure 3.16 The evolution of the absorbance of Chrysoidine in time when influenced by 30 % H ₂ O ₂ at pH=7, Right corner: The Napierian logarithm of the ratio of absorbance and the initial absorbance of Chrysoidine vs. time	53
Figure 3.17 The evolution of the liquid-liquid extraction of indigo by IL105 in time and pH.	54
Figure 3.18 The evolution of the absorbance of Indigo in time when influenced by 30 % H ₂ O ₂ at pH=7, Right corner: The Napierian logarithm of the ratio of absorbance and the initial absorbance of Indigo vs. time	56
Figure 3.19 The evolution of the liquid-liquid extraction of tartrazine by IL105 in time and pH.	57
Figure 3.20 The evolution of the absorbance of Tartrazine in time when influenced by 30 % H ₂ O ₂ at pH=7, Right corner: The Napierian logarithm of the ratio of absorbance and the initial absorbance of Tartrazine vs. time.....	59
Figure 3.21 The evolution of the liquid-liquid extraction of malachite green by IL105 in time	60
Figure 3.22 The evolution of the absorbance of Malachite green in time when influenced by 30 % H ₂ O ₂ at pH=7, Right corner: The Napierian logarithm of the ratio of absorbance and the initial absorbance of Malachite green vs. time.....	61
Figure 3.23 The evolution of the liquid-liquid extraction of methyl violet by IL105 in time and pH.	63
Figure 3.24 The evolution of the absorbance of Methyl violet in time when influenced by 30 % H ₂ O ₂ at pH=7, Right corner: The Napierian logarithm of the ratio of absorbance and the initial absorbance of Methyl violet vs. time.....	64
Figure 3.25 The evolution of the liquid-liquid extraction of methylene blue by IL105 in time	65
Figure 3.26 The evolution of the absorbance of Methylene blue in time when influenced by 30 % H ₂ O ₂ at pH=7, Right corner: The Napierian logarithm of the ratio of absorbance and the initial absorbance of Methylene blue vs. time.....	67
Figure 3.27 First order reaction rate vs. time for the oxidation of pigments with 30% hydrogen peroxide with respectively Amaranth	68

List of Tables

Table 1.1 Common cations and anions of ionic liquids.....	2
Table 1.2 Cyclic voltammetric data for ferrocene at a Pt electrode, in different ionic liquids.....	10
Table 3.1 Structures and common designations of ionic liquids used for electrochemical stability window studies.	29
Table 3.2 The oxidation potential, the reduction potential and the electrochemical window available in [P6.6.6.14][DCA], [P6,6,6,14][Cl], Alliquat 336, [C4mim][NTf2], [C6mim][NTf2], [C8mim][NTf2] and [C6mim][Cl] at a platinum disk working electrode; v, 200 mVs-1.....	31
Table 3.3 Half-wave potential values for the[Fe(C5H5)2]+/0 redox process in different ionic liquids.....	37
Table 3.4 Selected data for the catalytic oxidation of cyclohexane to cyclohexanol and cyclohexanone catalyzed by ferrocene in [P6.6.6.14][DCA].	38
Table 3.5 Wavelength of Maximum Absorbance for the pigments at the studied pH values	41
Table 3.6 Visual comparison of respectively Amaranth, Rhodamine 6G Chrysoidine, Indigo, Tartrazine, Malachite green, Methyl violet and Methylene blue at a pH of 2, 7 and 12 after 5 minutes and 2.5 hours.....	44
Table 3.7 Sun exposure of Amaranth with and without IL105 at pH=7	45
Table 3.8 Oxidation of Amaranth by 30% H2O2 with and without IL105 at pH=7.....	47
Table 3.9 Sun exposure of Rhodamine 6G with and without IL105	48
Table 3.10 Oxidation of Rhodamine 6G by 30% H2O2 with and without IL105.....	49
Table 3.11 Sun exposure of Chrysoidine with and without IL105	51
Table 3.12 Oxidation of Chrysoidine by 30% H2O2 with and without IL105	52
Table 3.13 Sun exposure of Indigo with and without IL105	53
Table 3.14 Oxidation of indigo by 30% H2O2 with and without IL105	55
Table 3.15 Sun exposure of Tartrazine with and without IL105	56
Table 3.16 Oxidation of Tartrazine by 30% H2O2 with and without IL105.....	58
Table 3.17 Sun exposure of Malachite green with and without IL105.....	59
Table 3.18 Oxidation of Malachite green by 30% H2O2 with and without IL105	61
Table 3.19 Sun exposure of Methyl violet with and without IL105	62
Table 3.20 Oxidation of Methyl violet by 30% H2O2 with and without IL105.....	64
Table 3.21 Sun exposure of methylene blue with and without IL105.....	65
Table 3.22 Oxidation of Methylene blue by 30% H2O2 with and without IL105.....	66

Chapter 1:INTRODUCTION

1.1 Ionic liquids

To meet the demands of a growing population, the chemical processing industry has used yield oriented procedures, without including in the process design a way of minimizing the waste production. One of the major sources of waste is solvent losses that end up in the atmosphere or in ground water [1-6]. Solvent use has been reported to account for about 60% of the overall energy in pharmaceutical production, and it has been responsible for 50% of post-treatment greenhouse gas emissions [7,8]. The use of these materials has a detrimental effect on human health, safety and the environment. This combined with their volatility and flammability led to increasing pressure for minimizing their use. Therefore, solvent selection should be considered systematically to improve synthesis conditions within the framework of green chemistry principles, [9] and there are a number of solvent selection guides available in the literature [1-8]. Chemically, the solvent would have a high capacity to dissolve the solute, in a little amount of volume. It would need to be inexpensive to produce, recyclable and robust, to face various processing environments [9-11]. In fact, a large quantity of organic solvents is used as liquid media for chemical reaction, extraction and formulation. Various methods and tools have been developed for the identification and selection of appropriate solvents for synthesis.[1-8]

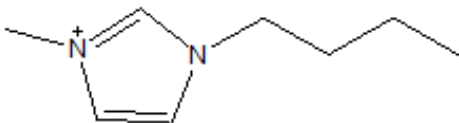
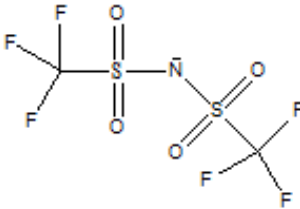
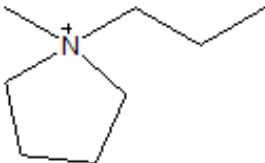
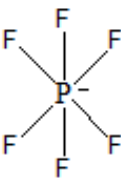
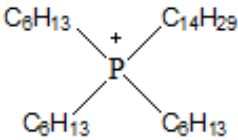
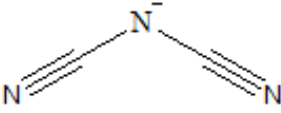
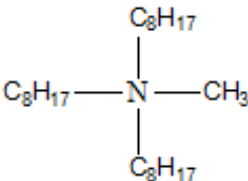
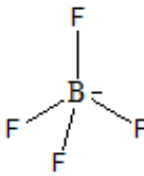
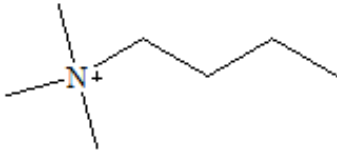
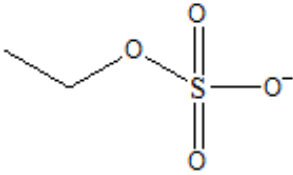
Recently, however, a new class of solvent has emerged that fit perfect in the idea of green chemistry, namely ionic liquids. These solvents are often fluid at room temperature, and consist entirely of ionic species. They're non-flammable, have high thermal stability and are relatively undemanding and inexpensive to manufacture. Another big advantage is the absence of a measurable vapor pressure, with no emission of toxic, volatile organic compounds (VOC). Their special properties make them a field of interest for chemists. Although ILs display many advantages, they have a high viscosity compared with molecular solvents. This will have to be taken into account during experiments and further use. [9,12,13]

1.1.1 Structure

Ionic liquids exist in two main categories, simple salts that consist of a single anion and cation, and binary ionic liquids, where more than one cation or anion is present. [9,12,13]

The cation is an organic species, such as 1-butyl-3-methylimidazolium ([C₄mim]⁺), 1-methyl-1-propyl-pyrrolidinium ([C₃mpyr]⁺), trihexyl(tetradecyl)phosphonium ([P_{6,6,6,14}]⁺), 1-methyl-1-butyl-pyrrolidinium ([C₄mpyr]⁺) and trioctyl(methyl)ammonium ([OMA]⁺) as shown in. The anion can be organic or inorganic. Examples are bis(trifluoromethylsulfonyl)imide ([NTf₂]⁻), hexafluorophosphate ([PF₆]⁻), dicyanamide ([DCA]⁻), tetrafluoroborate ([BF₄]⁻) and ethyl sulfate ([C₂SO₄]⁻), Table 1.1. [1]

Table 1.1 Common cations and anions of ionic liquids.

Cation	Structure	Anion	Structure
[C ₄ mim] ⁺		[NTf ₂] ⁻	
[C ₃ mpyr] ⁺		[PF ₆] ⁻	
[P _{6,6,6,14}] ⁺		[DCA] ⁻	
[OMA] ⁺		[BF ₄] ⁻	
[N _{4,1,1,1}] ⁺		[C ₂ SO ₄] ⁻	

ILs are called “designer solvents” because it is possible to tune the properties of the IL by changing one of the components. In this way, the solvents can be designed with a particular end use in mind. Melting point, density, hydrophobicity and also miscibility of water in ionic liquids can be changed dependent on the structure. Preferentially ILs which are liquid at ambient temperature are used; they are referred to as room temperature ionic liquids RTILs. [9,12,13] The reason why these salts are liquid below 100 °C, is the low symmetry and bulkiness of the cation. This lack of symmetry promotes a reduction of the lattice energy of the crystalline form of the salt, lowering their melting points. The anion on the other hand, mostly controls water miscibility, but the cation can also influence the hydrophobicity or hydrogen bonding ability.

Since ILs are ionic, they will bear a charge. This charge is not localized on an atom, but it is distributed all over the molecular structure. There is one exception on this matter and that is IL's with a halogen anion. The charge is worn by the halogen function itself. [14]

Supposedly ILs demonstrate a structural heterogeneity, where the aspects of chemical physics of ILs can be ascribed to; this includes solvation, dynamics and transport. [15]

Phosphonium-based ILs are more recent than the imidazolium- and pyridinium-based ILs, and cheaper to produce. They are more thermally stable (in some cases up to nearly 400°C!) [16] in comparison with ammonium and imidazolium salts, and this remarkable property makes them suitable for reactions that are carried out at temperatures greater than 100°C. Phosphonium- based ILs are used as the catalyst and solvent for hydroformylation [17], palladium-catalyzed Heck reactions [17] and palladium-mediated Suzuki cross-coupling reactions. [17] In addition, they are also powerful phase-transfer catalysts for the Halex reaction [18]. Recently, phosphonium-based ILs have been used for CO₂ capture. [19]. Along with their application in the synthesis of the styrenic derivatives of phosphonium-based ILs, they are used as monomers in the synthesis of phosphonium-containing random copolymers. [20]

1.1.2 Physicochemical properties

The nature and size of both anion and cation are determinative for the physicochemical properties of IL's.

1.1.2.1 Electrical Conductivity

ILs are molten salts at room temperature, which means they are conductive liquids. As published previously [21] the electrical conductivity of pure ILs is relatively low, which is an impediment to progress in numerous fields of the proposed electrochemical applications. In Figure 1.1 the trend of imidazolium based ionic liquids is present.

The electrical conductivity dramatically increases with temperature, changing 1 order in magnitude in the liquid state in a temperature increase of about 200 K. The theoretical analysis of the temperature dependence of the electrical conductivity in liquid state indicates that most of the imidazolium and phosphonium based ILs follows Vogel-Tamman-Fulcher (VTF) equation. The increase in the conductivity with temperature also depends on the size of the anion and cation. The ratio in size of both species and their interaction with one another seems to be the base for this behavior. Unfortunately, there is still an unfilled gap in this area, giving space for new studies in this field.

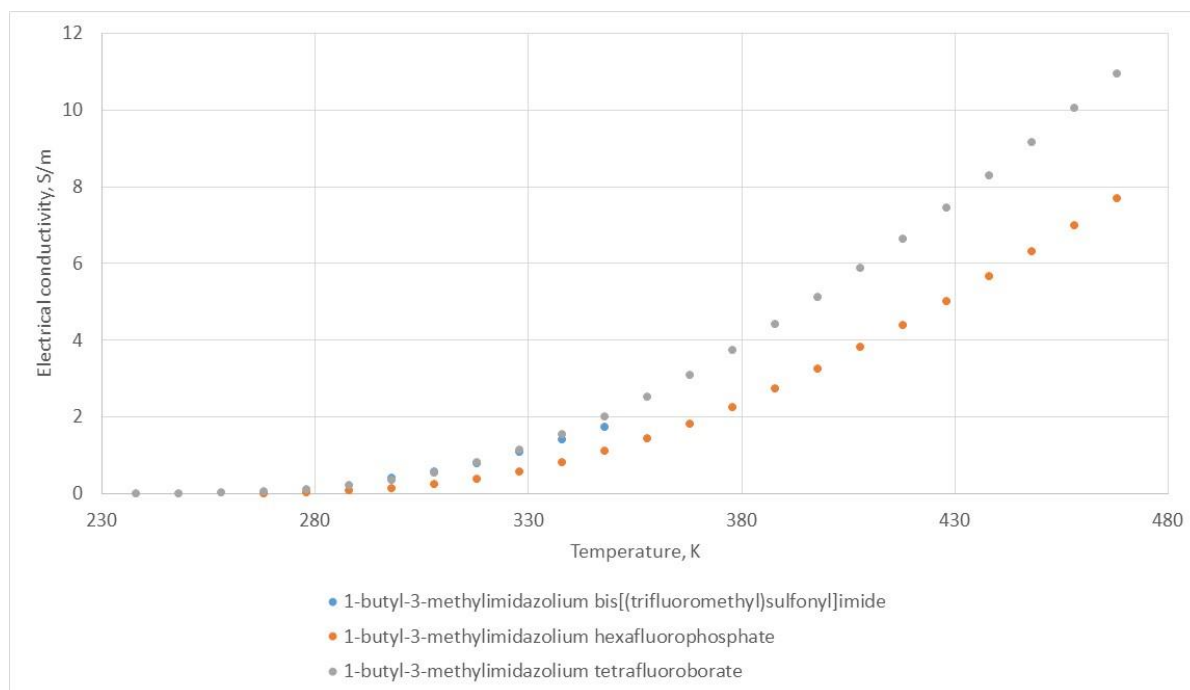


Figure 1.1 A comparison of electrical conductivity versus temperature for ionic liquids with 1-butyl-3-methylimidazolium ($[C_4mim]^+$) as the cation and several anions, namely bis[(trifluoromethyl)sulfonyl]imide ($[NTf_2]^-$), hexafluorophosphate ($[PF_6]^-$) and tetrafluoroborate ($[BF_4]^-$) [21]

1.1.2.2 Density

Density is an important factor in defining the nature of an ionic liquid. Usually ILs show a linearly decrease in density with an increase in temperature. This is common in both phosphonium and imidazolium based ionic liquids, over a wide range of temperature. As is determined in previous studies on different ILs over a wide range of temperatures. [22-23] This is a logical consequence, since an increase in temperature makes the molecules more mobile, resulting in a thermal expansion. The differences in density, for very similar structures of ionic liquids are attributed to the presence of additional hydrogen bonds. [22-23]

The evolution of the density vs. temperature is given for trihexyl(tetradecyl)phosphonium $[P_{6.6.6.14}]^+$ based and dicyanamide based ILs, in respectively Figure 1.2 [24-27] and Figure 1.3 [24,25,28,29]. A linear decrease with an increase in temperature is observed in both cases.

Figure 1.2 demonstrates the impact of several anions on the density of trihexyl(tetradecyl)phosphonium ($[P_{6.6.6.14}]^+$) ILs. The density decreases in the following order; $[NTf_2]^-$, $[DCA]^-$, $[Cl]^-$ and $[Br]^-$.

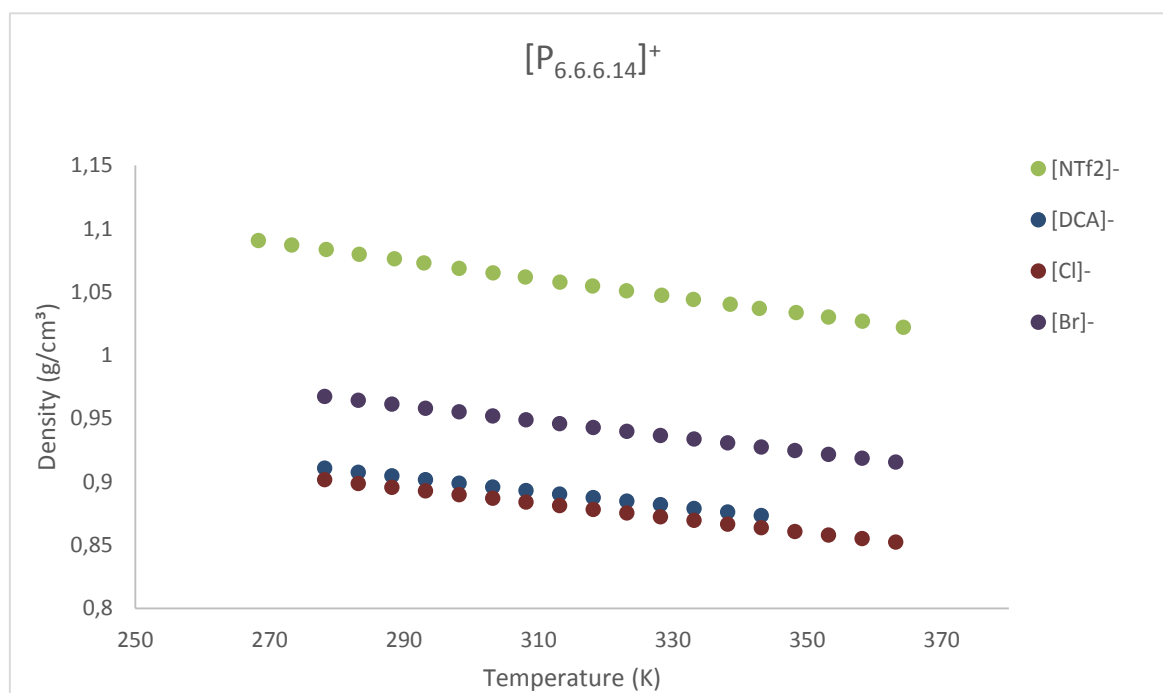


Figure 1.2 A comparison of density versus temperature for ionic liquids with $[P_{6.6.6.14}]^+$ as the cation and several anions with a mentioning of the water content in percentages; $[DCA]^-$ [24] (0.01 %), $[Cl]^-$ (0.03 %) [27], $[NTf_2]^-$ (0.04 %) [24] and $[Br]^-$ (0.02 %) [27]

In Figure 1.3 the impact of the cation on the density of dicyanamide ($[DCA]^-$) based ILs is exhibited. The density decreases in the following order; $[C_2mim]^+$, $[C_4mim]^+$, $[C_4mpyr]^+$, and $[P_{6.6.6.14}]^+$.

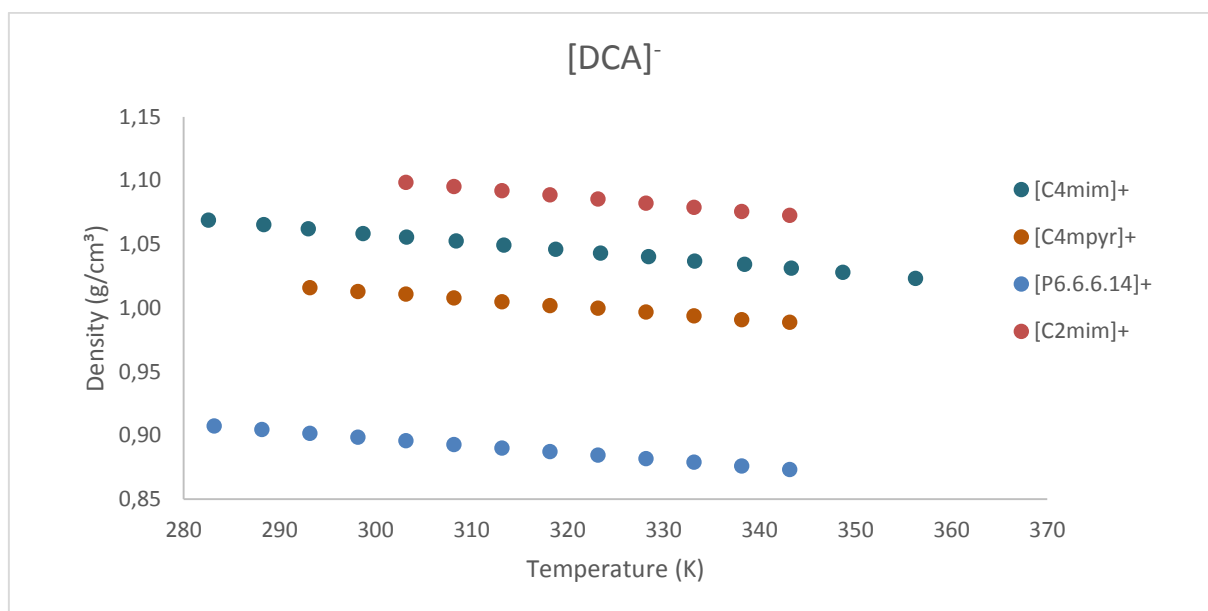


Figure 1.3 A comparison of density versus time for ionic liquids with $[DCA]^-$ as the anion and several cations with a mentioning of the water content in percentages; $[C_4mim]^+$ (0.00 %) [29], $[C_4mpyr]^+$ (<0.15 %) [29], $[P_{6.6.6.14}]^+$ (0.01 %) [24] and $[C_2mim]^+$ (0.17 %) [28]

Both the anions as the cations have a considerable impact on the density of the ionic liquids, which can be attributed to the presence of additional hydrogen bonds. [21,22]

1.1.2.3 Viscosity

Viscosity is an important macroscopic property of ionic liquids. This property is of considerable importance for fluid flow calculations and equipment design. It determines the possibility of using fluids as reaction media or solvents for transportation purposes. Mapping these values precisely, can reduce the energy requirements for processing these fluids drastically. [21] It results from several microscopic interactions such as van der Waals, columbic, hydrogen bonding and is considerably dependent upon the size and shape of the ions. IL's have a relatively high viscosity, which can be explained by IL structure. [21,23]

The effect of both the anion as the cation on the viscosity is analyzed in Figure 1.4, using several ionic liquids; $[P_{6.6.6.14}][DCA]$, $[N_{4.1.1.1}][NTf_2]$, $[OMA][NTf_2]$, $[C_2mim][NTf_2]$, $[C_2mim][DCA]$ and $[C_2mim][C_2SO_4]$. [30-33] The structure of the anion has a tremendous impact on the viscosity of an ionic liquid. When $[NTf_2]^-$ is taken as the anion, and only the cation is differed a considerable difference is seen. The viscosity of the IL decreases in the order of $[OMA]^+$, $[N_{4.1.1.1}]^+$ and $[C_2mim]^+$ with values, respectively 676.3, 140.7 and 38.6 mPa.s at 293.15 K. Considering $[DCA]^-$ as the anion, the same phenomenon is seen with $[P_{6.6.6.14}]^+$ and $[C_2mim]^+$, giving viscosities of 532.45 and 140.7 mPa.s at 293.15 K.

In order to determine the effect of the anion on the viscosity of ionic liquids, $[C_2mim]^+$ is considered as the cation, and the anion is altered. If $[NTf_2]^-$, $[DCA]^-$ and $[C_2SO_4]^-$ are compared a smaller change is observed, with viscosities, being respectively 22.8, 38.6 and 125.6 mPa.s at 293.15K.

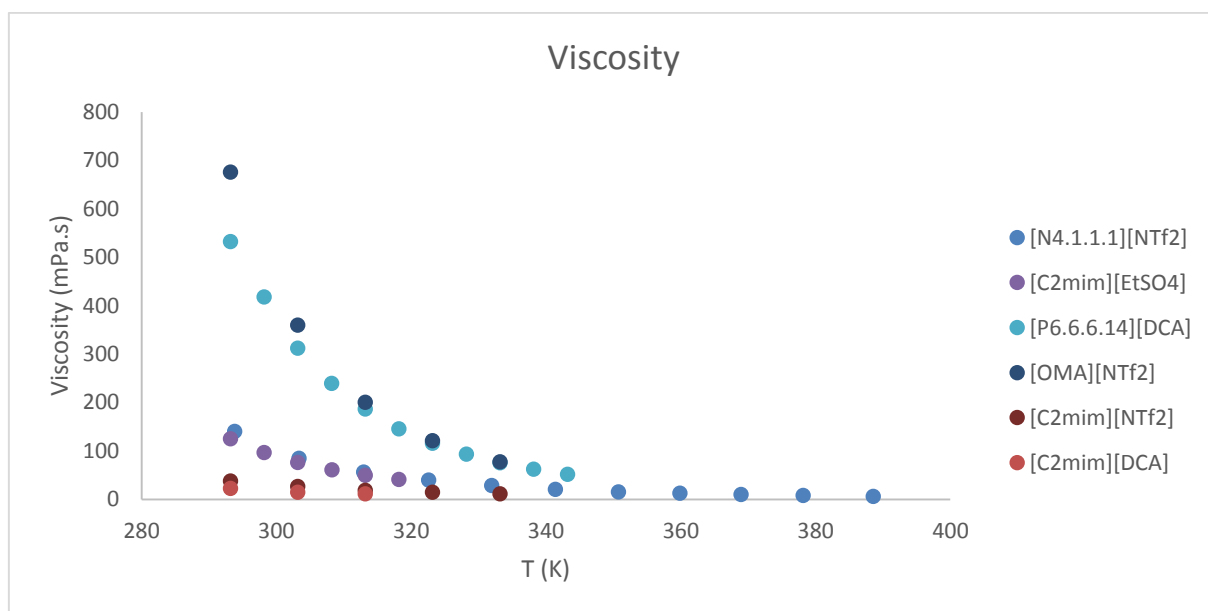


Figure 1.4 Viscosity versus time for ionic liquids with a mentioning of the water content in percentages; [P_{6.6.6.14}][DCA] (0.01 %) [31], [N_{4.1.1.1}][NTf₂] (0.01 %) [30], [OMA][NTf₂] (0.05 %) [33], [C₂mim][NTf₂] (0.05 %) [33], [C₂mim][DCA] (0.19 %) [33] and [C₂mim][EtSO₄] (0.01 %-0.04 %) [33]

Water and other impurities change the viscosity of ILs drastically. It can be assumed that polar water molecules modify the properties of the ions, which decreases the viscosity tremendously. [34] Another reason is the lowering of the electrostatic attractions among the ions and thus the cohesive energy of the system. [23] In IL's with alkylimidazolium as a cation, the addition of chloride will, even in low concentrations, decrease the viscosity of ionic liquids substantially. This is due to the interaction via hydrogen bonds between the protons and the chloride of the imidazolium ring [34]

1.1.3 Electrochemical behavior

In electrochemical experiments, the conductivity of a solvent is of vital importance. ILs have inherent ionic conductivity thereby eliminating the need for using an additional supporting electrolyte in electrochemical devices. The conductivity of a pure ionic liquid depends on the mobility of the ions, which is influenced by the ion size, ion association and viscosity (a decrease in viscosity enhances the mass transport of analyte to the electrode surface).

In general, an ideal electrolyte should have high ionic conductivity ($>10^{-4}$ S/cm), fast ion mobility during redox reactions ($>10^{-14}$ m².(V.s)⁻¹), large electrochemical potential windows (>1 V) and low volatility. ILs exhibit many of these properties and characteristics. [35]

In fact, it has been shown that ionic liquids are highly effective electrolytes making possible their applications in batteries [36-39], capacitors [40-42], solar [43-48] and fuel cells [49]. The non-volatility and non-combustibility should contribute to the long-term durability and safety of these devices.

Most properties of ILs relevant to electrochemistry are centrally based on the above-mentioned conductivity and viscosity, and on electrochemical potential windows.

The electrochemical potential window of stability of an ionic liquid is generally characterized by the reduction potential of its cation and the oxidation potential of its anion.

$$\text{Potential window} = E_{\text{anodic limiting potential}} - E_{\text{cathodic limiting potential}} \quad (1)$$

These limits are tunable based on the cation and anion selection, and the electrochemical window can be widened or narrowed to include or exclude certain potential window ranges, an indication of the versatility of ionic liquids in different applications. [9]

It is currently known that some electrodepositions, that are not possible to be studied in aqueous or inorganic electrolyte solutions, are possible in IL's, due to their wide electrochemical window. [9,12,13]

The major impurities contained in ILs are water and oxygen, even in highly pure samples, since these molecules are dissolved easily into the ILs from the atmosphere. Their electrochemical activity makes the removal of these molecules essential before any voltammetric measurement. [9]

The water miscibility and hydrophobicity is influenced by the identity of the anion of the IL. This needs to be taken into account when drying an IL and it also determines the difficulty that comes with reaching very low moisture contents. Certain precautions will have to be taken, to get the water content to a very low level. An example is the use of an imidazolium-based IL with a hydrophilic anion. When it is mixed with water a micelle is formed. If the cation contains a long side chain, it is more likely for the cation to get included in a micelle, because of the hydrophobicity of the alkyl side chain. By exchanging the anion for a hydrophobic one, the structure becomes non-micellar, thus excluding water out of the IL. [9,50]

The effect of water on the electrochemical window of trihexyl(tetradecyl)phosphonium dicyanamide [P_{6.6.6.14}][DCA] has not yet been reported while has been thoroughly studied [51] at room temperature, for 1-alkyl-3-methylimidazolium based ILs [C_nmim][X], with the n being 4 or 6, making it a 1-butyl- or 1-hexyl-3methylimidazolium salt with the [X] being [NTf₂]⁻ or [PF₆]⁻.

More hydrophobic IL's such as [C_nmim][PF₆] will form a biphasic system with water, when saturation is reached. The concentration in which this happens depends again on the alkyl chain length of the cation and on the anion type. [51]

It should be kept in mind that ionic liquids are in fact hygroscopic. An experiment wherein IL's got exposed to the atmosphere at ambient temperature showed the water uptake in function of time, Figure 1.5. The hydrophobicity of the anions decreases in the following order; [PF₆]⁻ > [BF₄]⁻ > [NO₃]⁻ > Cl⁻. It turned out that even the considered 'hydrophobic' ones such as [C_nmim][PF₆] extract 1w/w% over a 3 h period of exposition. In the water-soluble IL's, the water uptake will be even more severe. [51] It should also be noted that the presence of water in [PF₆]⁻ can lead to decomposition reactions, producing e.g., HF. [52]

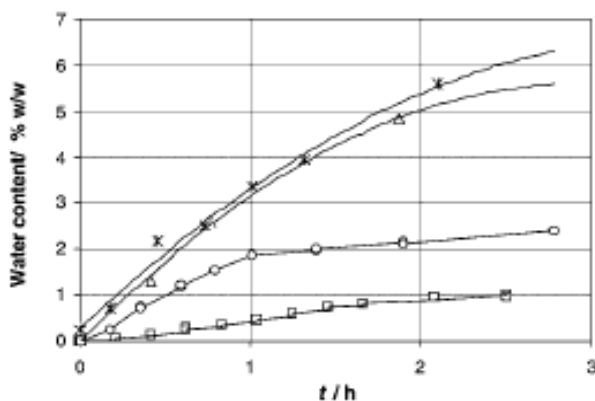


Figure 1.5 Absorption of water from atmospheric air at ambient temperature and moisture, with constant stirring as a function of exposure. (Δ) corresponds to $[\text{C}_8\text{mim}][\text{NO}_3]$, (*) to $[\text{C}_8\text{mim}]\text{Cl}$, (O) to $[\text{C}_4\text{mim}][\text{BF}_4]$ and (\square) to $[\text{C}_4\text{mim}][\text{PF}_6]$. [51]

The presence of water may have a rather dramatic effect on the reactivity of ILs. The influence of water on hydrogen bonds between ionic liquids and cellulose was investigated. [9] It was found that water gets included in the hydrogen bond-accepting sites of the anions. In other words, if a hydrogen-bond between an anion and cellulose breaks, the chance that it will be replaced by a water molecule increases. Therefore, to make results comparable it is very important to take note of the water content in the ILs used. [53]

The ferrocene/ferrocenium $[\text{Fe}(\text{C}_5\text{H}_5)_2 / \text{Fe}(\text{C}_5\text{H}_5)_2^+, \text{Fc}^\circ/\text{Fc}^+]$ couple is widely used as an internal standard in voltammetric studies in conventional non-aqueous media containing electrolytes. In order to make a comparison in RTIL's, the IUPAC recommends the use of the same couple as an internal potential reference. [54] However, in many ionic liquids the solubility of ferrocene is rather low. Heterogeneities in the ionic liquids can cause the measured current to differ from the normal situation due to, for example, the accumulation of ferrocene on the electrode surface. [54] Moreover, since the oxidation potential of Fc° is very close to the anodic potential limit of some IL's, the reversibility of the $\text{Fc}^\circ/\text{Fc}^+$ process can be negatively influenced. Some irreversible voltammetric behavior was observed, probably due to the reaction of Fc^+ with the IL itself or the oxidation products of the IL. [54]

To date, the electrochemical behaviour of ferrocene in trihexyl(tetradecyl)phosphonium dicyanamide, $[\text{P}_{6.6.6.14}][\text{DCA}]$ (IL105), has not been reported. The behavior of ferrocene in other ionic liquids, on the other hand, is already tested [55-56]. As an example, the cyclic voltammogram of the common ionic liquid $[\text{C}_4\text{mim}][\text{BF}_4]$ is shown in Figure 1.4.

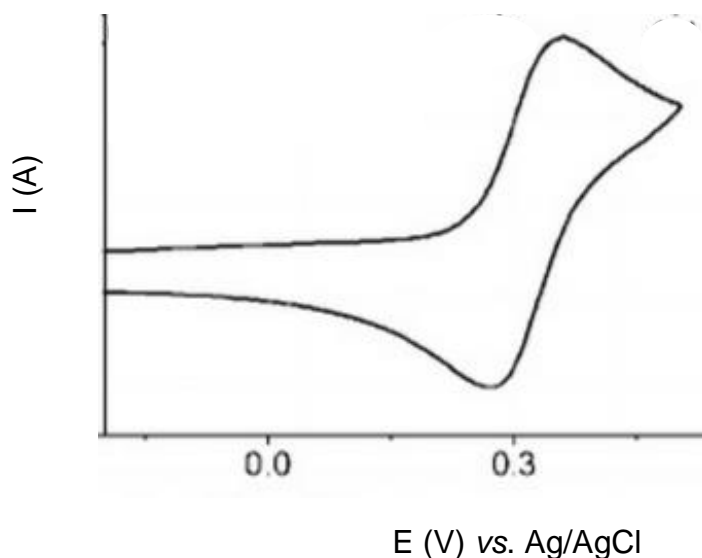


Figure 1.4 Cyclic voltammogram of Fc in [C₄mim][BF₄] at a scan rate of 0.100V/s at 298K: Potentials are vs. an Ag/AgCl reference electrode. [55]

The electrochemical potential values for the Fe(C₅H₅)₂ / Fe(C₅H₅)₂⁺, Fc⁰/Fc⁺ redox couple in different ionic liquid media is presented in Table 1.2.

Table 1.2 Cyclic voltammetric data for ferrocene at a Pt electrode, in different ionic liquids.

Ionic liquid	E _{1/2} ^{ox} /mV ^a	Reference
[C ₂ mim][BF ₄]	410	[56]
[C ₄ mim][BF ₄]	313	[55]
[C ₄ mim][PF ₆]	-0.03	[57]
[C ₆ mim][PF ₆]	248	[55]
[C ₄ mim][N(SO ₂ CF ₃) ₂]	-0.02	[57]
[C ₄ mim][CF ₃ SO ₃]	-0.01	[57]

^a Reference electrode: Ag(I)/Ag; counter electrode: Pt

When comparing results it is important to keep in mind that, the formal potential is dependent on multiple factors, such as the ionic liquid and the working and reference electrodes used.

1.1.4 Catalytic application for the oxidation of cycloalkanes

Selective partial oxidation of alkanes is an important topic with potential in terms of economic and ecological perspectives of sustainable chemistry [21,58-67]. However, efficient catalytic oxidation of alkanes [68-69] still remains a challenging topic. The development of more active catalysts, under mild conditions, at room temperature and using low toxicity media and oxidizing agents is needed. Hydrogen peroxide is one of the best options in this regard since H₂O is the sole by-product. Thus, peroxidative alkane oxidations were the selected reactions for the present study.

Cyclohexane was the chosen substrate in view of the significance of the oxidized products (cyclohexanol and cyclohexanone, Figure 1.6) for the manufacturing of adipic acid, Nylon-6,6' and polyamide-6 [58-66]. Moreover, the industrial process of cyclohexane oxidation needs to be improved, since it requires considerably harsh conditions (150 °C) and leads to low yields (*ca.* 4%) to assure a good selectivity (*ca.* 85%)[67]. The difficulty finds its origin in the activation of the C(sp³)-H bond in such unreactive saturated hydrocarbons, thus inhibiting their wider use for the direct use of added-value chemical products. [70]

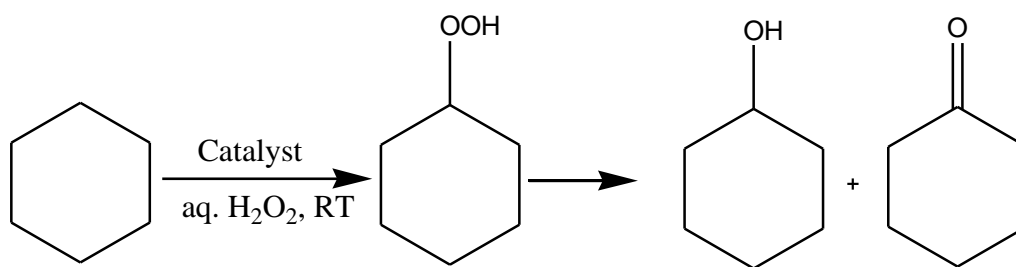


Figure 1.6 Peroxidative oxidation of cyclohexane to cyclohexanol and cyclohexanone.

It has been a pursuit for many years now, to replace the classical process by other systems that can catalyze the selective oxidation of alkanes at ambient temperature. [71-73]

The oxidation reaction of cyclohexane to cyclohexanol and cyclohexanone was investigated in [C₂mim][BF₄] with titanium silicate 1 (TS-1), which is a titanium-containing molecular sieve, as a catalyst and tert-butyl-hydroperoxide (t-BuOOH, TBHP) as oxidant. The maximum conversion and yield was found at a mole ratio of 2:1 of TBHP to cyclohexane at 90 °C, with a conversion of 13.20 %, a yield of 12.88 % and 97.6 % selectivity for the oxidation of cyclohexane to cyclohexanol and cyclohexanone. It was found that the yield and conversion increased with an increasing temperature, while the selectivity lowered slightly at high temperatures (between 70 °C and 100 °C). No significant increase in oxidation was found between 90 °C and 100 °C, conceivably due to the decomposition of TBHP. [72]

1-Glycyl-3-methyl imidazolium chloride was used as a complex with Cu(II) ([Gmim]Cl–Cu(II) complex), for the C-H oxidation reaction on several alkyl-arenes. A 70% yield was obtained for the oxidation of cyclohexane to cyclohexanone, when the reaction oxidation reaction was performed for 12 hours with 0.1 mmol of catalyst at ambient temperature. The recyclability of the catalyst was tested for the oxidation of ethylbenzene to acetobenzene. A decrease from 85% to 82% yield was observed after 6 reaction cycles for the oxidation of ethylbenzene to acetobenzene specifically, when extracted and dried under vacuum. [71]

Only a few studies on ferrocene for the cyclohexane oxidation have been done. [75,76]

The combination of ferrocene as a catalyst with potassium persulfate ($K_2S_2O_8$) as a co-catalyst dissolved in acetonitrile when exposed to 20 atm of CO was tested. A yield of 18.3, 0.8 and 0.3 for respectively cyclohexylperoxide, cyclohexanol and cyclohexanone at 60 °C with a reaction time of 4 hours, was obtained. [75]

Ferrocene, in combination with pyrazine carboxylic acid ([PCA]) in a 1:2 molar ratio catalyzes the homogeneous oxidation of cyclohexane and benzene with H_2O_2 as an oxidant in an acetonitrile medium. [76]

The combination of ferrocene derivatives and ionic liquids are being used for several catalytic purposes, such as the oxygen reduction reaction [77], Suzuki Miyaura reaction [78] and the isomerization of allylic alcohol [79].

To the best of our knowledge, no research on the catalytic oxidation of cyclohexane in ionic liquid media is found. In this work, the oxidation of cyclohexane in trihexyl(tetradecyl)phosphonium dicyanamide ($[P_{6.6.6.14}][DCA]$, IL105) with ferrocene as a catalyst will be studied.

1.1.5 Possible ecological effects

The major concern in the use of ILs related to the fact that some anions are not so *green*, and the risk of hydrolysis stability of the anion with the formation of an acid can occur. Lower homologues of alkylsulfate anions for example, namely methanesulfate and ethanesulfate may be sensitive to hydrolysis, with the formation of the corresponding alcohol and hydrogensulfate as a consequence. [3,21]. The antimicrobial activity increased as the alkyl chain length of pyridinium, imidazolium, and quaternary ammonium salts increased, thus increasing the toxicity for bacteria. [80-85]

Cho et al. showed that the toxicity of ILs increased with an increase in alkyl chain length, when investigation series of imidazolium based ionic liquids. [86] In the investigation for the toxicity of 1-butyl-3-methylimidazolium, 1-butyl-3methylpyridinium, tetrabutylammonium, 1-butyl-1-methylpyrrolidinium and tetrabutylphosphonium bromides a toxicity between two and four orders of magnitude greater than those of organic solvents was found. [87] Varying the anion has a minimal effect on the toxicity of imidazolium and pyridinium salts, which suggests that toxicity is largely driven by the cation. [81,88-90]

1.2 Pigments

1.2.1 Hazards

Dyes are an important class of synthetic organic compounds used in many industries, especially textiles. Consequently, they have become common industrial environmental pollutants during their synthesis and later, during fiber dyeing. Textile industries are facing a challenge in the field of quality and productivity due to the globalization of the world market. The textile industry utilizes about 90% of all dyes, while the remaining 10% are used in food, printing, and plastics. The greatest amounts come from Asia, with China as the largest producer. This big release of major quantities of dyes has a significant detrimental effect on the environment, due to the high chemical oxygen demand (COD) and toxicity of these effluent streams. [88]

Pigments are organic compounds that consist of two main groups, chromophores and auxochromes. A chromophore is the structural part that gives the dye its characterizing color. It consists of conjugated double bonds and a delocalized electron group. Double-bonded carbons, cyano, carbonyl groups and double bonded nitrogen groups are the more typical examples of this kind. The color intensity exists because of the presence of an auxochrome. This is usually an electron-donor such as an amine, a carboxylic acid, a sulfate or a hydroxyl group. In Figure 1.7 violet is taken as an example to show the presence of auxochromes (blue) and chromophores (red). [89]

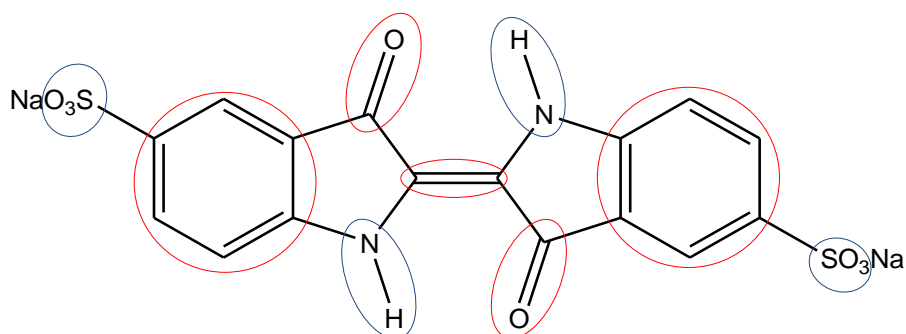


Figure 1.7 The structure of Indigo and the presence of auxochromes (blue) and chromophores (red).

Textile wastewaters, containing dyes tend to be high in chemical oxygen demand (COD), biochemical oxygen demand (BOD), total organic carbon (TOC), suspended solids (SS), turbidity, and toxicity. The characterization of wastewater and setting of regulatory levels is often done by the first four factors. Turbidity of water will cause clouding of water, blocking the sunlight and thus inhibiting photosynthetic processes of plants in water. [88] Some pigments are toxic, not only for the aquatic environments, but also for a variety of organisms, ranging from bacteria to humans. Even when dyes are marketed as being safe, they can be potentially dangerous due to their degradation products. Since natural colors are not as uniform, stable etc. synthetic dyes are still being used in big quantities, even though there are a lot of detrimental effects connected to their use. [90]

1.2.2 Treatment of wastewater

The development of techniques for the removal of dyes from aqueous waste streams has become a big field of interest for researchers, for the reasons mentioned in 1.2.1. Most of the removal methods consist of a physical, biological and chemical step. The used approaches are found to be expensive and ineffective.

The parameters of wastewater can vary significantly, depending on the different dyeing and washing processes used. Consequently the characteristics and treatment of wastewater will be altered, when a change of these factors is present. With pH being a very important factor, this needs to be taken into account

Pang et al. found that a combination of a chemical treatment, coupled with a physical treatment, followed by a biological treatment, ending with another physical treatment to be ideal. Physical treatments usually separate the different components in the wastewater, with adsorption, ion exchange and filtration being the main ones. Micro-organisms such as bacteria, plants or fungi are the basis of the biological treatment. They will breakdown the organic compounds in wastewater and convert them to water and carbon dioxide under aerobic and/or anaerobic conditions. In most cases pretreatment is required, because most dyes aren't biodegradable. [88] Another problem occurring in this method is the toxicity of the dyes, causing the extinction of most plant types. [91]

The chemical processes embody a wide range of techniques. The generic way includes coagulation or flocculation process as well as an oxidation. Alternatives have been investigated as a replacement for oxidations reactions. This is due to the increased toxicity of the products in comparison to the reactants used. Therefore it needs to be used in combination with other techniques. Coagulation or flocculation is mostly used in co-operation with physical methods as it is the purpose to remove suspended particles. [88]

One of the techniques being researched is the liquid-liquid extraction (LLE). Here in dye-containing wastewaters are brought in contact with an immiscible organic solvent, into which the dyes dissolves. In 2007, Mahmoud et al. [92] examined a variety of more environmentally-friendly solvents for liquid-liquid extraction. Specifically, various plant oils were used in an attempt to extract the dye Remazol Brilliant Blue (an anionic dye). These authors concluded that the increase in the extraction efficiency observed is directly proportional to the viscosity of the liquids.

This new method, employing ionic liquids has already been tested in several dyes. [92-98] Being a topic of interest, LLE will be further investigated in this work.

1.2.3 Characterization of dyes

Amaranth (C.I. 16185) is a dark red to purple azo dye, that's used as a food and cosmetics dye. It is anionic and can be applied to natural and synthetic fibers, leather, paper and phenol-formaldehyde resins. Since 1976 Amaranth has been banned in the USA, due to carcinogen effects, but it is still used in some countries. Another dye that belongs to the anionic ones is indigo (C.I. 73015 A). It is commonly used as a pH indicator, because of the dependence of the color on the pH. This pigment is found to be blue below the first pKa (11.4) and yellow above its second pKa (13.0). When used as a redox indicator indigo turns yellow upon reduction.

Tartrazine (C.I. 19140) is a synthetic anionic lemon yellow azo dye, mostly used as a food coloring, but can also be used in cosmetics and medication.

Malachite green (C.I. 42000) is an organic compound which owes its color to the presence of a cation. It find its use as a pH indicator with a yellow color below pH is 0.2 and green between a pH of 1.8 and 11.5. A loss in color will appear above a pH of 13.2.

Methyl violet (C.I. 42535) is a cationic dye that is mostly used as a purple dye for textiles and also, to give deep violet colors to paint. It is mutagen and mitotic poison, therefore concerns exist when it comes to the impact it has on the environment.

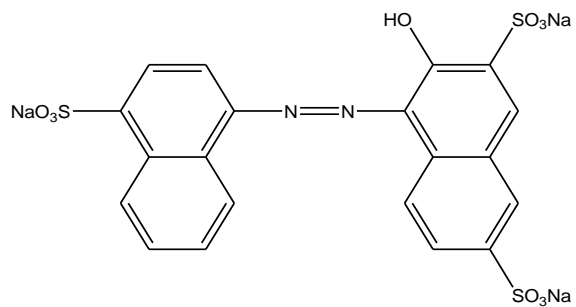
Methylene blue (C.I. 52015) is a heterocyclic aromatic chemical compound, used as a cationic dye in a big range of fields, such as biology and chemistry. It is frequently found in biological stains and occasionally as a redox indicator. In the health care industry methylene blue can battle certain cancers, when combined with other drugs.

Rhodamine 6G (C.I. 45160) is highly fluorescent, thus is often used as a cationic tracer dye within water to determine the rate and direction of flow and transport in water. The fluorescent behavior make them usable in an extensive range of biotechnology applications such as fluorescence microscopy, flow cytometry and fluorescence correlation spectroscopy.

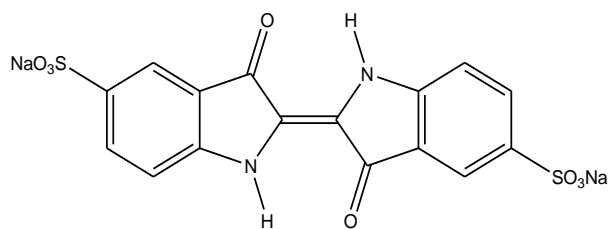
Chrysoidine (C.I. 11270) also named basic orange 2, is a cationic azo dye that changes color depending on the pH. It will shift from orange at pH 4.0 or bellow to yellow at pH 7.0 or above. Photographic material, inks, toners and detergents are some of the application.

The structures of the dyes used in this work can be found in Figure 1.8.

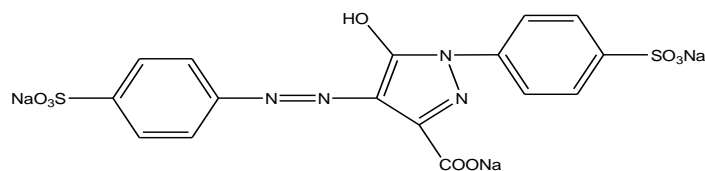
Anionic dyes



Amaranth

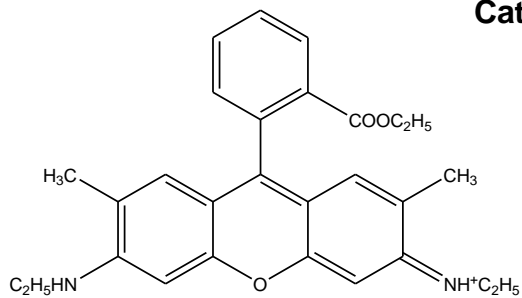


Indigo

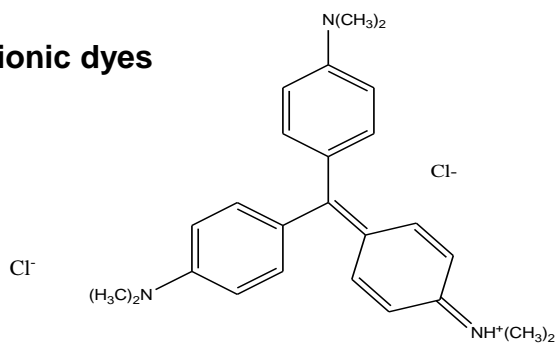


Tartrazine

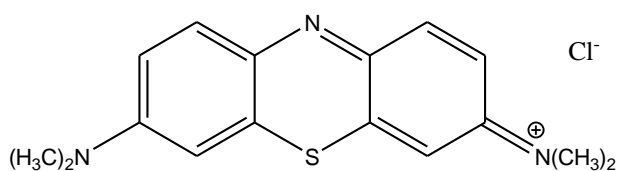
Cationic dyes



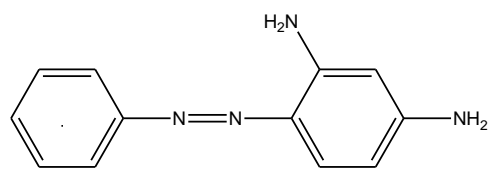
Rhodamine 6G



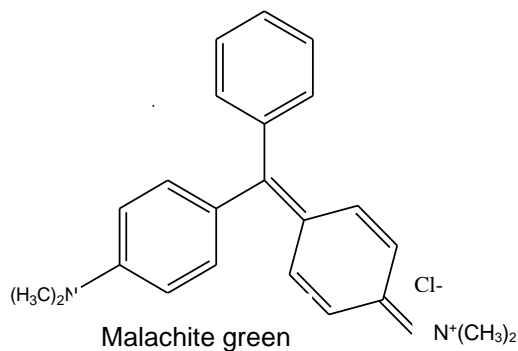
Methyl violet



Methylene blue



Chrysoidine



Malachite green

Figure 1.8 Structure and designation of the considered dyes.

1.2.4 Extraction of dyes from aqueous solution with ionic liquids

Several works have been conducted on the use of ionic liquids in the extraction of dyes. [93-100] For these extraction to be feasible, the dye components need to dissolve into the ionic liquid, withdrawing it from the wastewater. It is very important for the ionic liquid not to dissolve into the aqueous layer in significant amounts, as it would have an even more detrimental effect on the environment.

To quantify the extracted amount, the distribution ratio (D), defined in 2 is used. Therein the dye concentration in the IL is divided by the dye concentration in the aqueous layer.

$$D = \frac{[dye]_{org}}{[dye]_{aq}} \quad (2)$$

If the D value is greater than 10 it is considered efficient and inefficient when it is less than 1. [99]

Pei et al. found that when cationic dyes and $[PF_6]^-$ based ionic liquids were brought in contact, associates were formed between the cationic dye and the anion of the IL in a ratio that came close to 1:1. Aqueous solutions of malachite green and methylene blue formed precipitates, when a $[PF_6]^-$ based ionic liquid was added. After agitation, these precipitates dissolved into the ionic liquids. A strong enough interaction between ionic liquids and cationic dyes is thus implied. [100]

The dye-IL associates were investigated, and association constants were calculated utilizing theoretical models established by the determination of the deviation from linear behavior. It was found that the association reached values as high as 10^6 (L.mol⁻¹)², which is a sign of a strong interconnection. An exothermic nature was ascribed to the formation process of the association, which was implied by the thermodynamic results found by Y. Pei et al. [100]

No actual research was done on the use of IL105 in the liquid-liquid extraction of pigment out of aqueous media. More commonly used IL's are those, containing a 1-alkyl-3-methylimidazolium cation. Ali et al. attempted to extract several dyes into $[C_4mim][PF_6]$, $[C_4mim][BF_4]$, $[C_4mim][NTf_2]$, and $[C_6mim][Br]$. The cationic dyes studied included Methylene blue among others. The extraction efficiencies were as high as 99%. No mechanism was determined, but the researchers concluded that hydrophobicity of an ionic liquid has no effect on extraction efficiency. [95]

1.2.5 Effect of physical properties on the LLE of dyes

A work by Mahmoud et al. suggested that the more viscous a solvent, the higher D_{dye} got. In other words, the more viscous an IL, the more efficient it would extract dyes. [92,101] As already mentioned in 1.1.2.3 the viscosity is influenced by several factors. An increase in cation size is normally accompanied by an increase in viscosity. In addition the choice of anion can significantly influence viscosity as well.

Zhang et al. on the other hand, found that the least viscous IL's extracted the cationic dyes the most efficiently, with D_{dye} being slightly higher for $[\text{C}_6\text{mim}][\text{NTf}_2]$ than for $[\text{C}_6\text{mim}][\text{PF}_6]$. For anionic dyes the opposite is true, the most viscous IL's extracted the anionic dyes the most efficiently. The relationship between viscosity and extraction efficiency appears to be strong but is possibly coincidental. A more precise way to approach the difference in extraction ability is the hydrophobicity of its constituent cation and anion. [101]

In this work, several anionic and cationic dyes will be tested, using an ionic liquid. Most of these pigments have not been reported previously in a LLE experiment.

Chapter 2: EXPERIMENTAL PROCEDURE

2.1 Material

Different ionic liquids are used, including [P_{6.6.6.14}][Cl], IL105 ([P_{6.6.6.14}][DCA] which were kindly donated by cytec industries inc. Alliquat336 was acquired at Alfa Aesar and [C₆mim]Cl, [C₆mim][NTf₂], [C₄mim][NTf₂] and [C₆mim][NTf₂] were homemade using the synthesis procedure as described in 2.53. The ionic liquids are being dried for 12 h, using the vacuum line, with Edwards RV3 pump. When this is done they need to be put under nitrogen, using the vacuum line. Ferrocene, 99 % dichloromethane, sodiumtetrafluoroborate, acetone and acetonitrile were purchased at Sigma- Aldrich. The ultra-pure water, used for calibration, was purified at Faculdade de Ciências da Universidade de Lisboa. The distilled water, used for extraction, was purified in *Centro de Quimica Estrutural I.S.T.* University of Lisbon.

The dyes; Amaranth, Rhodamine 6G, Chrysoidine, Indigo, Tartrazine, Malachite green, methyl violet and Methylene blue were purchased at Sigma-Aldrich as well as hydrogen peroxide solution (30% H₂O₂). 100mL of a 40mg/L basic solution of all the pigments was made, dissolving 4mg of pigment in 100mL of distilled water. When altering the pH a 1.0M solution of sodium hydroxide was used to obtain a pH of 12 and 0.1M of hydrochloric acid was used to obtain a pH of 2. Both the granulated NaOH as the 37% HCL solution, used to make the diluted solutions, were acquired at Sigma-Aldrich. pH-papers were used to test measure the pH of the pigment solutions and the pH adjusted by adding either acid or base.

2.2 Equipment

The DSA 5000M Anthon Paar densitometer was used for the density measurements. The accuracy of the apparatus needs to be checked every day, before being used. Here for ultra-pure degassed water is used.



Figure 2.1 The DSA 5000 M Anthon Paar densitometer

Potentiostat/Galvanostat Model 273 A by EG&G Princeton Applied Research (Figure 2.2) with PowerSuite software is used for all the experiments. A three electrode system (Figure 2.3) is utilized with a Platinum quasi-reference electrode and a Platinum auxiliary- and working electrode. The cyclic voltammetry (CV) cell was made in Centro de Quimica Estrutural I.S.T. University of Lisbon. The water content of every ionic liquid was measured with the Karl Fischer 831 Coulometer.

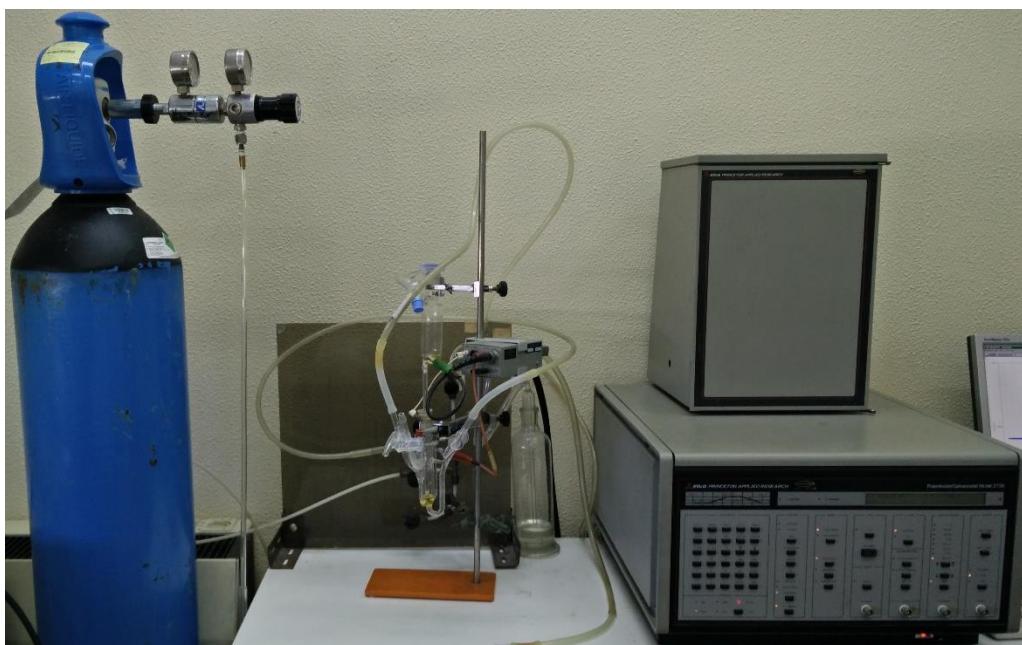


Figure 2.2 Nitrogen bottle, with a valve connected to a three electrode electrolyses cell, connected to the Potentiostat/galvanostat Model 273 A by EG&G Princeton Applied Research



Figure 2.3 A three electrode system with a Silver pseudo-reference electrode and a Platinum auxiliary- and working electrode.

A heating plate with a set temperature and an agitation function was used, Figure 2.4, to keep the reaction at a constant temperature, making convection possible and thus preventing diffusion to become a restrictive factor. The gas chromatograph MFC 8000 from Fisons instruments, was utilized for the analysis of the product containing water phase. It is a GC with flame ionization detector and capillary column (DB-WAX, column length: 30 m; internal diameter: 0.32 mm) and the Jasco-Borwin v.1.50 software. 0.045 μL of the sample got injected and subsequently analyzed. A temperature program with an initial temperature of 100 $^{\circ}\text{C}$ (1 min) and a ramp of 10 $^{\circ}\text{C}/\text{min}$ with a final temperature of 180 $^{\circ}\text{C}$ (1 min)



Figure 2.4 Oil bath on a heating plate

The pH was tested using a pH-paper. Different UV-VIS spectrometers were used. PerkinElmer's Lambda 35 UV-VIS spectrophotometer, Jasco 7800 and the UV-3101 PC, UV-VIS-NIR Scanning spectrophotometer Shimadzu were used. Hellman quartz cells, with 1cm path length, were utilized for all the measurements.

The vacuum line, Figure 2.5, has multiple use, as it can be used to add nitrogen or create a vacuum. In this work all of the drying steps were performed in this line.



Figure 2.5 Vacuum and inert atmosphere line



Figure 2.6 Karl Fischer 831 Coulometer

The 831 Karl Fischer Coulometer, as shown in Figure 2.6 is used to measure the water content of the ionic liquids, when doing electrochemistry experiments

2.3 Procedure

2.3.1 Density

To get reproducible results IL105 is to be degassed and preheated to the starting temperature of the measurements, being 50°C. The measuring cell is to be filled carefully to prevent the appearance of bubbles in the cell.

Several measurements have to be done in order to have a reproducible result. If the density starts to stagnate, the temperature can be adjusted. The final value is the average of all the results, excluding the extremely aberrant ones. In order to get a clear view of the evolution of density versus temperature, values are taken between 50 °C and 15 °C; starting at 50 °C decreasing the temperature in steps of 5°C.

The results are to be compared with data found in the literature.

2.3.2 Cyclic voltammetry

The cyclic voltammetric experiments were performed using an EG&G PAR 273A potentiostat/galvanostat connected to a personal computer through a GPIB interface.

The studies were conducted at a platinum disc working electrode ($d = 0.5 \text{ mm}$) and at room temperature, in a three-electrode-type cell with a Luggin capillary connected to a silver wire pseudo-reference electrode (to control the working electrode potential) and a Pt wire as the counter electrode for the CV cell. The solutions were saturated by bubbling N_2 before each run. The redox potentials of the complexes were measured by CV in the presence of ferrocene as the internal standard.

Room - temperature ionic liquids are usually prepared from a variety of organic and inorganic salts. Because both ionic liquids and halide salts are hygroscopic in most cases, they must be dried under vacuum at elevated temperatures and handled in a dry atmosphere.

Cyclic voltammetry is a very sensitive technique, so when the setup is done, one needs to make sure that every piece of equipment that is involved in the measurement is properly cleaned. All experiments were carried out at ambient temperature in a N₂-atmosphere, saturating the ionic liquid with N₂ before every measurement.

5 mL of dried ionic liquid is added to the electrochemical cell withdrawing the IL from a schlenk, using a syringe. Both the cyclic voltammetry cell as the schlenk are to be under a N₂-atmosphere. Cyclic voltammetry is applied as a technique to measure the electrochemical window, which ranges from the potential of the cathodic peak to the potential of the anodic peak of the ionic liquid.

The water content of the ionic liquid will be studied as an influential factor. Therefore a CV-scan will be taken of the dried IL and subsequently after the addition of 100 mg of water. This process will be repeated until the electrochemical window remains the same. A sample needs to be taken after every measurement, followed by the determination of the water content of every sample by Karl Fischer titration.

The same procedure as mentioned above will be used, for the addition of ferrocene to the IL. The characteristic peak potential will be calculated out of the potential of both the cathodic as the anodic peak of the reversible ferrocene oxidation. Ferrocene will be added to several ILs and the peak potential is to be compared.

2.3.3 Peroxidative oxidation of cyclohexane

IL105 is being used in combination with ferrocene as catalyst for the oxidation of cyclohexane to cyclohexanol and cyclohexanone. A solution of ferrocene in ionic liquid will be made with a differing concentration, given in Table 3.4.

Making use of a magnetic stirrer, the solution will be stirred until homogeneity is reached. The reagent, cyclohexane namely, is added to the homogeneous solution at a concentration of 129.68 g/L. Afterwards an addition of 486.2 g/L of the oxidant TBHP takes place after homogenizing the solution.

The flask was placed in an oil bath and kept at 50°C. A reaction time of 2 hours was used, combined with stirring. After two hours the flask is taken out of the oil bath and cooled down by rinsing it with tap water.

The ionic liquid has a very small vapor pressure, therefore cannot be evaporated. 3mL of water was added to extract the products. Since water and IL105 are immiscible, a biphasic solution will get formed, Figure 2.5. It will be stirred thoroughly, by a magnetic stirrer, to make all the products migrate to the aqueous phase. The water phase is separated from the ionic liquid, making use of a glass pipet. IL105 is then dried under vacuum overnight and stored in a N₂ atmosphere.



Figure 2.7 Biphasic mixture of IL105 and H₂O

2.3.4 Pigments

2.3.4.1 Calibration curves

Dye solution of different concentration were made, by adding different quantities of the stock-solution and supplementing it to create a 3 mL solution. The quantity of this addition depends on the absorbance of the dyes at that certain concentration. Absorbance values were kept below one. Three solutions for each pH (2, 7 and 12) were measured. The volumes were converted to concentration via molar mass and density. Subsequently first order graphs of absorbance versus concentration were made.

2.3.4.2 Sun exposure

A dilution was made adding 100 μ L of the 40mg/L pigment solution and 2.9mL of water to a flask, followed by a homogenization. Pictures were taken before and after 5, 10 and 30min of sun-exposure.

2.3.4.3 pH

The difference in color of all the dyes at different pH's (2, 7 and 12) was investigated. Making a solution of different volumes of pigment solution 40 mg/L, depending on the absorbance of the pigment and diluting it to 3 mL with distilled water. The addition of 1 M NaOH brought the pH to 12 and 0.1 M HCl to 2. The pH was analysed using a pH-paper. Photos were taken and the color/intensity between the different samples were compared.

2.3.4.4 Advanced oxidation procedure using H₂O₂ (30%)

A dilution was made adding 100 µL of the 40 mg/L pigment solution and 2.9 mL of water to a flask, followed by a homogenization. 150 µL of the solution is to be replaced by 150 µL of 30 % H₂O₂. The evolution of the color was visualized making pictures before and after the addition of the hydrogen peroxide. When 5, 10, 30 min and 72 h passed, pictures were taken again.

To quantify the change in intensity of the pigments with the addition of hydrogen peroxide, the PerkinElmer's Lambda 35 UV-VIS spectrophotometer was used. Solutions were prepared according to method in the previous paragraph, subsequently measuring the absorbance over the 700-200 nm range before and then immediately after the addition of 30 % H₂O₂. Spectra's need to be taken after 5, 10 and 30 minutes as well. The exact absorbance of the pigment can be read at the isosbestic point.

The values are to be used to calculate the rate of reaction (k) for the oxidation of the dye by 30 % hydrogen peroxide. A linear behavior is seen after the induction period, the first 10 minutes, where a change in reaction rate is seen. Therefor the first order integrated rate law (3) can be used with A being the absorbance at the endpoint of the graph and A₀ the initial point of the linear behavior.

$$\ln(A) = -kt + \ln(A_0) \quad (3)$$

2.3.4.5 Liquid-liquid extraction

The influence of the sun on the intensity of the pigment with exposure to the sun is to be tested. Therefor a dilution was made, adding 100 µL of the 40 mg/L pigment solution and 2.9 mL of water to a flask, followed by a homogenization. 300 µL of this solution was subtracted, followed by an addition of 300 µL of IL105. It was mixed rigorously, in order to start the extraction of the dye out of the aqueous solution. Pictures were made before and after 5, 10 and 30 min of sun-exposure.

A qualitative investigation was done on the impact of ionic liquid on the color intensity of the pigments. 100 µL of the 40 mg/L pigment solution was diluted with distilled water until a volume of 3 mL was reached. The subtraction of 150 µL of the aqueous solution and subsequently the addition of 150 µL of hydrogen peroxide followed thereafter. The evolution was visualized making pictures before and after the addition of the hydrogen peroxide. When 5, 10, 30 min and 72 h passed, pictures were taken again.

For the dyes that were found to have a great affinity for the considered ionic liquid, quantification of the extraction capacity was done, making use of the UV-3101 PC, UV-VIS-NIR Scanning spectrophotometer by Shimadzu. Dilutions of different dye concentrations were made. The absorbance in function of the wavelength was measured. In order to compare the difference in intensity (absorbance) of the dye in the aqueous solution before and after the addition of ionic liquid; 300 µL of the 3 mL diluted solution was subtracted, followed by the addition of the same amount of the ionic liquid. Spectra of 10 %IL solution were taken 30 minutes after the ionic liquid is added, in order to give the ionic liquid time to extract the dye. The exact absorbance of the pigment can be read at the isosbestic point.

The distribution coefficient (D) can be calculated by converting the absorbance at the isosbestic points to concentration determined via the calibration curve. Subsequently equation 4 will be used by filling in the initial- and final concentration with the liquid-liquid extraction. Since a solution of 3 mL was used, containing 2.7 mL of dye solution and 0.300 mL of IL105 (9:1 phase-to-volume ratio), a factor nine needs to be added to the equation.

$$D = \frac{[\text{Initial concentration in aqueous layer}] - [\text{Final concentration in aqueous layer}]}{[\text{Final concentration of aqueous layer}]} \times 9 \quad (4)$$

Different volumes of dye-solution were added to the cell, depending on the intensity of the dye at that certain concentration. The absorbance can't be greater than 1. All the solutions were diluted to a volume of 2.7 mL with distilled water. A measurement is done without the addition of the ionic liquid and there after 300 μL of IL105 will get added to the solution. Spectra are taken immediately after the addition and at 5, 10, 30 and 60 minutes, with the Jasco 7800 UV-VIS spectrophotometer.

The percentage of extraction (E) was calculated by the following equation (4) where $[\text{dye}]_{\text{aq}0}$ the initial dye concentration of aqueous phase ($\text{mg}\cdot\text{L}^{-1}$), and $[\text{dye}]_{\text{aq}}$ the dye concentration of aqueous phase after extraction ($\text{mg}\cdot\text{L}^{-1}$).

$$E = 100 * \frac{[\text{dye}]_{\text{aq}0} - [\text{dye}]_{\text{aq}}}{[\text{dye}]_{\text{aq}0}} \quad (5)$$

2.3.5 Synthesis C_6mimBF_4

The $[\text{C}_6\text{mim}][\text{BF}_4]$ was synthesized using the procedure published by Dupont et al. [71]

Before the actual synthesis starts, the ionic liquid needs to be dried. Therefore 30 mL (0.0513 mol) of $[\text{C}_6\text{mim}][\text{Cl}]$ is added to a round bottom flask, which needs to get dried under vacuum at 60 $^\circ\text{C}$.

The actual reaction consists of the reaction of 1-Hexyl-3-methylimidazolium chloride with an aqueous sodiumtetrafluoroborate solution. Since it is a 1:1 reaction, both of the reagents need to be present in the same molar quantity. These reagents are stirred for 20 hours, with a magnetic stirrer.

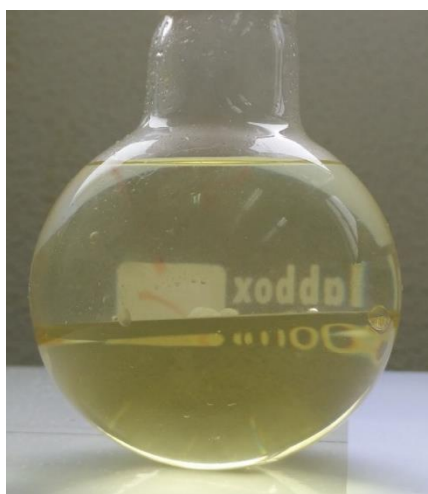


Figure 2.8 The biphasic solution generated at the synthesis of $[\text{C}_6\text{mim}][\text{BF}_4]$

99,9% dichloromethane (30 mL) is used to extract the ionic liquid from the aqueous biphasic solution. Afterwards the two layers are separated by decantation. The upper layer is clear and needs no further removal of solid compounds, while as the bottom, $[\text{C}_6\text{mim}][\text{BF}_4]$ containing, layer will need to be filtrated, making use of a Büchner funnel under vacuum. Both of the solutions are to be purified by evaporation, so the solvents are removed out of the solution.

Chapter 3: RESULTS AND DISCUSSION

In this chapter results of the experiments will be given and discussed. Starting with a comparison of density vs temperature for the ionic liquid trihexyl(tetradecyl)phosphonium dicyanamide ([P_{6.6.6.14}][DCA], IL105). Subsequently, cyclic voltammetry will be used as a technique to investigate the electrochemical properties of several ionic liquids. The influence of water on the usable potential window will be investigated. The behaviour and peak potential of ferrocene in some of the previously handled ILs is presented.

The catalytic activity of ferrocene with IL105 as a medium, as was applied in the electrochemical studies is also used for the oxidation of cyclohexane. The effect of different influential factors is shown.

The adsorption of multiple pigments by the ionic liquid trihexyl(tetradecyl)phosphonium dicyanamide is examined in several conditions, such as exposure to the sun and change in acidity/basicity of the aqueous pigment solution. Oxidation of those pigments by 30 v/v% hydrogen peroxide and the effect of the ionic liquid on this process is shown.

3.1 Density

In Figure 3.1 a comparison is shown between densities of trihexyl(tetradecyl)phosphonium dicyanamide, [P_{6.6.6.14}][DCA], at several temperatures. Therein the values indicated by a red dot are measurement obtained in this work. [24,25,27,31]

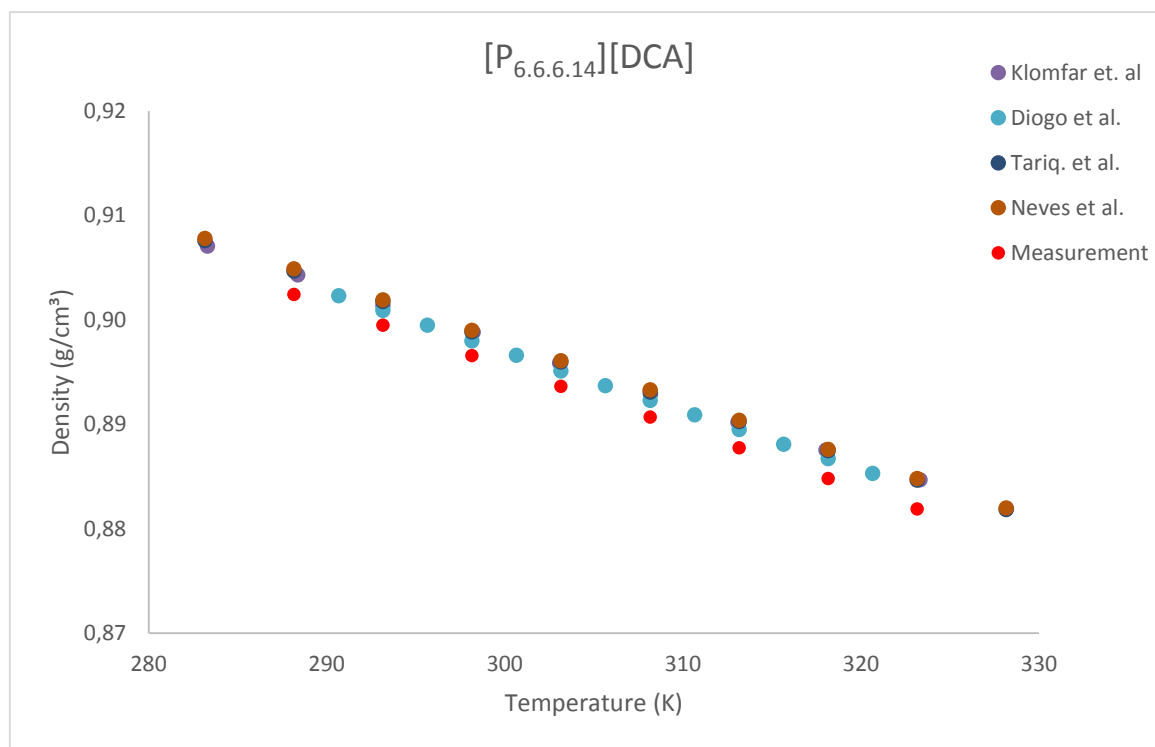


Figure 3.1 Density plotted against the temperature; a comparison between literature results by Klomfar *et al.* [139], Diogo *et al.* [140], Tariq *et al.* [141], Neves *et al.* [142] and measurements using the DSA 5000M Anthon Paar density meter.

Density measurements for $[P_{6.6.6.14}][DCA]$ were done in trifold or more in order to get reproducible results, thus diminishing the chance of errors occurring. The result obtained is situated in the uncertainty range of the literature results. [24,25,27,31]

3.2 Electrochemical behaviour of ionic liquids

The use of ionic liquids as electrolytes for electrochemical applications has been investigated in this study.

An initial carried out to establish the electrochemical window and stability against oxidation and reduction processes of selected ILs characterisation was (Table 3.1). The cathodic and anodic potential limits, that is, the electrochemical stability window, of seven room-temperature ionic liquids formed from a combination of cations 1-alkyl-3-methylimidazolium (alkyl = butyl, hexyl or octyl, $[C_n\text{mim}]^+$, $n = 4, 6$ or 8), trihexyl(tetradecyl)phosphonium ($[P_{6.6.6.14}]^+$) or *N*-methyl-*N,N,N*-trioctyloctan-1-ammonium ($[N_{8.8.8.1}]^+$), and anions bis(trifluoromethylsulfonyl)imide ($[(CF_3SO_2)_2N]^-$, $[NTf_2]^-$), dicyanamide ($[DCA]^-$) or chloride, were investigated by cyclic voltammetry (CV, scan rate 200 mV s^{-1}) at a platinum working electrode, under dinitrogen and at room temperature.

Table 3.1 Structures and common designations of ionic liquids used for electrochemical stability window studies.

Formula	Structure
$[P_{6.6.6.14}][DCA]$	
$[P_{6.6.6.14}][Cl]$	

Formula	Structure
<u>Alliquat 336</u>	
[C ₄ mim][NTf ₂]	
[C ₆ mim][NTf ₂]	
[C ₈ mim][NTf ₂]	
[C ₆ mim][Cl]	

The limits of the useful potential range are indicated by a sharp and steady rise in the current (see Figure 3.2) due to the electrochemical decomposition of the IL ions. These limits and the width of the stable potential windows determined under the experimental conditions used (see 2.3.2) are listed in Table 3.2.

Table 3.2 The oxidation potential, the reduction potential and the electrochemical window available in [P_{6.6.6.14}][DCA], [P_{6.6.6.14}][Cl], Alliquat 336, [C₄mim][NTf₂], [C₆mim][NTf₂], [C₈mim][NTf₂] and [C₆mim][Cl] at a platinum disk working electrode; v, 200 mVs⁻¹. Potentials are vs. an Ag quasi-reference electrode (QRE).

IL	E ^{ox} / V vs. Ag QRE	E ^{red} / V vs. Ag QRE	ΔE / V
[P _{6.6.6.14}][DCA]	1.7	-1.8	3.5
[P _{6.6.6.14}][Cl]	1.0	-3.0	4.0
Alliquat 336	1.0	-2.1	3.1
[C ₄ mim][NTf ₂]	1.0	-1.7	2.7
[C ₆ mim][NTf ₂]	1.8	-1.5	3.3
[C ₈ mim][NTf ₂]	1.5	-2.0	3.5
[C ₆ mim][Cl]	0.9	-1.5	2.4

The range of potentials available for the electrochemical processes not affecting the solvent potential window covers in each case a somewhat different region of the potential spectrum.

As an example, cyclic voltammograms presented in Figure 3.2, shows the differences on the electrochemical stability range existing between [C₄mim][NTf₂] and [C₈mim][NTf₂], two ILs with a common anion, where the cations present different length of methylimidazolium alkyl chains. Also, the flatness of the imidazolium ring seems to allow a higher conductivity than in commonly used cations, such as, the ammonium salts.

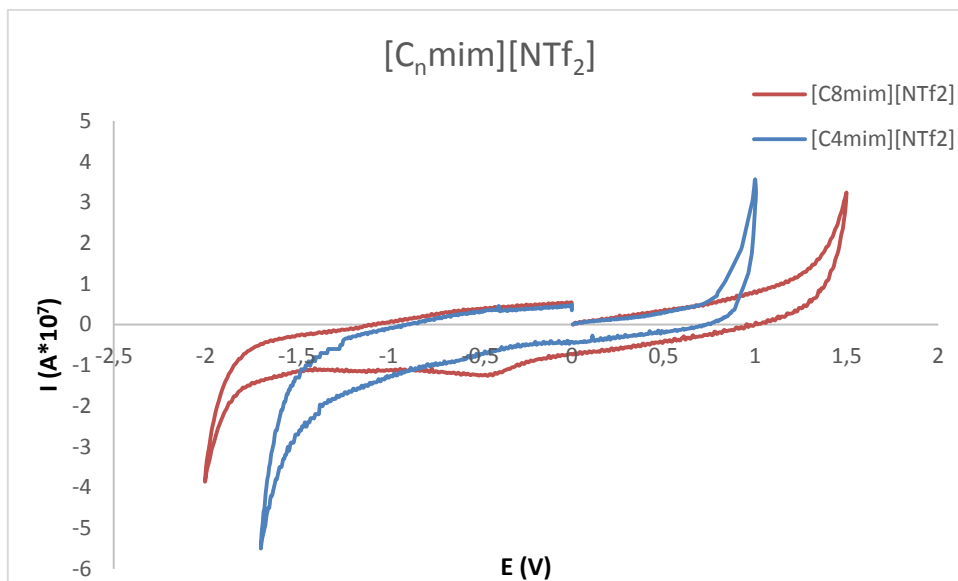


Figure 3.2 Cyclic voltammograms of [C4mim][NTf₂] (blue) and [C8mim][NTf₂] (red), at a platinum disk working electrode; ν , 200 mVs⁻¹. Potentials are vs. an Ag quasi-reference electrode (QRE).

Hydrophobicity of an ionic liquid increases with increasing alkyl chain length. Adding CH₂ groups to the alkyl chain on the imidazolium cation promotes a larger surface area with more hydrogen available, making the interaction with the water molecules less relevant.

As expected, the ILs with halides, and in particular the ones with the chloride anion (Table 3.2), are limited for oxidation applications above ca. 1 V, since the chloride undergoes oxidation at that potential. [102]

The best overall stability is delivered by [P_{6.6.6.14}][DCA] which exhibits similar, and wide, useful limits at both positive and negative potentials (Figure 3.3).

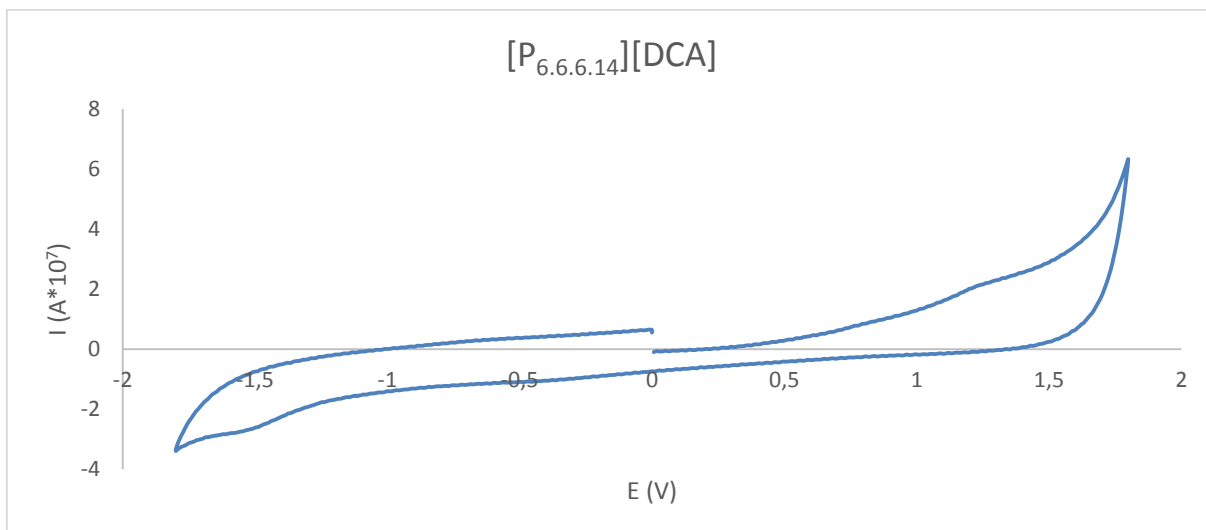


Figure 3.3 Cyclic voltammogram of [P6.6.6.14][DCA] (0.19 % water) at a platinum disk working electrode; ν , 200 mVs⁻¹. Potentials are vs. an Ag quasi-reference electrode (QRE).

The electrochemical potential window of room temperature ionic liquids is sensitive to impurities. As mentioned in section 1.1.3, a change in the water content of an ionic liquid will affect conductivity: as the water content increases, so does conductivity, whereas viscosity decreases.

A decrease in viscosity with the increase of the water content (section 1.1.2.3) and subsequent increase in conductivity of a RTIL used as solvent may appear to be advantageous for an electrochemical experiment. However, the performed cyclic voltammetric studies, as well as previous ones found in the literature, [102] have shown that an increase in water content significantly narrows the electrochemical window of each ionic liquid, as can be observed in Figure 3.4, e.g., for [C₄mim][NTf₂].

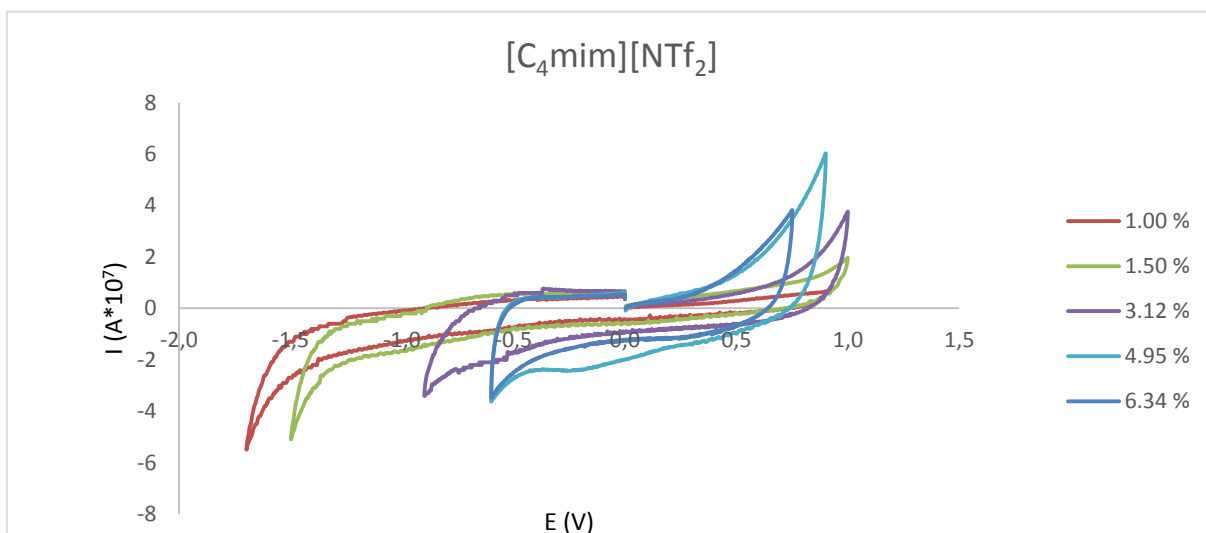


Figure 3.4 Cyclic voltammograms of [C₄mim][NTf₂] for different water contents; 1.00 % (red), 1.50 % (green), 3.12 % (purple), 4.95 % (light-blue) and 6.34 % (dark-blue) at a platinum disk working electrode; ν , 200 mVs⁻¹. Potentials are vs. an Ag quasi-reference electrode.

For the series $[C_n\text{mim}][\text{NTf}_2]$ ($n = 4, 6, \text{ or } 8$) a small increase in the water content of the IL leads to a considerable reduction on the potential range available for electrochemical stability of the IL (Figure 3.5), $[C_4\text{mim}][\text{NTf}_2]$ being the most affected. That can be due to the fact that $[C_4\text{mim}]$ is the smaller and more symmetric of the three, so it has the less surface area to interact with the water molecules.

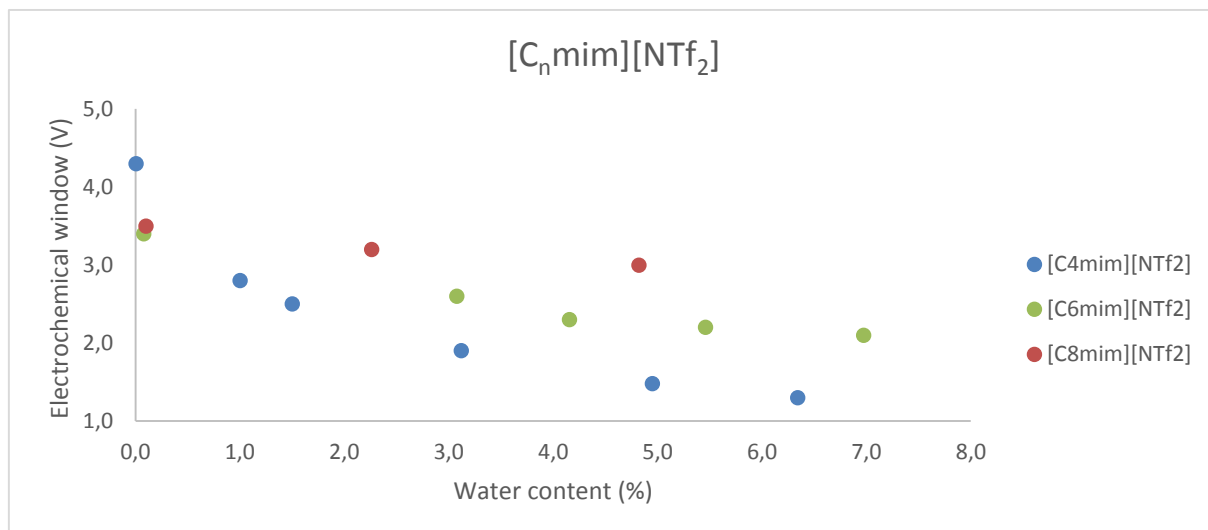


Figure 3.5 Potential window available in $[C_4\text{mim}][\text{NTf}_2]$, $[C_6\text{mim}][\text{NTf}_2]$ and $[C_8\text{mim}][\text{NTf}_2]$ for different water contents at a platinum disk working electrode; v , 200 mVs⁻¹. Potentials are vs. an Ag quasi-reference electrode (QRE).

A similar behaviour was found for the ILs containing $[\text{Cl}]^-$ as an anion at which the cation was differed. Trihexyl(tetradecyl)phosphonium ($[\text{P}_{6.6.6.14}]^+$), methyl(trioctyl)ammonium ($[\text{N}_{1.8.8.8}]^+$) and 1-hexyl-3-methylimidazolium ($[\text{C}_6\text{mim}]^+$), where ($[\text{N}_{1.8.8.8}]^+$) is the cation in Aliquat 336, are being used, Figure 3.6. However, these ILs are not so sensitive to the presence of water as the series $[\text{C}_n\text{mim}][\text{NTf}_2]$, what can be rationalized in terms of the large size of the cationic part, that promotes hydrophobicity, and therefore, less sensitivity to the presence of water molecules.

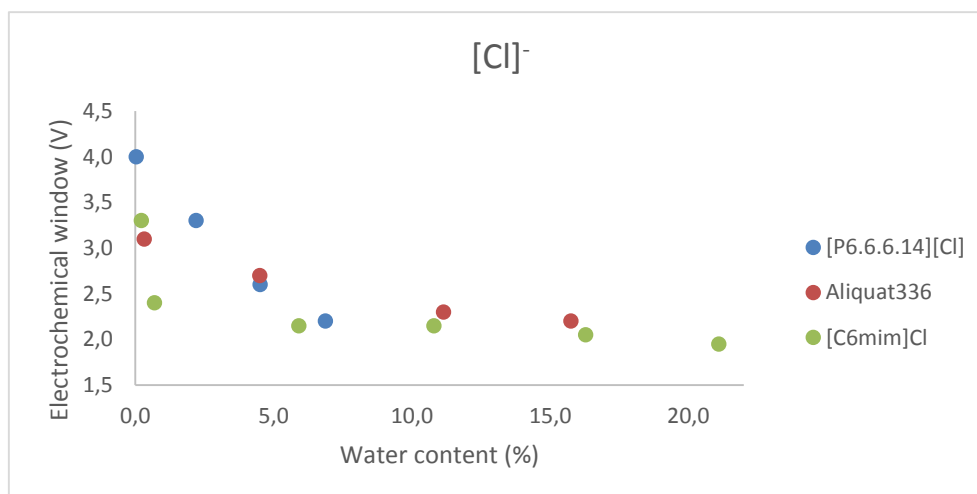


Figure 3.6 Potential window available in ILs consisting of $[\text{Cl}]^-$ as an anion and $[\text{P}_{6.6.6.14}]$, $[\text{N}_{1.8.8.8}]$ (in Aliquat 336) and $[\text{C}_6\text{mim}]$ as a cation for different water contents at a platinum disk working electrode; v , 200 mVs⁻¹. Potentials are vs. an Ag quasi-reference electrode

A bigger decrease in electrochemical window is seen at $[\text{P}_{6.6.6.14}]\text{Cl}$ as is in $[\text{P}_{6.6.6.14}][\text{DCA}]$, Figure 3.7. The difference between the two $[\text{P}_{6.6.6.14}]$ ILs with changing anion is not comparable to the change that is seen when the cation is changed.

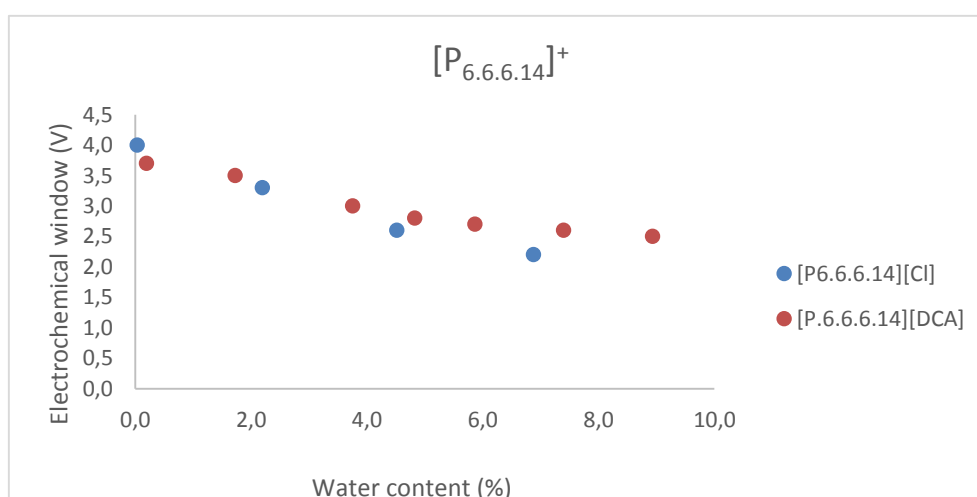


Figure 3.7 Potential window available in ILs consisting of $[\text{P}_{6.6.6.14}]^+$ as a cation and $[\text{Cl}]^-$ and $[\text{DCA}]^-$ as an anion for different water contents at a platinum disk working electrode; v , 200 mVs⁻¹. Potentials are vs. an Ag quasi-reference electrode (QRE).

In figure 3.8 the influence of the anion on the potential window is investigated at different water contents. $[\text{C}_6\text{mim}]^+$ is considered as cation and the anions are respectively $[\text{NTf}_2]^-$ and $[\text{Cl}]^-$. A significant decrease in potential range for an increasing water content is seen in both cases. If the evolution of the two is compared on the other hand, no significant difference is seen.

O'Mahony et al. did not see a change in the potential window (3.3 V), when increasing the water content from 0.22 % to 6,10 %, when measuring at a Pt working electrode. This is opposed to the results that are found in this work, which are showing a considerable decrease in the potential window when water is added.

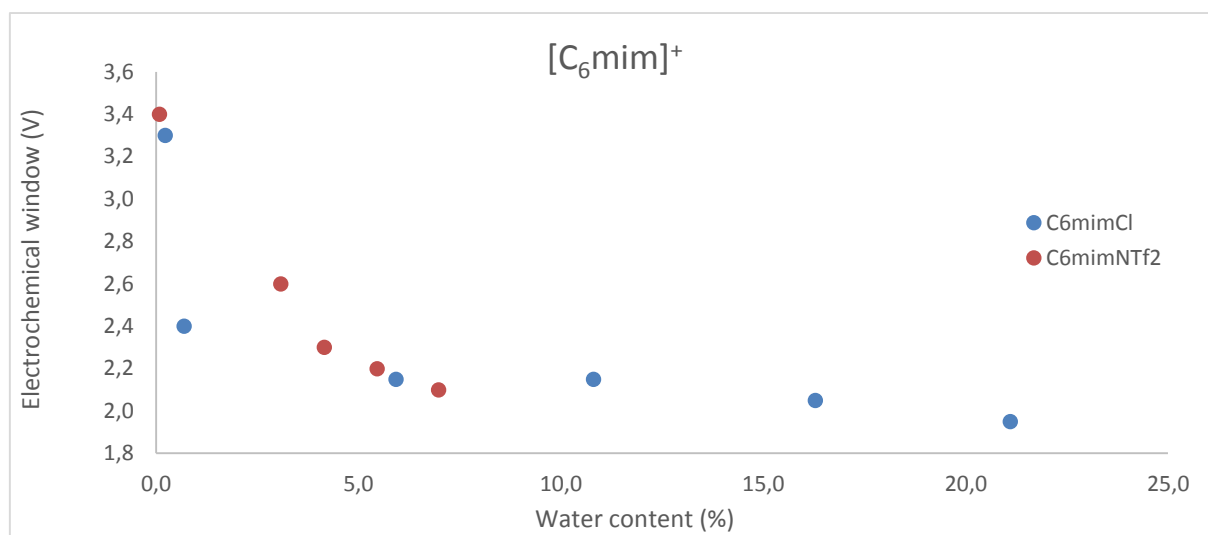


Figure 3.8 Potential window available in ILs consisting of $[\text{C}_6\text{mim}]^+$ as a cation and $[\text{Cl}]^-$ and $[\text{NTf}_2]^-$ as an anion for different water contents at a platinum disk working electrode; v , 200 mVs⁻¹. Potentials are vs. an Ag quasi-reference electrode (QRE).

The anion, in particular, was found to affect the level of water uptake. The hydrophobicity of the anions adhered to the following trend: $[\text{NTf}_2]^- > [\text{DCA}]^- > [\text{Cl}]^-$.

The process $[\text{Fe}(\text{C}_5\text{H}_5)_2]^{+/0}$ of the traditionally used reference compound ferrocene has been studied at a platinum disk electrode in the ionic liquids $[\text{C}_6\text{mim}][\text{Br}]$, $[\text{C}_6\text{mim}][\text{NTf}_2]$ and $[\text{P}_{6.6.6.14}][\text{DCA}]$.

A reversible, one-electron reduction process was observed (a typical cyclic voltammogram is shown on Figure 3.9), and the measured half wave potential *versus* a silver quasi-reference electrode are presented in Table 3.3.

Table 3.3 Half-wave potential values for the $[\text{Fe}(\text{C}_5\text{H}_5)_2]^{+0}$ redox process in different ionic liquids.

Ionic Liquid	$E_{1/2}^{\text{ox}} / \text{V}^a$	i_{p_a} / i_{p_c}	Water content %
$[\text{C}_6\text{mim}][\text{NTf}_2]$	0.25	1.1	0.08
$[\text{P}_{6.6.6.14}][\text{DCA}]$	0.52	1.0	0.24
	0.57	1.5	0.19

^a Potentials are vs. an Ag quasi-reference electrode (QRE).

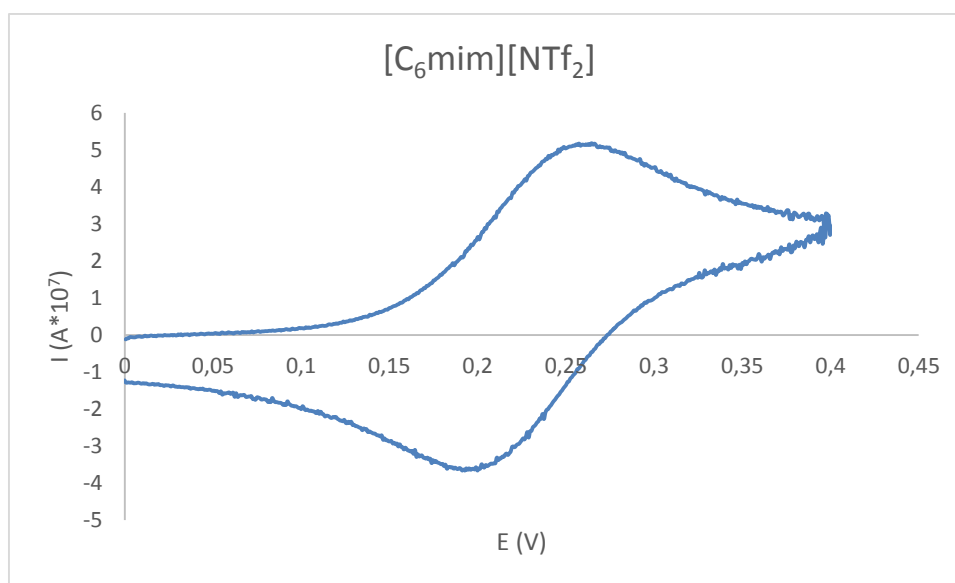


Figure 3.9 Cyclic voltammograms of ferrocene in $[\text{C}_6\text{mim}][\text{NTf}_2]$ at a platinum disk working electrode; v , 200 mVs^{-1} . Potentials are vs. an Ag quasi-reference electrode (QRE).

3.3 Peroxidative oxidation of cyclohexane

The catalytic activity of ferrocene in trihexyl(tetradecyl)phosphonium dicyanamide, [P_{6.6.6.14}][DCA], was tested as catalyst for the oxidation of cyclohexane with aqueous tert-butylhydroperoxide (ButOOH, TBHP) as oxidizing agent, at 50 °C. Results are given in Table 3.4.

Table 3.4 Selected data for the catalytic oxidation of cyclohexane to cyclohexanol and cyclohexanone catalyzed by ferrocene in [P_{6.6.6.14}][DCA].

Entry	Catalyst amount (mol L ⁻¹)	Additive (mol L ⁻¹)	Yield % ^b			Total TON ^c	Total TOF ^d (h ⁻¹)	
			Cyclo-hexanone	Cyclo-hexanol	Total			
1			30	1.5	0	1.5	91.1	182.2
2			60	0.7	0	0.7	44.6	44.6
3	2.47x10 ⁻⁴	-	120	7.2	0	7.2	448.6	224.3
4			180	10.1	0	10.1	629.9	210.0
5			360	10.2	0	10.2	639.2	106.5
6	2.47x10 ⁻⁴	Na ₂ CO ₃ (7.30x10 ⁻²)	120	14.3	0	14.3	892.9	446.5
7		HNO ₃ (1.60x10 ⁻¹)	120	15.7	0	15.7	980.0	490.0
8	1.32x10 ⁻²		120	5.8	0	5.8	7.2	3.6
9	3.70x10 ⁻²	-	120	7.7	0	7.7	3.3	1.7
10	4.94x10 ⁻²		120	6.9	0	6.9	2.2	1.1

^aYield and TON determined by GC analysis (upon treatment with PPh₃). ^bMolar yield (%) based on substrate, *i.e.* moles of product (alcohol (OL) or ketone (ONE)) per 100 mol of cycloalkane. ^cTurnover number = number of moles of products per mol of catalyst. ^d TOF = TON per hour.

Only cyclohexanone was produced by oxidation of cyclohexane in the above-mentioned conditions (cyclohexanol was not detected, not even traces). A maximum cyclohexanone yield of 15.7% was obtained (entry 7, Table 3.4) in the presence of acidic medium. This selectivity is rare, being the cyclohexanol and cyclohexanone mixture the common products obtained.

Interestingly, both acidic and basic additives led to an enhancement of the amount of cyclohexanone produced.

Martins *et al.* also found that the addition of HNO₃ promotes the activity of the [FeCl₂{η³-HC(pz)₃}] / CNT-Oxi-Na combination for the catalytic conversion of cyclohexane to both cyclohexanol and cyclohexanone. [70]

G.B. Shul'pin et al. showed that the addition of a base can have an accelerating-, retardation- or inhibiting effect on the decomposition of hydro peroxides. It is dependent on the composition of the base, oxidant and the catalyst used. Some complexes, heterocyclic N-bases for say, probably play the role of proton transfer reagent in a lot of oxidations. Thus stimulating the oxidation of alkanes. In other cases, however, a base can deprotonate a reactive species, which leads to its inactivation. If a base is added to manganese complex, the H_2O_2 decomposition will be greatly enhanced, accelerating the oxidation rapidly. [75]

A reaction pathway for this reaction as is suggested by Nowotny *et al.* [103] is the direct-oxidation reaction via the free-radical chain reaction pathway, Figure 3.10. It is the presumed mechanistic pathway for the one-pot oxidation of cyclohexane with TBHP as an oxidant. This was the proposed way of reaction with both the use of cobalt carboxylate complexes and vanadium exchanged zeolite Y. In this case TBHP would be initiated by the combination of ferrocene and IL105, forming a butylperoxide- and butyloxy radical. The exact change in the structure of both, causing the radicalization isn't sure, but the conversion from Fe(II) to Fe(III) seems the most probable. In the propagation step these radicals would deprotonate cyclohexane, resulting in a cyclohexyl radical which immediately converts to a cyclohexyl peroxy radical by oxygen dissolved in the reaction medium. Nowotny *et al.* proposed a conversion to both cyclohexanone and cyclohexanol, but since only cyclohexanone is formed the alcohol formation step can be discarded. As a termination step the cyclohexyl peroxy radical will combine with butylperoxide radical to form cyclohexanone releasing both oxygen and *tert*-butanol as byproduct. [103,104]

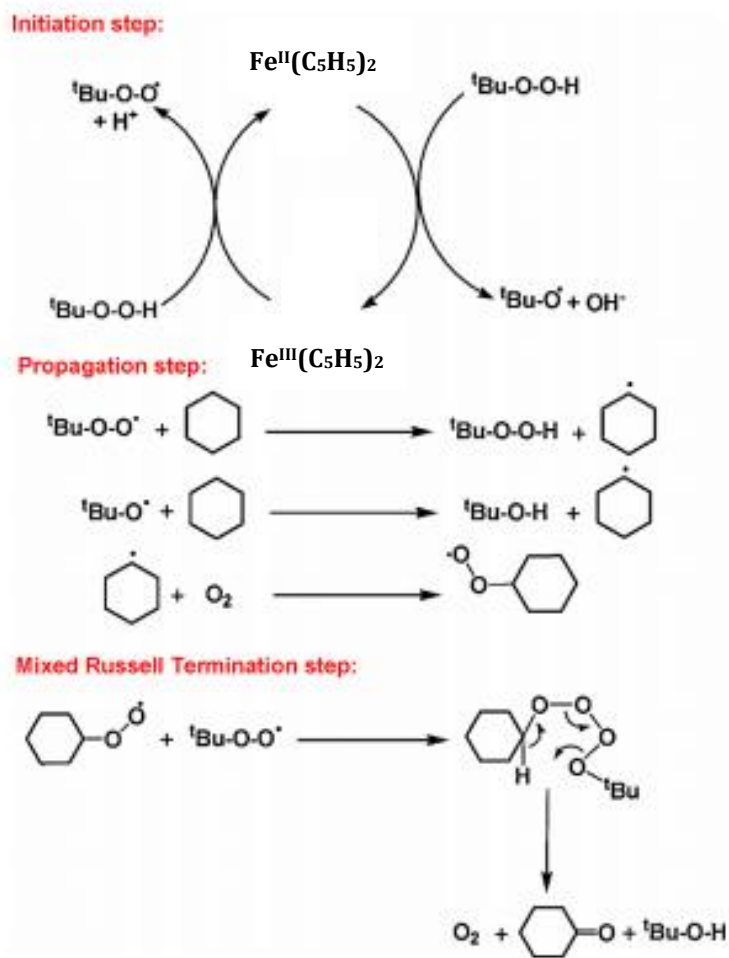


Figure 3.10 Proposed mechanism for cyclohexane oxidation via free-radical reaction pathway over ferrocene as catalyst, making use of TBHP as oxidant. [104]

3.4 Pigments

For determining the influence of the concentration and pH for each pigment, a calibration curve was made for the working range of concentration and with the pH values used in the studies. (See section 2.3.4.3 for procedure and Annex 1 for figures). In all the pigments studied, a linear behavior for absorbance vs concentration was found at all the pH values studied.

Therefore UV- spectra were taken, reading the absorbance's at the highest point in the absorbance vs wavelength graph. A linear behavior was observed for all the pigments. Table 3.5 Shows the absorbance's at the highest point determined for each pigment at the different pH values.

Table 3.5 Wavelength of Maximum Absorbance for the pigments at the studied pH values

Pigment	λ (pH=2) /nm	λ (pH=7) /nm	λ (pH=12) /nm
Amaranth	521	521	493
Rhodamine 6G	524	524	524
Chrysoidine	455	450	403
Indigo	610	610	610
Tartrazine	421	423	425
Malachite green	616	616	/
Methyl violet	582	582	/
Methylene blue	662	662	662

A qualitative experiment subjecting both pigment, as a mixture of pigment and ionic liquid to the sun is done to investigate the evolution of the color intensity of the aqueous pigment solution. The ultimate goal is to see which pigment will migrate from the aqueous phase to the ionic liquid, comparing the color intensity of the aqueous phase as a function of time. To complement the study, examination of the change in color of the ionic liquid before and after the addition to the pigment solution by UV measurements was performed. Only values above 1% are mentioned. This value was chosen because it represents the minimum average value, in color variation, detected by a human eye.

For the liquid-liquid extraction, the pigments that showed a decrease in color intensity of the aqueous phase and an increase in color intensity of the ionic liquid phase, were subsequently investigated. The UV-spectra of several concentrations of pigment solution were taken. IL105 was added to the solution and left untouched for 30 minutes at room temperature for the pigment to migrate from the aqueous phase to the ionic liquid phase. UV-spectra were taken again and the absorbances were read at the predefined wavelength showed in Table 3.5. The distribution ratios were calculated, as well as the percentage of extraction. All the measurements were put in a graph of absorbance versus time. This was done at a pH of 2, 7 and 12. pH is a measure of acidity ($\text{pH} < 7$) or basicity ($\text{pH} > 7$) of an aqueous solution. The pH factor is very important in the adsorption process especially for dye adsorption. The pH of a medium will control the magnitude of electrostatic charges which are imparted by the ionized dye molecules. As a result the rate of adsorption will vary with the pH of an aqueous medium [106]. The effect of pH solution on the adsorption process can be studied by preparing adsorbent-adsorbate solution with fixed adsorbent dose and dye concentration but with different pH by adding NaOH (1 M) or HCl (0.1 M) solutions and then shaken until equilibrium.

The evolution of the color intensity of the aqueous solution and thus the magnitude in which the pigment gets adsorbed out of the aqueous solution by the ionic liquid is recorded.

Therefore the absorbance of the pigment solution was measured at the maximum absorbance wavelength point before the addition of IL105 and directly afterwards. Subsequently the mixture was stored in an ambient environment and after 5, 10 and 30 minutes the absorbance was measured again. Furthermore, the four aliphatic chains present in phosphonium-based IL (IL105) also confer a higher hydrophobicity to the IL and a consequent higher capability for phase separation.

Recently, advanced oxidation processes (AOPs) has been developed to oxidize organic pollutants into carbon dioxide, water and inorganic ions or transform into less complex structures. AOPs are based on the generation of highly reactive species such as hydroxyl radicals ($\cdot\text{OH}$), which have strong oxidation potential and oxidise a large number of organic pollutants using hydrogen peroxide. The influence of 30% H_2O_2 , as oxidant, was explored visually at different times. The color intensity of the aqueous phase of both the samples with as without IL105 were compared. The change in color of the ionic liquid before and after the addition to the pigment solution was examined as well.

For the quantification, in the case of the oxidation with hydrogen peroxide (30%, v/v) the absorbances were determined before and after the addition of the oxidant to the mixture of water and IL105. In order to examine the evolution of the absorbance in time, measurements at different times are done. Then the reaction rate was calculated. For amaranth this is given in Figure 3.11.

3.4.1.1 Influence of the pH

A visual comparison of the color at different pH's is given in Table 3.6. For amaranth only a basic pH of 12 has an influence on the color of the dye. This can be due to an alteration in the auxochromes of Amaranth, Figure 1.8, being the hydroxyl group. If this group gets deprotonated a loss in color intensity can be the consequence.

The influence of the pH on the color of Rhodamine 6G shows no difference between the samples is seen at respectively pH is 2, 7 and 12.

The color of samples Chrysoidine at respectively pH is 2, 7 and 12 are visually compared. No difference is seen between the samples at different pH's, but the intensity of the pigment solution at a pH of 12 decreased after 2.5 hours. This can be due to the change in the structure of chrysoidine. The higher pH causes the loss of protons at the amine-functions of chrysoidine, Figure 1.8, thus causing a loss in color intensity. In 1.2.1 amine-functions are mentioned as an auxochromic group, which determine the color intensity. A change in their structure can change the color intensity tremendously.

For indigo no difference in color is seen between pH=2 and pH=7. When increasing the pH to a value of twelve on the other hand, the color becomes yellow instead of blue and the intensity decreases slightly in time. The change in color is due to Indigo being a pH indicator, which by definition a halochromic chemical compound added in small amounts to a solution so the pH (acidity or basicity) of the solution can be determined visually. Hence, a pH indicator is a chemical detector for hydronium ions (H_3O^+) or hydrogen ions (H^+) in the Arrhenius model. The decrease in color intensity can be clarified by the amine functions getting deprotonated.































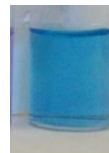

















The qualitative investigation on the influence of pH on the color intensity of Tartrazine shows that no visual difference in color is seen at any of the pH's (2, 7 and 12).

Table 3.6 shows a visual comparison of Malachite green at several pH's, being 2, 7 and 12. A change in color is seen when raising or lowering the pH, to respectively 2 and 12. A complete disappearance of color at pH 12 is observable. In 1.2.3 it was mentioned that the pigment is green between a pH of 1.8 and 11.5 and loses its color above a pH of 13.2. The early disappearance of color is probably due to the pH being slightly higher than 12. As the pH decreases the color shifts more to a blue-green as opposed to blue, when neutral. The change in color is due to Malachite green being a pH indicator.

The influence of the pH on Methyl violet is shown in Table 3.6. The increase in acidity to a pH of 2, does not have a visual impact on methyl violet. When NaOH is added, the aqueous solution clears out gradually, with a complete loss of color after 2.5 hours. Since Methyl violet is a protonated amine it is to be suspected that the color intensity of the pigment would decrease tremendously with an increase in pH, resulting in the formation of a neutral dye.

For methylene blue, at different pH's (2, 7 and 12), it can be concluded that the pH does not have an influence on the color of the dye, Table 3.6.

Table 3.6 Visual comparison of respectively Amaranth, Rhodamine 6G Chrysoidine, Indigo, Tartrazine, Malachite green, Methyl violet and Methylene blue at a pH of 2, 7 and 12 after 5 minutes and 2.5 hours.











Time (h)	Amaranth		Rhodamine 6G		Chrysoidine		Indigo	
	0.083	2.5	0.083	2.5	0.083	2.5	0.083	2.5
pH=12								
pH=7								
pH=2								
Time (h)	Tartrazine		Malachite green		Methyl violet		Methylene blue	
	0.083	2.5	0.083	2.5	0.083	2.5	0.083	2.5
pH=12								
pH=7								
pH=2								

3.4.2 Amaranth C.I. 16185

3.4.2.1 Sun exposure

In Table 3.7 Table 3.7 Sun exposure of Amaranth with and without IL105 the behavior of amaranth is analyzed when exposed to the sun. No change is seen when the dye is affected by the sun for 30 minutes. With the addition of IL105 on the other hand a migration of pigment to the ionic liquid is observed, thus clearing out the aqueous solution. The sorption of pigment by the IL mostly takes place directly after its addition, proceeding until 30 minutes with a stagnation of the sorption afterwards.

Table 3.7 Sun exposure of Amaranth with and without IL105 at pH=7

Time (min)	0	5	10	30	60
Sun exposure					
Sun exposure + IL105					

3.4.2.2 Extracted concentration

In order to quantify the magnitude in which the pigment is desorbed by the ionic liquid, the distribution ratio is calculated and the values are given in annex 2.1.

3.4.2.3 Evolution of the extraction in time

Figure 3.11 shows the magnitude in which Amaranth migrates to the ionic liquid in function of time at different pH's. We can see in the figure that the maximum (15%) is achieved by pH=12. Immediately after the addition of IL105, at pH=2, promotes an 8% extraction while at pH= 7 or 12, the value is smaller. Until 10 minutes the acid and basic form of the pigment have similar values of extraction, but at 30minutes the highest values belongs to the basic form of the pigment. This is due to the anionic form prevailing over the acidic one. As can be seen, higher values of extraction are obtained at higher pH than at low, consistent with the preferential extraction of the anionic, since pKa is 10.36.

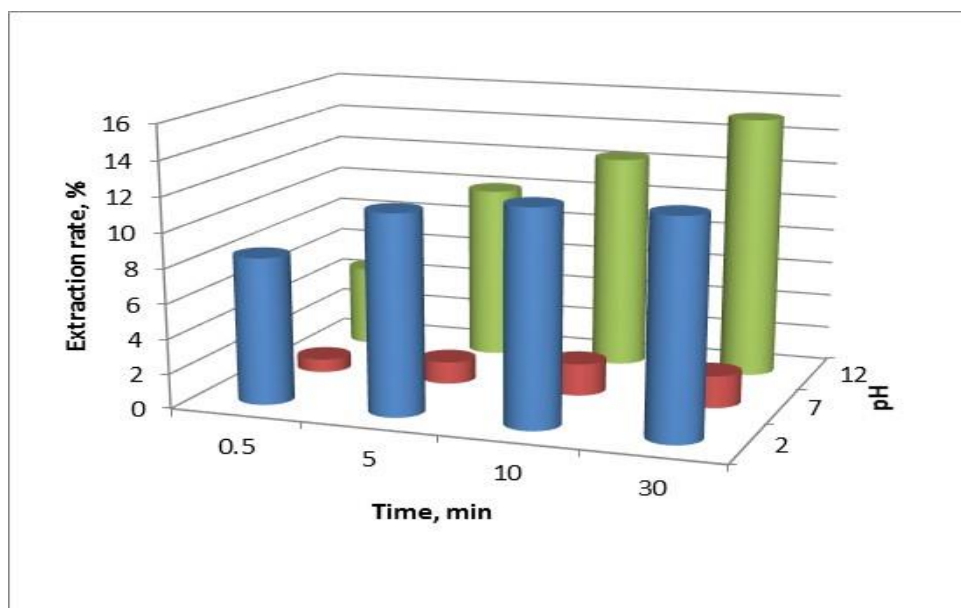


Figure 3.11 The evolution of the liquid-liquid extraction of amaranth by IL105 in time at pH's of 2, 7 and 12.

3.4.2.4 Oxidation by 30% H₂O₂

The influence of IL105 on the intensity of Amaranth is investigated, when influenced by 30% hydro peroxide. In Table 3.8 Table 3.8 Oxidation of Amaranth by 30% H₂O₂ with and without IL105 the result is given. It is noticeable that the color intensity of the pigment decreases gradually, with a total disappearance at the end. In the presence of ionic liquid on the other hand, the change in intensity is much slower than it is in the absence of IL. The amount of hydrogen peroxide was not sufficient to cause the disappearance of the coloring effect of the pigment entirely. The ionic liquid ensures a protection against the oxidative effect of the hydrogen peroxide. This is due to the IL withstanding the effect of hydrogen peroxide almost completely. A decrease in color intensity is seen, but only in a small magnitude. The aqueous phase in the same sample undergoes the same effect as the one without ionic liquid, losing its color completely.

Table 3.8 Oxidation of Amaranth by 30% H₂O₂ with and without IL105 at pH=7






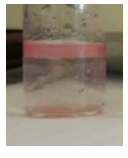


Time (h)	0	0.166	0.5	72
30%H ₂ O ₂				
Time (h)	0	0.166	0.5	72
30%H ₂ O ₂ + IL105				

Figure 3.12 shows the evolution of the dye intensity after the addition of hydrogen peroxide. Qualitatively it wasn't clear that the dye already showed that much of a difference after 30min. In order to quantify this decrease, UV-VIS was used as a technique. After 30 minutes the absorbance of the pigment solution already reduced from 0.054 to 0.040, making it a significant degradation of the pigment.

In the same figure a graph is shown that displays the speed in which the oxidation reaction of amaranth by 30% hydrogen peroxide occurs. The slope presents the first order reaction rate for the oxidation of Amaranth.

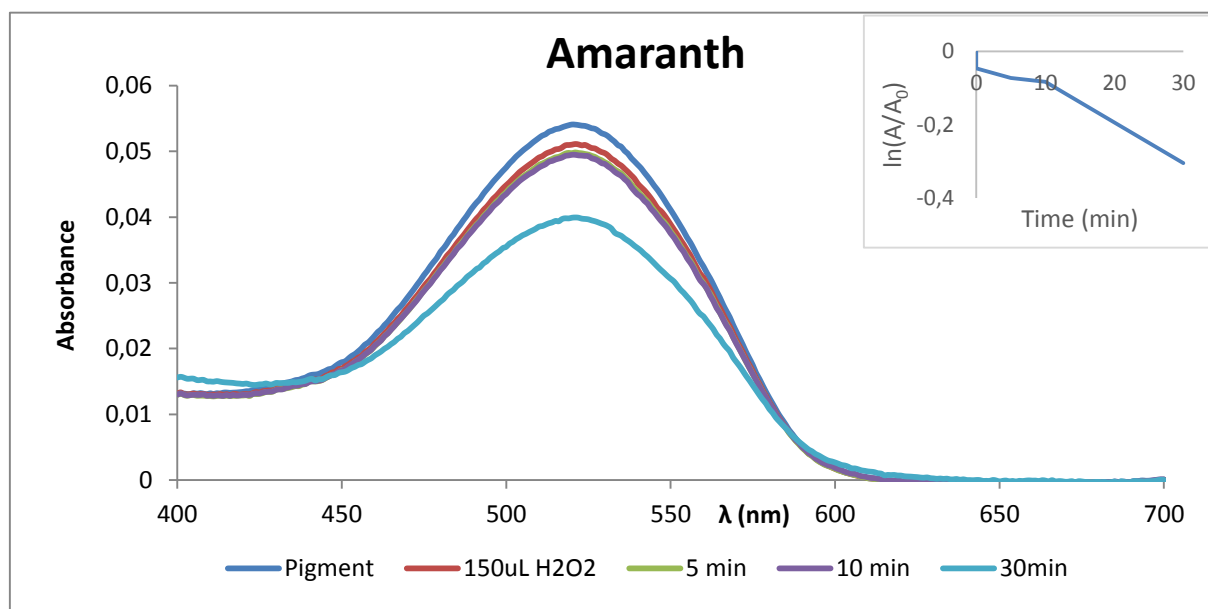


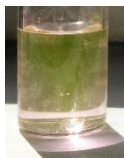


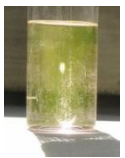




Figure 3.12 The evolution of the absorbance of Amaranth in time when influenced by 30 % H₂O₂ at pH=7, Right corner: The Napierian logarithm of the ratio of absorbance and the initial absorbance of Amaranth vs. time

3.4.3 Rhodamine 6G C.I. 45160

3.4.3.1 Sun exposure

In Table 3.9 the behavior of Rhodamine 6G is analyzed when exposed to the sun. No change is seen when the dye is affected by the sun for 1 hour. With the addition of IL105 on the other hand a small migration of dye from the aqueous solution to the IL is seen. The extraction by the ionic liquid is not as strong as the one found in 3.4.2.1, but it is considerable.

Table 3.9 Sun exposure of Rhodamine 6G with and without IL105

Time (min)	0	5	10	30
Sun exposure				
Sun exposure + IL105				

3.4.3.2 Evolution of the extraction in time

In Figure 3.13 the extraction of Rhodamine 6G by the ionic liquid, IL105 is displayed. A big increase extraction occurs, when the basicity is increased to a pH of 12. It shows a big initial increase of 15% and increases until 30 minutes.

The migration of pigment from the aqueous solution to the IL in a neutral solution has a small magnitude, with a stagnation of this process after 10 minutes. In acid media, no decrease in absorbance is seen whatsoever. In other words, acidity is detrimental for the sorption process of Rhodamine 6G to IL105.

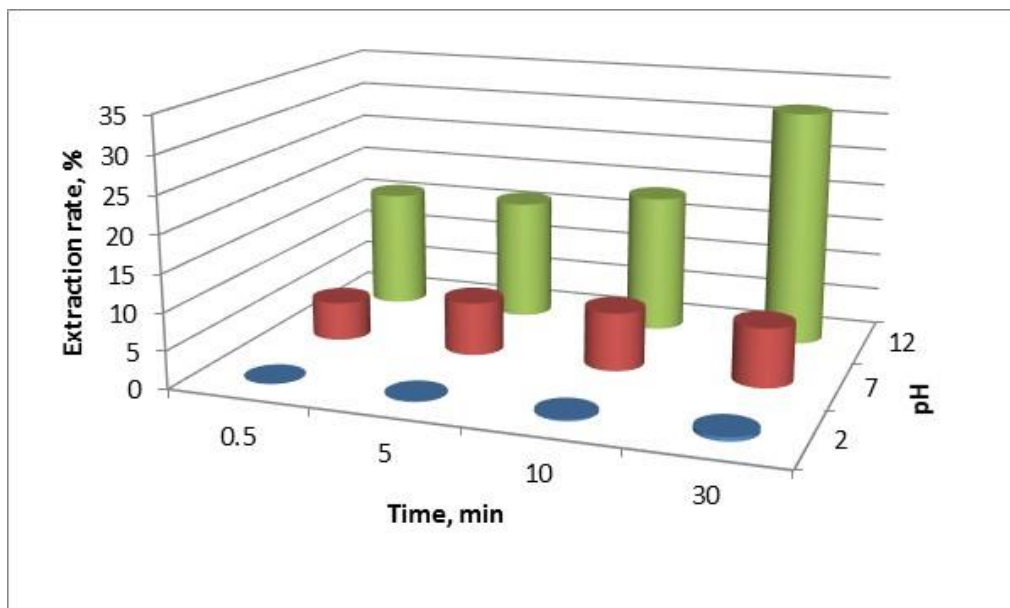


Figure 3.13 The evolution of the liquid-liquid extraction of Rhodamine 6G by IL105 in time and pH.

As already mentioned the acidity of the pigment solution interferes in the sorption process of Rhodamine 6G from the aqueous solution to the IL, thus explaining the value being close to 0. In a neutral medium the extraction is found to be smaller (approximately 10%), with an average efficiency in basic media at a pH of 12 (32%).

3.4.3.3 Oxidation by 30% H₂O₂

The influence of IL105 on the intensity of Rhodamine 6G is investigated, when influenced by 30% hydrogen peroxide. In Table 3.10 the evolution is given. It is noticeable that the fortitude of the pigment gradually decreases, with a total disappearance at the end. The same effect is seen in the presence of ionic liquid. A small migration of pigment to IL105 is seen ones again, as was already found in the sun exposure test, 3.4.3.1.

Table 3.10 Oxidation of Rhodamine 6G by 30% H₂O₂ with and without IL105

Time (h)	0	0.166	0.5	72
30% H ₂ O ₂				
Time (h)	0	0.166	0.5	72
30% H ₂ O ₂ + IL105				

Figure 3.14 shows the evolution of the pigment intensity without IL105, after the addition of hydrogen peroxide. The graph shows that the decrease in intensity is gradual, as was suspected out of the qualitative tests. Another graph is shown in the right corner that displays the speed in which the oxidation reaction of rhodamine 6 G by 30% hydrogen peroxide occurs.

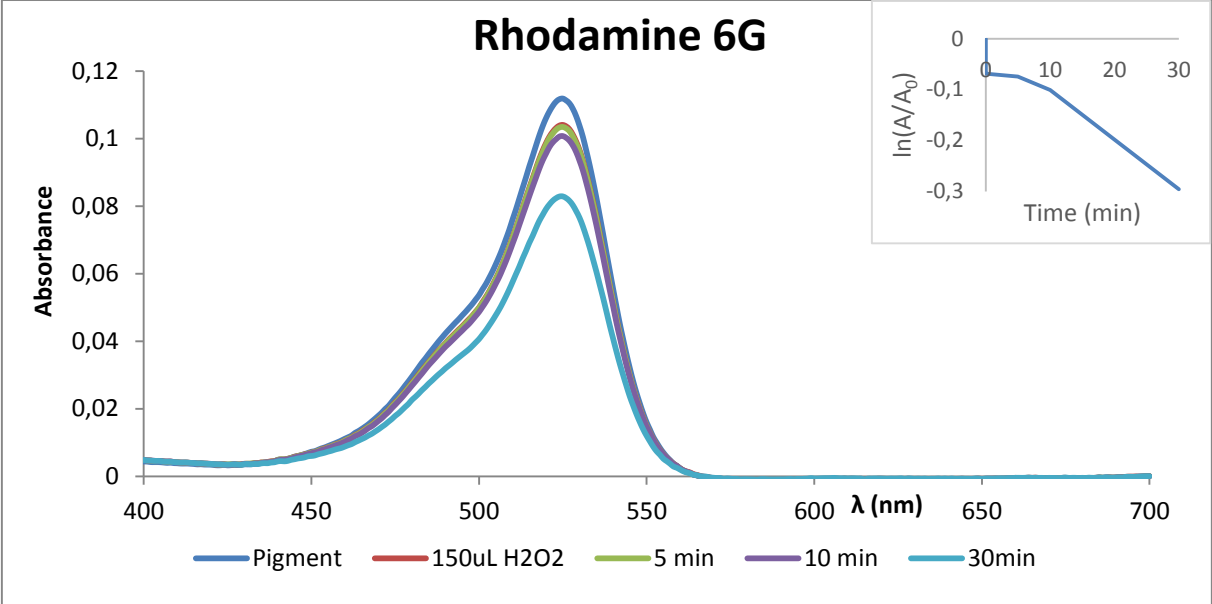


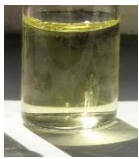
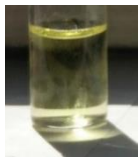

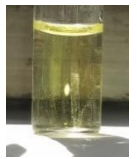
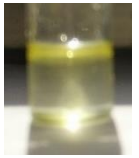



Figure 3.14 The evolution of the absorbance of Rhodamine 6G in time when influenced by 30 % H₂O₂ at pH=7, Right corner: The Napierian logarithm of the ratio of absorbance and the initial absorbance of Rhodamine 6G vs. time.

3.4.4 Chrysoidine C.I. 11270

3.4.4.1 Sun exposure

Table 3.11 shows a visual comparison between the behavior of Chrysoidine in an aqueous solution in the absence and in the presence of IL105. It behaves the same as Amaranth, as is explained in 3.4.2.1.

Table 3.11 Sun exposure of Chrysoidine with and without IL105

Time (min)	0	5	10	30
Sun exposure				
Sun exposure + IL105				

3.4.4.2 Evolution of the extraction in time

In Figure 3.15 the evolution of the absorbance of Chrysoidine by the ionic liquid, IL105, at a pH of 2, 7 and 12 is displayed. A big increase of the extraction, from 5 to 10 minutes occurs, when basicity is increased to a pH of 12. The extraction after 30 minutes was 55%, which is more than considerable compared to the extraction ratios of the other pigments in IL105; excluding Indigo since it has a higher extraction ratio at a pH of 12.

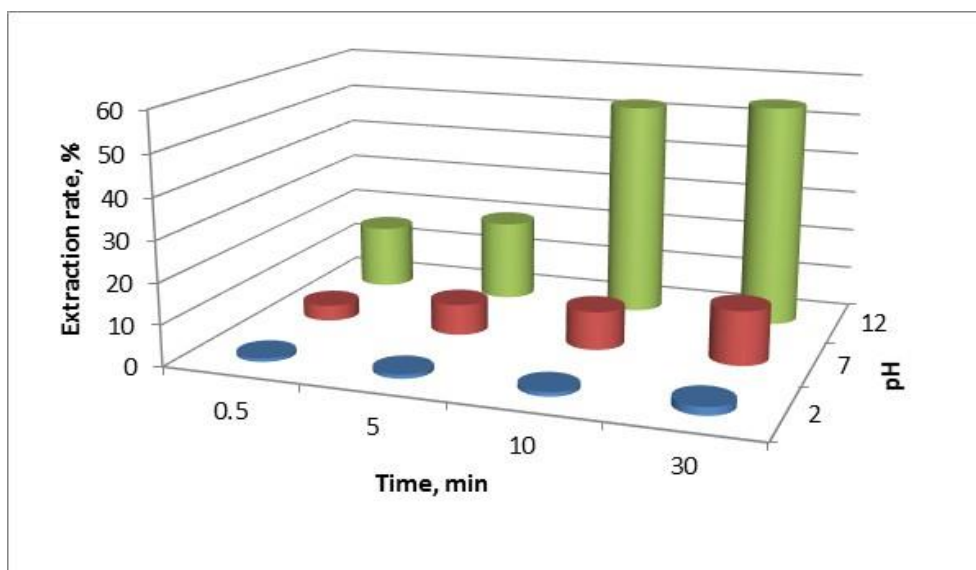


Figure 3.15 The evolution of the liquid-liquid extraction of chrysoidine by IL105 in time.

No comparison is possible because the use of ionic liquids with this pigment never been tested before.

3.4.4.3 Oxidation by 30% H₂O₂

The influence of IL105 on the intensity of Chrysoidine is investigated, when influenced by 30% hydrogen peroxide, in Table 3.12 the evolution is given. Same behavior is seen as with Amaranth, 3.4.2.4, with the only difference that the IL withstands the effect of hydrogen peroxide completely. No degradation of Chrysoidine in the IL is seen at all. This could be explained by a stronger association between IL 105 and Chrysoidine.

Table 3.12 Oxidation of Chrysoidine by 30% H₂O₂ with and without IL105

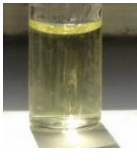
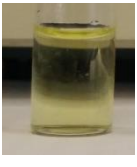


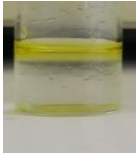
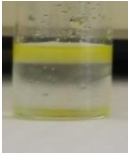
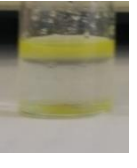

Time (h)	0	0.166	0.5	72
30% H ₂ O ₂				
Time (h)	0	0.166	0.5	72
30% H ₂ O ₂ + IL105				

Figure 3.16 shows the evolution of the dye intensity after the addition of hydrogen peroxide. No measurement directly after the addition of 30% H₂O₂ was done. Since this addition will dilute the pigment solution slightly, the initial effect of the hydrogen peroxide can only be estimated. The comparisons will have to be done for the measurements after 5, 10 and 30 minutes, in order to decently compare the results.

The graph shows that the decrease in dye intensity is little with an absorbance of 0.1265 after 5 and 0.1108 after 30 minutes, thus only decreasing 12.41%.

In Figure 3.16 a graph is shown on the right, which displays the speed in which the oxidation reaction of Chrysoidine by 30% hydrogen peroxide occurs, with the slopes being of the first order reaction rates.

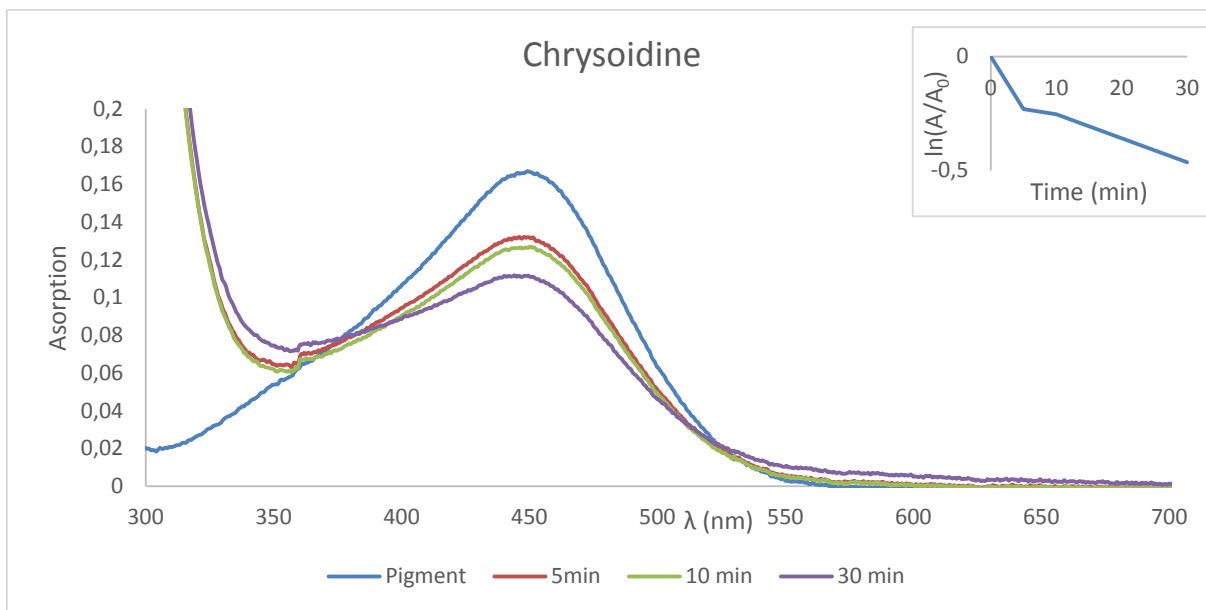


Figure 3.16 The evolution of the absorbance of Chrysoïdine in time when influenced by 30 % H₂O₂ at pH=7, Right corner: The Napierian logarithm of the ratio of absorbance and the initial absorbance of Chrysoïdine vs. time

3.4.5 Indigo C.I. 73015 A

3.4.5.1 Sun exposure

Table 3.13 shows a visual comparison between the behavior of Indigo in an aqueous solution in the absence and in the presence of IL105, when exposed to the sun. It behaves the same as Amaranth, as is explained in 3.4.2.1.

Table 3.13 Sun exposure of Indigo with and without IL105

Time (min)	0	5	10	30
Sun exposure				
Sun exposure + IL105				

3.4.5.2 Extracted concentration

The absorption of Indigo is given at concentrations of pigment solution, both in the presence as absence of IL105. The behavior of Indigo in contact with IL105 is comparable with the behavior of Amaranth, 3.4.2.2.

Preceding the concentrations of indigo extracted by the ionic liquid can be calculated out of the difference in absorbance between both. The distribution ratios, directly linked to the extraction of the dye, out of the ionic liquid are given in annex 2.2.

3.4.5.3 Evolution of the extraction in time

In Figure 3.17 the extraction of indigo by the ionic liquid IL105 at a pH of 2, 7 and 12 is displayed. A big increase of the extraction rate occurs in both basic and acidic medium. An extraction with a small to non-existent magnitude is seen in neutral media. It is quite peculiar that no real extraction is to be seen at pH is 7, a significant distribution ratio was found (annex 2.2) plus a extraction rate is seen in basic aqueous solutions (63%), only after 30 minutes.

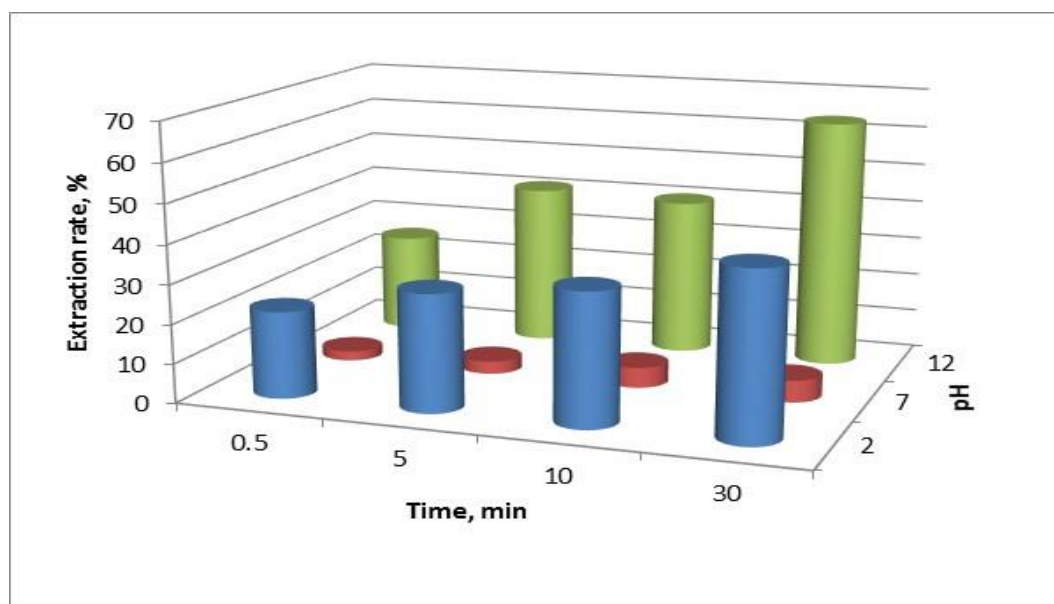


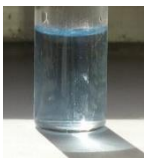
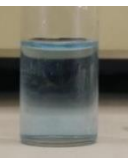



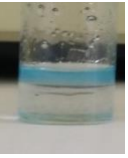


Figure 3.17 The evolution of the liquid-liquid extraction of indigo by IL105 in time and pH.

As explained in the previous paragraph, no significant decrease in absorbance is seen at pH = 7 . This makes the sorption process inefficient in those conditions. Both at a pH of 2 as 12, on the other hand, the extraction ratios increase significantly with values being respectively 42% and 63% after 30 minutes.

3.4.5.4 Oxidation by 30% H₂O₂

Table 3.14 shows the influence of 30% H₂O₂ on the discoloring of indigo. A gradual change is noticeable in the one without ionic liquid, with a complete disappearance of color after 72 hours. If IL105 is added, the same thing is seen, with the only difference that the pigment migrates to the ionic liquid, making the aqueous solution colorless. The IL-phase shows no decrease in color after 30 minutes, but when the period is extended to 72 hours; no color remains. A complete degradation of Indigo is seen after 72 hours.

Table 3.14 Oxidation of indigo by 30% H₂O₂ with and without IL105

Time (h)	0	0.166	0.5	72
30%H ₂ O ₂				
Time (h)	0	0.166	0.5	72
30%H ₂ O ₂ + IL105				

In Figure 3.18 the change in intensity of the color can be seen, when 30% hydrogen peroxide is added to the pigment solution. It is a gradual decrease over time. The same figure, contains a graph displaying the speed in which the oxidation reaction of Indigo by 30% hydrogen peroxide occurs, with the slope of graphs being the first order reaction rate constant.

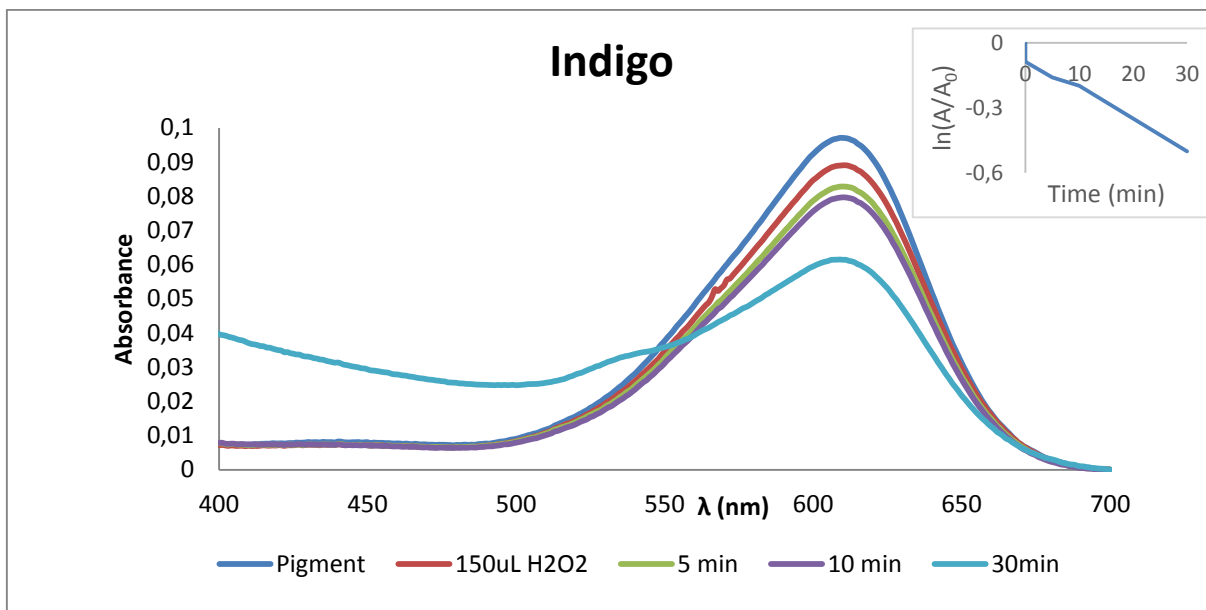



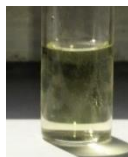

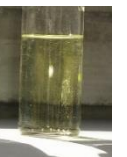

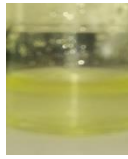

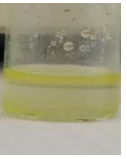
Figure 3.18 The evolution of the absorbance of Indigo in time when influenced by 30 % H₂O₂ at pH=7, Right corner: The Napierian logarithm of the ratio of absorbance and the initial absorbance of Indigo vs. time

3.4.6 Tartrazine C.I. 19140

3.4.6.1 Sun exposure

Table 3.15 shows a visual comparison between the behavior of Tartrazine in an aqueous solution in the absence and in the presence of IL105. It behaves the same as Amaranth, as is explained in 3.4.2.1, with the only difference that the extraction is slower and only partial.

Table 3.15 Sun exposure of Tartrazine with and without IL105

Time (min)	0	5	10	30
Sun exposure				
Sun exposure + IL105				

3.4.6.2 Evolution of the extraction in time

In Figure 3.19 the extraction of Tartrazine by the ionic liquid, IL105 is displayed. A decrease in absorbance and thus the migration of pigment to the ionic liquid is seen at all the pH values studied. The magnitude in which it appears is the highest at a pH of 7. The alteration of the pH affects the sorption process of pigment from the aqueous phase to the ionic liquid negatively.

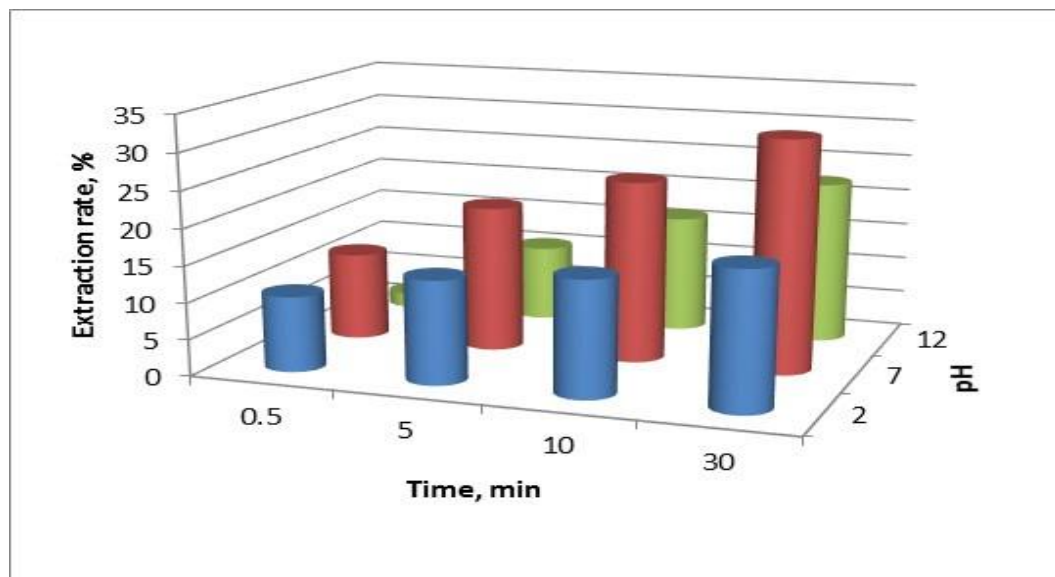


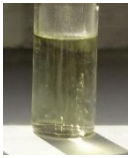
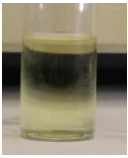


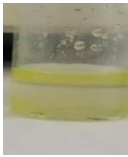
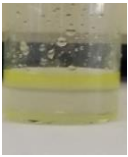
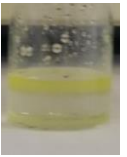
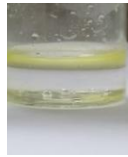
Figure 3.19 The evolution of the liquid-liquid extraction of tartrazine by IL105 in time and pH.

As was expected in the previous paragraph, the distribution ratio is the highest in neutral media (7.1909). The D-values at a pH of 2 and 12 are comparable, with values of respectively 2.5358 and 1.8878 (See annex 2.2). Since the ratios are in the 1-10 range the sorption process is of average efficiency.

3.4.6.3 Oxidation by 30% H₂O₂

In Table 3.16 the influence of ionic liquid on the oxidation of Tartrazine with and without IL105 is visually presented. The impact seems the same as was seen in Amaranth, 3.4.2.4. When a closer look is taken, it is clear that the color of the pigment remains partially in the sample where no IL was added as opposed to Amaranth where it disappears completely.

Table 3.16 Oxidation of Tartrazine by 30% H₂O₂ with and without IL105

Time (h)	0	0.166	0.5	72
30%H ₂ O ₂				
Time (h)	0	0.166	0.5	72
30%H ₂ O ₂ + IL105				

The presence of 30% hydrogen peroxide barely has influence on Tartrazine, which can be concluded by the small decrease in color intensity, Figure 3.20. The absorbance is 0.06259 after the addition of hydrogen peroxide and 0.05814 after 30 minutes. On the right a graph is shown, that displays the speed in which the oxidation reaction of Tartrazine by 30% hydrogen peroxide occurs. The rate of reaction was calculated, as explained in the last paragraph of 2.3.4.4; the evolution will be shown in section 3.4.10.

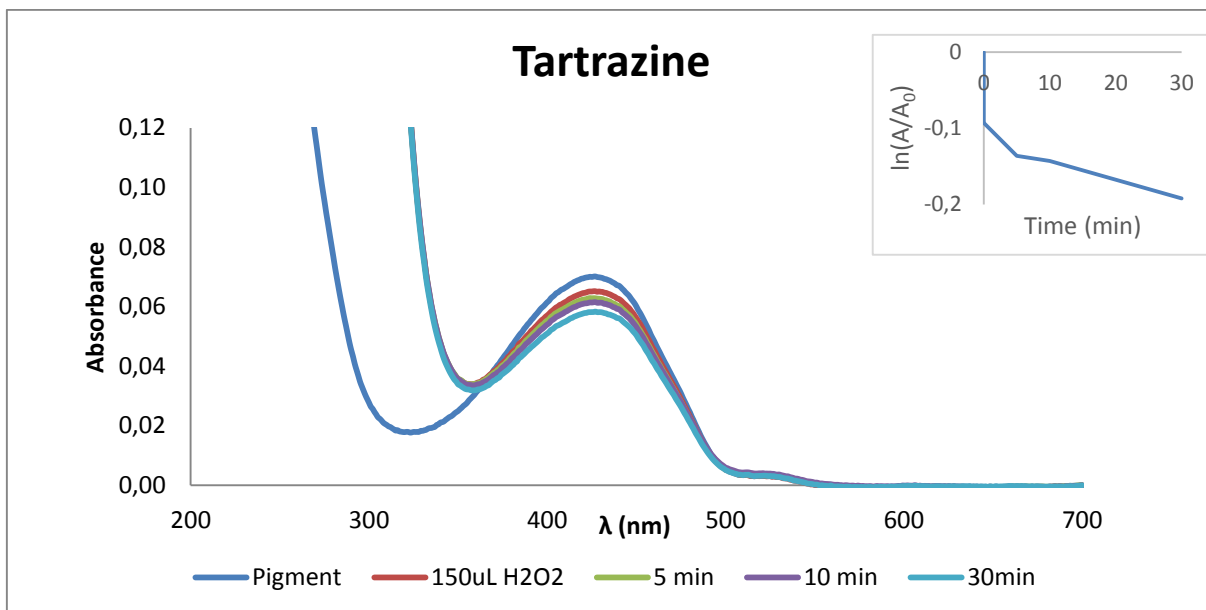


Figure 3.20 The evolution of the absorbance of Tartrazine in time when influenced by 30 % H_2O_2 at pH=7, Right corner: The Napierian logarithm of the ratio of absorbance and the initial absorbance of Tartrazine vs. time.

3.4.7 Malachite green C.I. 42000

3.4.7.1 Sun exposure

Table 3.17 shows a visual comparison between the behavior of Malachite green in an aqueous solution in the absence and in the presence of IL105. Malachite green is distributed over both the aqueous phase as the IL phase. No preference for any of the phases is visually noticeable, while Rhodamine 6G clearly prefers the IL phase.

Table 3.17 Sun exposure of Malachite green with and without IL105

Time (min)	0	5	10	30
Sun exposure				
Sun exposure + IL105				

3.4.7.2 Evolution of the extraction in time

In Figure 3.21 the extraction of malachite green by the ionic liquid, IL105 is displayed. Since the aqueous solution, becomes colorless immediately after the base is added and the pH of 12 is reached, no curve is shown. The addition of acid boosts the decrease in absorbance, since no significant reduction of the absorbance is seen without.

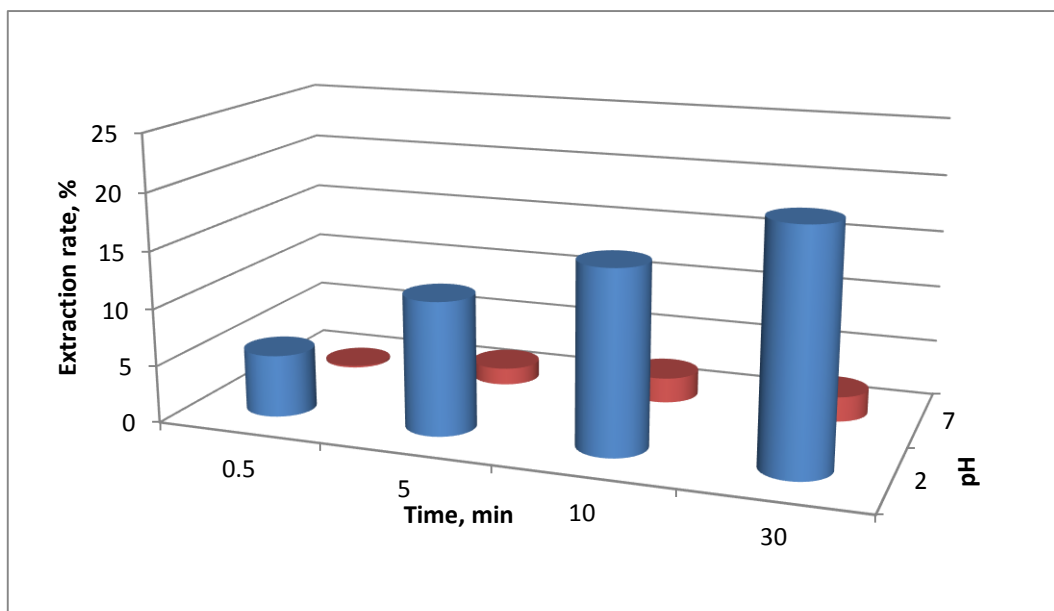



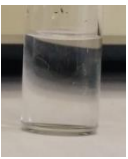






Figure 3.21 The evolution of the liquid-liquid extraction of malachite green by IL105 in time

The calculation of extraction ratios is especially useful for the extraction in an acidic environment. Therein an extraction ratio of 20% is found after 30 minutes, making it a sorption process of pigment from the aqueous phase to the IL of average efficiency, while in a neutral medium the distribution ration is only 5%, making it inefficient.

3.4.7.3 Oxidation by 30% H₂O₂

The influence of IL105 on the intensity of Malachite green is investigated, when influenced by 30% hydrogen peroxide; in Table 3.18 the evolution is given. The pigment starts oxidizing almost immediately after the oxidizing agent is added. No real difference is seen between the measurement with and without ionic liquid present.

Table 3.18 Oxidation of Malachite green by 30% H₂O₂ with and without IL105

Time (h)	0	0.166	0.5	72
30% H ₂ O ₂				
Time (h)	0	0.166	0.5	72
30% H ₂ O ₂ + IL105				

Out of the visual representation of the solution of malachite green and hydrogen peroxide one could conclude that the color already disappears after 10 minutes. When UV-VIS measurements are done on the other hand, it is seen that a longer time is needed to fully degrade Malachite green, thus retaining its color partially. This change in absorbance versus time, can be seen in Figure 3.22. A graph displaying the speed in which the oxidation reaction of Malachite green by 30% hydrogen peroxide occurs is shown in the right hand corner.

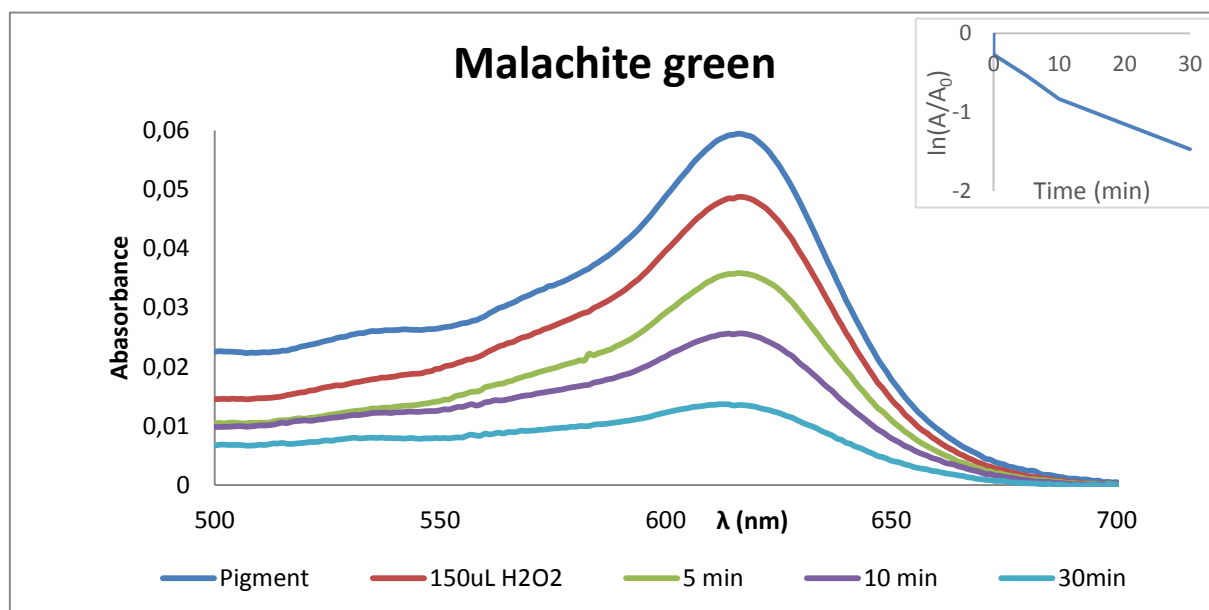



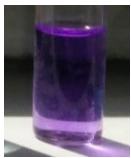



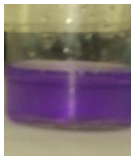


Figure 3.22 The evolution of the absorbance of Malachite green in time when influenced by 30 % H₂O₂ at pH=7, Right corner: The Napierian logarithm of the ratio of absorbance and the initial absorbance of Malachite green vs. time.

3.4.8 Methyl violet C.I. 42535

3.4.8.1 Sun exposure

Table 3.19 shows a visual comparison between the behavior of methyl violet in an aqueous solution in the absence and in the presence of IL105. No difference is seen between both, since Methyl violet does not show any affinity for the ionic liquid.

Table 3.19 Sun exposure of Methyl violet with and without IL105

Time (min)	0	5	10	30
Sun exposure				
Sun exposure + IL105				

3.4.8.2 Evolution of the extraction in time

Methyl Violet (MV) is a protonated amine. Not unexpectedly then, MV partitioning is more sensitive to changes in the aqueous pH than is the distribution of the other cationic dyes, like methylene blue. Specifically, increasing pH, which would be accompanied by deprotonation of MVH^+ to yield the neutral dye, results in a decrease in the extraction. In Figure 3.23 the evolution of the absorbance in time is given for the contact between IL105 and Methyl violet.

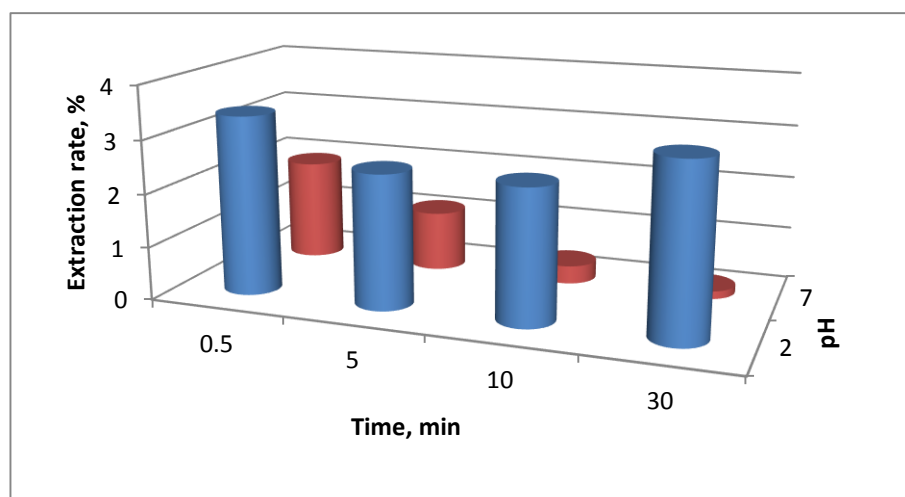


Figure 3.23 The evolution of the liquid-liquid extraction of methyl violet by IL105 in time and pH.


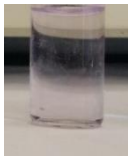






Because Methyl violet is a protonated amine it is not unexpected that the methyl violet partitioning is sensitive to changes in the aqueous pH. Increasing the pH, would be accompanied by deprotonation of the amine-function, yielding a neutral dye, results in a decrease of the distribution ratio, annex 2.2. In this case it is seen indeed, that in an acidic medium the sorption of methyl violet by IL105 is of more significance than in a neutral medium.

3.4.8.3 Oxidation by 30% H_2O_2

The influence of IL105 on the intensity of methyl violet is investigated, when influenced by 30% hydrogen peroxide; in Table 3.20 the evolution is given. The pigment starts oxidizing quite rapidly after the oxidizing agent is added, almost losing its color after 30 minutes.

Extraction of the dye by IL105 is seen after 5minutes. The aqueous phase will lose its color even faster than it does without the presence of ionic liquid. In the ionic liquid phase on the other hand, the degradation of Methyl violet is much slower compared to the speed of degradation in the pigment solution without IL added.

Table 3.20 Oxidation of Methyl violet by 30% H₂O₂ with and without IL105

Time (h)	0	0.166	0.5	72
30% H ₂ O ₂				
Time (h)	0	0.166	0.5	72
30% H ₂ O ₂ + IL105				

If only Table 3.20 would be examined, it would appear that almost all the pigment is degraded after 10 minutes. If Figure 3.24 is taken into account it can be seen that, that is not entirely true. The intensity of the dye decreases gradually. The graph also contains a graph displaying the speed in which the oxidation reaction of Methyl violet by 30% hydrogen peroxide occurs. It is shown in the right hand corner.

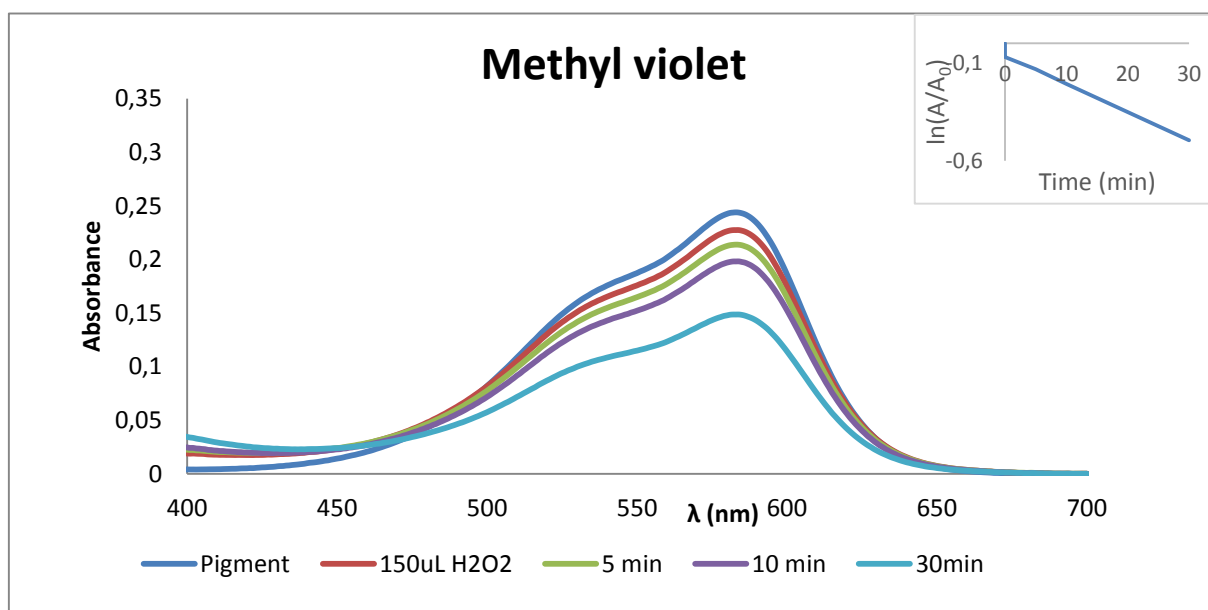










Figure 3.24 The evolution of the absorbance of Methyl violet in time when influenced by 30 % H₂O₂ at pH=7, Right corner: The Napierian logarithm of the ratio of absorbance and the initial absorbance of Methyl violet vs. time.

3.4.9 Methylene blue C.I. 52015

3.4.9.1 Sun exposure

Table 3.21 shows a visual comparison between the behavior of methyl violet in an aqueous solution in the absence and in the presence of IL105. Methylene blue is distributed over both the aqueous phase and the IL phase, with a preference for the IL phase.

Table 3.21 Sun exposure of methylene blue with and without IL105

Time (min)	0	5	10	30
Sun exposure				
Sun exposure + IL105				

3.4.9.2 Evolution of the extraction in time

In Figure 3.25 the evolution of the absorbance in time is given for the contact between IL105 and methylene blue. It is noticeable that no real extraction of Methylene blue out of the aqueous phase by IL105 takes place at a pH of 2 nor 7. This can be seen by the lack of extraction in the qualitative investigation of sun exposure, 3.4.9.1. With the addition of a base (pH=12) on the other hand, a considerable decrease in absorbance is seen.

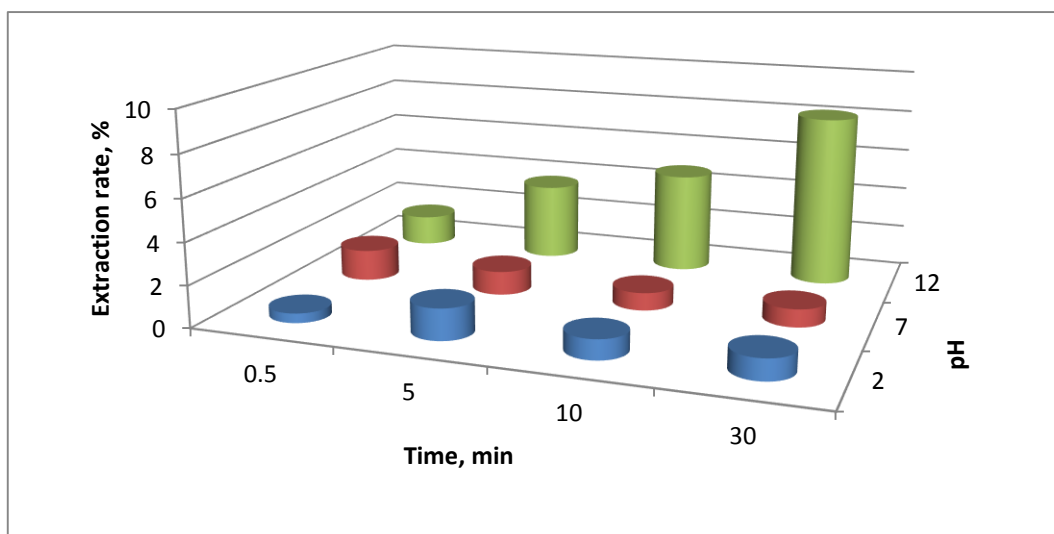


Figure 3.25 The evolution of the liquid-liquid extraction of methylene blue by IL105 in time

The extraction ratio of Methylene blue between water and IL105 is only useful for the extraction in a basic environment, pH is 12. Therein an extraction ratio of 8% is found after 30 minutes, making it a sorption process of pigment from the aqueous phase to the IL of small efficiency. The changes in the behavior of the dye could be attributed to the hydrolysis or aggregation at these pH conditions [106]. In both neutral as acidic (pH=2) medium the extraction was below 2%.

3.4.9.3 Oxidation by 30% H₂O₂

The influence of IL105 on the intensity of methylene blue is investigated, when influenced by 30% hydrogen peroxide; in Table 3.22 Table 3.8 Oxidation of Amaranth by 30% H₂O₂ with and without IL105 the evolution is given. No real difference is seen between both. The pigment is divided evenly over the two liquids. The dye still retains its color after a period of 72 hours when exposed to the oxidizing agent.

Table 3.22 Oxidation of Methylene blue by 30% H₂O₂ with and without IL105









Time (h)	0	0.166	0.5	72
30% H ₂ O ₂				
Time (h)	0	0.166	0.5	72
30% H ₂ O ₂ + IL105				

Figure 3.26 confirms what is seen on the pictures in Table 3.22, little to no decrease in pigment intensity is seen with the addition of 30% hydrogen peroxide. In the right hand corner a graph is shown, that displays the speed in which the oxidation reaction of Methylene by 30% hydrogen peroxide occurs. The slope of the curve, and thus the first order reaction rate is found to be very low, which was expected, since the absorbance was 0.2568 directly after the addition of hydrogen peroxide and 0.2283 after 30 minutes.

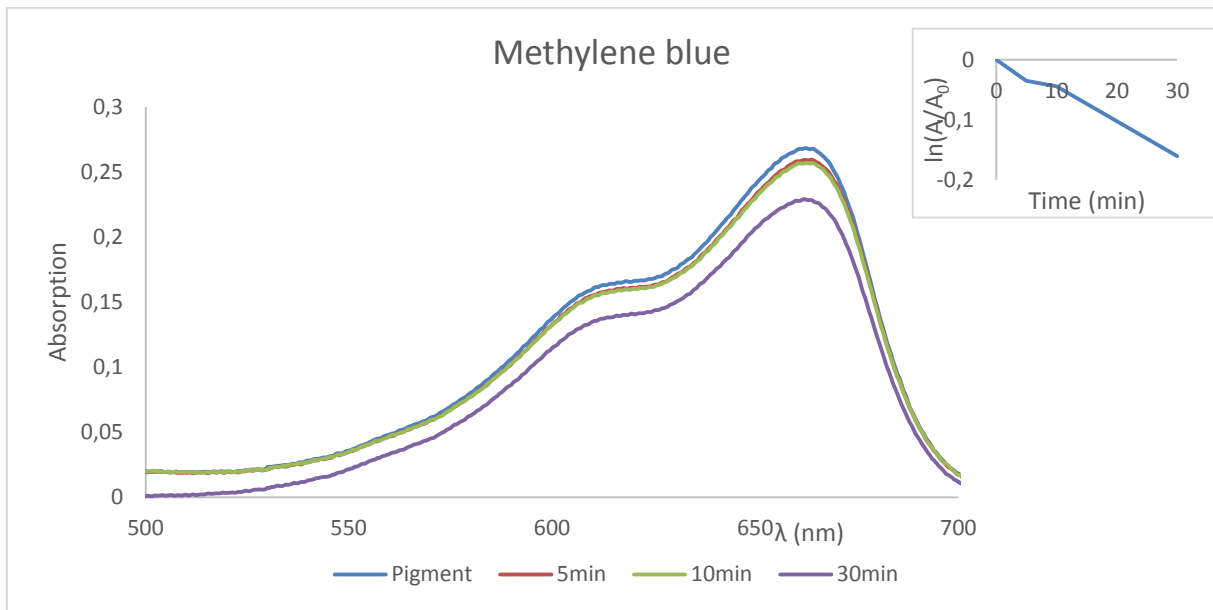


Figure 3.26 The evolution of the absorbance of Methylene blue in time when influenced by 30 % H_2O_2 at $\text{pH}=7$, Right corner: The Napierian logarithm of the ratio of absorbance and the initial absorbance of Methylene blue vs. time.

3.4.10 Rate of reaction

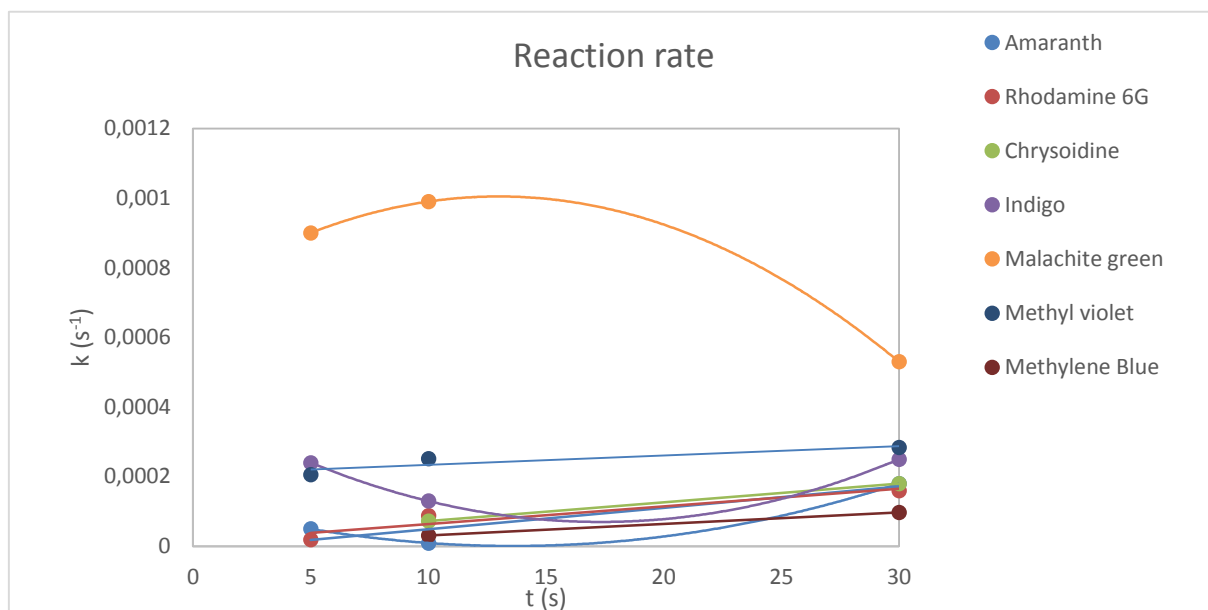


Figure 3.27 First order reaction rate vs. time for the oxidation of pigments with 30% hydrogen peroxide with respectively Amaranth

The first order reaction rate is given in function of time for the oxidation of pigments, Figure 3.27. Methyl violet, Chrysoidine, Methylene blue and Rhodamine 6G show a linear behavior, thus being a first order reaction. The oxidation of Amaranth, Indigo and Malachite green on the other hand show a second order equation and will go through via a second order reaction. Tartrazine has more complex reaction rate, that will need to be further investigated.

3.5 Discussion

3.5.1 Density

Density measurements for [P_{6.6.6.14}][DCA] were done in trifold or more in order to get reproducible results, thus diminishing the chance of errors occurring. The result obtained is situated in the uncertainty range of the literature results.

3.5.1 Electrochemical behaviour of ionic liquids

As expected, the ILs with halides, and in particular the ones with the chloride anion, are limited for oxidation applications above *ca.* 1 V, since the chloride undergoes oxidation at that potential. [14]

The best overall stability is delivered by [P_{6.6.6.14}][DCA] which exhibits similar, and wide, useful limits at both positive and negative potentials.

The electrochemical potential window of room temperature ionic liquids is sensitive to impurities. A change in the water content of an ionic liquid will affect conductivity: as the water content increases, so does conductivity; thus decreasing the electrochemical potential window.

Hydrophobicity of an ionic liquid increases with increasing alkyl chain length. Adding CH₂ groups to the alkyl chain on the imidazolium cation promotes a larger surface area with more hydrogen available, making the interaction with the water molecules less relevant. For the series [C_nmim][NTf₂] (n = 4, 6, or 8) this theory is confirmed. [C₄mim][NTf₂] is being the most affected. The magnitude in which ILs containing [Cl]⁻ as an anion and different cations got influenced by the water content is to be put in order as follows; [P_{6.6.6.14}]⁺, [N_{1.8.8.8}]⁺, [C₆mim]⁺. An increase in the size of the cationic part, showed to promote hydrophobicity and therefor lowered the sensitivity of the presence of water molecules.

A bigger decrease in electrochemical window with an increase in water content is seen at [P_{6.6.6.14}][Cl] as compared to [P_{6.6.6.14}][DCA].

The process [Fe(C₅H₅)₂]⁺⁰ of the traditionally used reference compound ferrocene has been studied at a platinum disk electrode in the ionic liquids [C₆mim][NTf₂] and [P_{6.6.6.14}][DCA]. A reversible, one-electron reduction process was observed.

3.5.2 Peroxidative oxidation of cyclohexane

The catalytic activity of ferrocene in trihexyl(tetradecyl)phosphonium dicyanamide, [P_{6.6.6.14}][DCA], was tested as catalyst for the oxidation of cyclohexane with aqueous tert-butylhydroperoxide (ButOOH, TBHP) as oxidizing agent, at 50 °C.

Only cyclohexanone was produced by oxidation of cyclohexane in the above-mentioned conditions (cyclohexanol was not detected, not even traces). A maximum cyclohexanone yield of 15.7% was obtained in the presence of acidic medium. This selectivity is rare, being the cyclohexanol and cyclohexanone mixture the common products obtained. Interestingly, both acidic and basic additives led to an enhancement of the amount of cyclohexanone produced.

Martins *et al.* also found that the addition of HNO₃ promotes the activity of the [FeCl₂{η³-HC(pz)₃}] / CNT-Oxi-Na combination for the catalytic conversion of cyclohexane to both cyclohexanol and cyclohexanone. [15]

G.B. Shul'pin *et al.* showed that the addition of a base can have an accelerating-, retardation- or inhibiting effect on the decomposition of hydro peroxides. It is dependent on the composition of the base, oxidant and the catalyst used. [16]

A reaction pathway for this reaction as is suggested by Nowotny *et al.* [103] is the direct-oxidation reaction via the free-radical chain reaction pathway. It is the presumed mechanistic pathway for the one-pot oxidation of cyclohexane with TBHP as an oxidant.

3.5.3 Pigments

The distribution ratios (annex 2.2) of the pigment between the aqueous phase and IL105 is to be used as a way of comparing the sorption capacity of the ionic liquid for that specific pigment.

Generally, at low pH solution, the percentage of dye removal will decrease significantly for cationic dye adsorption, with Malachite green and methyl violet being exceptions. Since the extraction of methyl violet was of such a small order, it is excluded. At a high pH solution the distribution ratio of the dyes increase significantly, with Malachite green showing a comparable distribution ratio compared to a neutral solution.

If the results of the high pH solutions of the anionic dyes are compared to the low pH solutions, an increase in the distribution ratio is seen in all the anionic dyes. The migration of Tartrazine to IL105 shows to be the most efficient at a pH of 7. This finding is opposed to the finding of Osma *et al.* [107] that found a decrease in the adsorption of reactive black 5 by seed shells with an increase in pH. It was attributed to the fact that the adsorption was driven by electrostatic attraction between the positive charge at the solution interface and the adsorbent surface that appeared to be negatively charged. An increase in pH will thus decrease the positive charge at the solution, subsequently decreasing the extraction rate.

The increased distribution ratio in cationic dyes could be attributed by the increase in negative charge at the solution interface, caused by the electrostatic interactions between OH⁻ groups and the cationic dyes. As for anionic dyes further investigation needs to be done, since a repulsive effect between the anionic dyes and the hydroxyl groups would be expected, taking only this explanation into account.

The extent in which the sorption process of the pigment to the aqueous phase appears at a neutral pH was determined using the results of annex 2.1 and the sun exposure tests. The pigments can be ordered as follows; Chrysoidine > Indigo > Amaranth > Tartrazine > Rhodamine 6G > Malachite green > Methylene blue > Methyl violet. With Methylene blue and Methyl violet showing no affinity for the ionic liquid at all. Only at a basic pH a small extraction of the pigment by IL105 is seen. The raise in the distribution ratio is not to be searched in a structural change of Methylene blue, with the increase in basicity as is stated by Oplawski. [108]

Amaranth, Chrysoidine and Tartrazine belong to the family of the azo dyes, whom are composed of an R=N=N-R' functional group. The sorption of those dyes by IL105 is superior compared to the other dyes, with one dye being extremely favorable, namely Chrysoidine. The distribution ratio shows values of up to 100 for this sorption process. Migration of Tartrazine to IL105 seems inferior to the absorption of the other two, if only visually compared. When comparing the distribution ratios, on the other hand, no difference is seen between Amaranth and Tartrazine. The inferiority of both Amaranth as Tartrazine to Chrysoidine can't be ascribed to the ionicity, which is used as a way of comparing the sorption capacity in several sources. [108-109] Adak et al. and Adak and Pal stated that Alumina has a lower affinity for anionic pigments as opposed to cationic pigments. The presence of the negative charge in anionic pigments makes a better interaction with the positively charged alumina feasible.

If the charge of the pigment would determine the absorption by the ionic liquid a bigger difference would be seen between the migration of Tartrazine and Amaranth to the IL. This means that the liquid-liquid extraction by IL105 does not occur by chemical sorption, which would form covalent and/or ionic bonds. Physical sorption on the other hand is more conceivable, since both Tartrazine and Amaranth show the same ability of hydrogen bonds formation. This capability is due to the presence of one hydroxyl group in both the pigments. The hydrogen bonds are expected to be established between the dicyanamide and the hydroxyl group.

Same accounts for Chrysoidine, where the presence of two primary amine functions, create a greater range of possibilities for hydrogen bond formation. Whereas Tartrazine and Amaranth only have one possible hydrogen bonding site, Chrysoidine has two primary amine groups and thus four sites at which this physical sorption process can take place.

The partial attribution of the improved absorption of the pigments, discussed in the previous paragraphs, by IL105 may not be due to the presence of the azo group. Considering that Indigo has a distribution ratio with a greater value than Tartrazine and Amaranth, and does not have the azo group. Physical sorption, as used for explanatory means in the previous paragraphs, is a better way of clarifying the bigger magnitude in which Indigo gets absorbed. Two secondary amines and thus an extra hydrogen bonding site is embodied in the structure. Hence the raise in distribution ratio.

Chapter 4: CONCLUSIONS AND FUTURE WORK

The use of ionic liquids is already a step in the right direction, when it comes to being 'green'. Of course it is preferred to search for the ones that are inherently non-toxic, such as $P_{6.6.6.14}Cl$. If the synthesis can be effected by a route involving non- or less toxic starting, it is even a bigger improvement. For example, it is shown that hydroxyl-functionalized analogs of the imidazolium cation can be synthesized from fructose, which occurs naturally.

The densities of IL105 at several temperatures were in the uncertainty range of the values obtained in the literature.

The alteration in water content of the ionic liquids showed to have an influence on all of the ionic liquids tested. Therein an increase in the length of methylimidazolium alkyl chains showed to decrease both the usable potential range as the magnitude in which the ILs get influenced by water addition.

Trihexyl(tetradecyl)phosphonium dicyanamide (IL105) showed to have a wide potential window, which was greatly influenced by the addition of water. A reversible, one-electron reduction process was observed with the addition of ferrocene, which is mostly used as an internal standard in molecular solvents.

More research needs to be done on the influence of water on the electrochemical behavior of ILs. Therein the field of search needs to be broadened to the alterations that are seen with other impurities, since they can greatly influence the usability of ionic liquids in electrochemical experiments. Ferrocene did not seem to be affected by the ionic liquids tested, namely trihexyl(tetradecyl)phosphonium dicyanamide and 1-hexyl-3-methylimidazolium bis(trifluoromethylsulfonyl)imide. Its behaviour in a broader range of ILs will have to be investigated.

As for the catalytic cyclohexane oxidation by ferrocene in an IL105 medium; a considerable yield was found. The interactions between ionic liquids and ferrocene and more specifically the catalytic oxidation of alkanes are to be investigated. The oxidation of cyclohexane and the reaction pathway in which the corresponding alcohols and ketones get formed, and the influence the pH has on this process, needs to be further investigated.

The ionic liquid IL105 was examined as an adsorbent for several pigments out of an aqueous pigment solution. A considerable extraction of several pigments by the IL was seen, with the extraction of Chrysoidine being the most successful. The pH of the aqueous pigment solution showed to be an influential factor of great importance. An alteration in the pH, can either promote or depress the adsorption process significantly. As for the oxidation of the pigments by hydrogen peroxide 30 v/v%; a considerable protective effect of the ionic liquid against the pigment oxidation was seen in Amaranth, Chrysoidine and Indigo.

It would be useful to examine the extraction efficiencies of a variety of ILs on different dyes. More commonly used pigments can be tested, to get a precise idea of which ionic liquids have the ability to adsorb which dyes. If all the data were to be categorized, an idea of interactions between both the IL and the dye and influences on the extraction capacity of the IL can be formed. Concerning the dyes, different dyes with a broad spectrum of properties should be utilized; those involve cationic-, anionic-, azo-dyes etc. In ionic liquids the influence of the length of the alkyl chain, hydrophobicity, viscosity, density, anion, cation and so on will be investigated.

Most beneficial would be tests on real wastewater samples with a variety of ionic liquids. Naturally, these experiments would create issues with measurements as it would be difficult to create calibration standards due to the variety of colors and color combinations that would be encountered. Instrumentation other than UV-VIS spectrometers could potentially be used, once a measurement methodology can be established.

REFERENCE

- [1] Jiménez-González J., Constable D. J. C. (2011), "Green Chemistry and Engineering—A Practical Design Approach," John Wiley & Sons Inc., Hoboken, 3-39.
- [2] Ahluwalia V. K. (2009), "Green Chemistry, Environmentally Benign Reaction," CRC Press & Francis Group, Boca Raton.
- [3] Sheldon R. A. (2012), "Fundamentals of Green Chemistry: Efficiency in Reaction Design," *Chemical Society Reviews*, 41 (4), 1437-1451.
- [4] Dunn P. J. (2012), "The Importance of Green Chemistry in Process Research and Development," *Chemical Society Reviews*, 41 (4), 1452-1461.
- [5] Ghernaout D., Ghernaout B. and Naceur M. W. (2011), "Embodying the Chemical Water Treatment in the Green Chemistry: A Review," *Desalination*, 271 (1-3), 1-10.
- [6] Capello C., Fischer U. and Hungerbuhler K. (2007), "What Is a Green Solvent? A Comprehensive Framework for the Environmental Assessment of Solvents," *Green Chemistry*, 9 (9), 927-934.
- [7] Slater C. S. and Savelski M. (2007), "A Method to Characterize the Greenness of Solvents Used in Pharmaceutical Manufacture," *Journal of Environmental Science and Health, Part A*, 42 (11), 1595-1605.
- [8] Rundquist E. M., Pink C. J. and Livingston A. G. (2012), "Organic Solvent Nanofiltration: A Potential Alternative to Distillation for Solvent Recovery from Crystallisation Mother Liquors," *Green Chemistry*, 14 (8), 2197-2205.
- [9] Huddleston J. G., Visser A. E., Reichert E. W., Willauer H. D., Broker G. A. and Rogers R. D. (2001), "Characterisation and comparison of hydrophilic and hydrophobic room temperature ionic liquids incorporating the imidazolium cation," *Green chemistry*, 3, 156-164.
- [10] Anastas P. and Warner J. (1998), "Green Chemistry: Theory and Practice," Oxford University Press: New York, 30.
- [11] United States Environmental Protection Agency (2014, October 16), "Basics of green chemistry," Retrieved from <http://www.epa.gov>.
- [12] Earle M.J. and Seddon K.R. (2009), "Ionic liquids: Green solvents for the future," *Pure applied sciences*, 72 (7), 1391-1398.
- [13] Yoshimoto S., Taguchi R., Tsuji R., Ueda H. and Nishiyama K. (2012), "Dependence on the crystallographic orientation of Au for the potential window of the electrical double-layer region in imidazolium-based ionic liquids," *Electrochemistry communications*, 20, 26-28.
- [14] Handy S. T. (2011), "Ionic liquids - Classes and Properties," Intech: Rijeka.
- [15] Castner E. W. Jr., Wishart J. F. (2010), "Spotlight on ionic liquids," *The journal of chemical physics*, 132, 120901.

- [16] Dake S. A., Kulkarni R. S., Kadam V. N., Modani S. S., Bhale J. J., Tathe S. B. and Pawar R. P. (2009), "Phosponium Ionic Liquid: A Novel Catalyst for Benzyl Halide Oxidation," *Synthetic Communications*, Vol. 39, No. 21, 3898-3904.
- [17] Cao H. and Alper H. (2010), "Palladium-Catalyzed Double Carbonylation Reactions of o-Dihaloarenes with Amines in Phosponium Salt Ionic Liquids," *Organic Letters*, 12 (18), 4126-4129.
- [18] Luska K. L., Demmans K. Z., Stratton S. A. and Moores A. (2012), "Rhodium Complexes Stabilized by Phosphine- Functionalized Phosponium Ionic Liquids Used as Higher Alkene Hydroformylation Catalysts: Influence of the Phosponium Headgroup on Catalytic Activity," *Dalton Transactions*, 41 (43), 13533-13540.
- [19] Fan A., Chuah G.K. and Jaenicke S. (2012), "Phosponium Ionic Liquids as Highly Thermal Stable and Efficient Phase Transfer Catalysts for Solid-Liquid Halex Reactions," *Catalysis Today*, 198 (1), 300-304.
- [20] Harper N. D., Nizio N. D., Hendsbee A. D., Masuda J. D., Robertson K. N., Murphy L. J., Johnson M. B., Pye C. C. and Clyburne J. A. C. (2011), "Survey of Carbon Dioxide Capture in Phosponium-Based Ionic Liquids and End-Capped Polyethylene Glycol Using DETA (DETA = Diethylenetriamine) as a Model Absorbent," *Industrial & Engineering Chemistry Research*, 50 (5), 2822-2830.
- [21] Wasserscheid P. and Welton T. (2002), "Ionic liquids in synthesis," Wiley-VCH Verlag GmbH & co. KGaA, Weinheim.
- [22] Mjalli F., Naser J., Jibril J., Alizadeh V., and Gano Z. (2014), "Tetrabutylammonium chloride based ionic liquids and their physical properties," *Journal of chemical engineering data*, 59 (7), 2242-2251.
- [23] Pratap K., Chhotaray P. K. and Gardas R. L. (2014), "Thermophysical properties of ammonium and hydroxylammonium protic ionic liquids," *Journal of chemical thermodynamics*, 72, 117-124.
- [24] Klomfar J., Soucková M. and Pátek J. (2014), "Low Temperature Densities from (218 to 364) K and up to 50 MPa in Pressure and Surface Tension for Trihexyl(tetradecyl)phosponium Bis(trifluoromethylsulfonyl)imide and Dicyanamide and 1-Hexyl-3-methylimidazolium Hexafluorophosphate," *Journal of chemical engineering data* 59 (7), 2263-2274.
- [25] Tariq M., Forte P. A. S., Gomes C. M. F., Lopes C. J. N. And Rebelo L. P. N. (2009), "Densities and refractive indices of imidazolium- and phosponium-based ionic liquids: Effect of temperature, alkyl chain length, and anion," *The journal of chemical thermodynamics*, 41 (6), 790-798.
- [26] Carrera G. V. S. M., Afonso C. A. M. and Branco L. C. (2010), "Interfacial properties, densities, and contact angles of task specific ionic liquids," 55 (2), 609-615.
- [27] Neves C. M. S. S. Carvalho P. J., Freire M. G., Coutinho J. A. P. (2011), "Thermophysical properties of pure and water-saturated tetradecyltrihexylphosponium-based ionic liquids," 43 (6), 948-957.

- [28] Quijada-Maldonado E., van der Boogaart S. Lijbers J. H., Meindersma G. W., de Haan A. B. (2012), "Experimental densities, dynamic viscosities and surface tensions of the ionic liquids series 1-ethyl-3-methylimidazolium acetate and dicyanamide and their binary and ternary mixtures with water and ethanol at T = (298.15 to 343.15 K)," *Journal of chemical thermodynamics*, 51, 51-58.
- [29] Sánchez L. G., Espel J. R., Onink F., Meindersma G. W. And de Haan A. B. (2009), "Density, viscosity, and surface tension of synthesis grade imidazolium, pyridinium, and pyrrolidinium based room temperature ionic liquids," *Journal of chemical engineering data*, 54, 2803-2812.
- [30] Jacquemin J., Husson P., Padua A. S. H. And Majer V. (2005), "Density and viscosity of several pure and water-saturated ionic liquids," *Green chemistry*, 8, 172-180.
- [31] Diogo J. C. F., Caetano F. J. P., Fareleira J. M. N. A., Wakeham W. A., Afonso C. A. M., and Marques C. S. (2011), "Viscosity Measurements of the Ionic Liquid Trihexyl(tetradecyl)phosphonium Dicyanamide [P6,6,6,14][dca]," *Journal of chemical & engineering data*, 57 (4), 1015-1025.
- [32] Diogo J. C. F., Caetano J. P., Fareleira J. M. N. A. And Wakeham W. (2014), "Viscosity measurements on ionic liquids: a cautionary tale," *International journal of thermophysics*, 35, 1615-1635.
- [33] Fröba A. P., Kremer H. and Leipertz A. (2008), "Density, refractive index, interfacial tension, and viscosity of ionic liquids [EMIM][EtSO₄], [EMIM][NTf₂], [EMIM][N(CN)₂], and [OMA][NTf₂] in dependence on temperature at atmospheric pressure," *The journal of physical chemistry B*, 112 (39), 12420-12430.
- [34] Seddon K. R., Stark A. and Torres M. (2000), "Influence of chloride, water, and organic solvents on the physical properties of ionic liquids," *Pure applied chemistry*, 72 (12), 2275-2287.
- [35] Hiroyuki O., "Electrochemical aspects of ionic liquids", John Wiley & Sons, Inc., Hoboken, New Jersey, 2011.
- [36] Fung Y. S. and Zhu D. R.. (2012), "Electrodeposited Tin Coating as Negative Electrode Material for Lithium-Ion Battery in Room Temperature Molten Salt," *Journal of the electrochemical society*, 149 (3), A319–A324.
- [37] Shobukawa H., Tokuda H., Susan M. A. B. H. and Watanabe M. (2005), "Ion Transport Properties of Lithium Ionic Liquids and Their Ion Gels," *Electrochimica acta*, 50 (19), 3872– 3877.
- [38] Shobukawa H., Tokuda H., Tabata S. I. and Watanabe M. (2004), "Preparation and Transport Properties of Novel Lithium Ionic Liquids," *Electrochimica Acta*, 50(2-3), 305–309.
- [39] Seki S., Kobayashi Y., Miyashiro H., Ohno Y., Usami A., Mita Y., Watanabe M. and Terada N. (2006), "Highly Reversible Lithium Metal Secondary Battery Using a Room Temperature Ionic Liquid/Lithium Salt Mixture and a Surface-Coated Cathode Active Material," *Chemical Communications* (5), 544–545.

- [40] Stenger-Smith J. D., Webber C. K., Anderson N., Chafin A. P., Zong K. and Reynolds J. R. (2002), "Poly(3,4-alkylenedioxythiophene)-Based Supercapacitors Using Ionic Liquids as Supporting Electrolytes," *Journal of the Electrochemical Society*, 149 (8), A973–A977.
- [41] Sato T., Masuda G. and Takagi K. (2004), "Electrochemical Properties of Novel Ionic Liquids for Electric Double Layer Capacitor Applications," *Electrochimica Acta*, 49 (21), 3603–3611.
- [42] Liu H., He P., Li Z., Liu Y. and Li J. (2006) "A Novel Nickel-Based Mixed Rare-Earth Oxide/Activated Carbon Supercapacitor Using Room Temperature Ionic Liquid Electrolyte," *Electrochimica Acta*, 51 (10), 1925–1931.
- [43] Kubo W., Murakoshi K. and Kitamura T. (2001), "Quasi-Solid-State Dye-Sensitized TiO₂ Solar Cells: Effective Charge Transport in Mesoporous Space Filled with Gel Electrolytes Containing Iodide and Iodine," *Journal of Physical Chemistry B*, 105 (51) 12809–12815.
- [44] Kubo W., Kitamura T., Hanabusa K., Wada Y. and Yanagida S. (2002), "Quasi-Solid-State Dye-Sensitized Solar Cells using Room Temperature Molten Salts and a Low Molecular Weight Gelator," *Chemical Communications*, (4), 374–375.
- [45] Wang P., Zakeeruddin S. M., Moser J. E. and Grätzel M., "A New Ionic Liquid Electrolyte Enhances the Conversion Efficiency of Dye-Sensitized Solar Cells," *Journal of Physical Chemistry B*, 107 (48), 13280–13285.
- [46] Xia J., Masaki N., Jiang K. and Yanagida S. (2006), "Deposition of a Thin Film of TiO_x from a Titanium Metal Target as Novel Blocking Layers at Conducting Glass/TiO₂ Interfaces in Ionic Liquid Mesoscopic TiO₂ Dye-Sensitized Solar Cells," *Journal of Physical Chemistry B*, 110 (50), 25222–25228.
- [47] Wang P., Zakeeruddin S. M., Moser J. E., Humphry-Baker R. and Grätzel M. (2004), "A Solvent-Free, SeCN⁻/(SeCN)₃-Based Ionic Liquid Electrolyte for High-Efficiency Dye-Sensitized Nanocrystalline Solar Cells," *Journal of the American Chemical Society*, 126 (23), 7164–7165.
- [48] Wang P., Zakeeruddin S. M., Comte P., Exnar I. and Grätzel M. (2003), "Gelation of Ionic Liquid-Based Electrolytes with Silica Nanoparticles for Quasi-Solid-State Dye-Sensitized Solar Cells," *Journal of the American Chemical Society*, 125 (5), 1166–1167.
- [49] Noda A., Susan M. A. B. H., Kudo K., Mitsushima S., Hayamizu K. and Watanabe M. (2003), "Brønsted Acid-Base Ionic Liquids as Proton-Conducting Nonaqueous Electrolytes," *Journal of Physical Chemistry B*, 107 (17) 4024–4033.
- [50] Martins V. L., Nicolau B. G., Urahata S. M., Ribeiro M. C. C. and Torresi R. M. (2013), "Influence of Water Content on the Structure and Physicochemical Properties of an Ionic Liquid and Its Li⁺ Mixture," *Journal of physical chemistry*, 117 (29), 8782-8792.
- [51] Aslanov L.A (2011), "Ionic liquids: liquid structure," *Journal of molecular liquids*, 162 (3), 101-104.

- [52] Visser A. E. , Swatloski R. P., Reichert W. M., Griffin S. T. and Rogers R. D., "Traditional extractants in nontraditional solvents: Groups 1 and 2 extraction by crown ethers in room-temperature ionic liquids," *Industrial & engineering chemistry research*, 39 (10), 3596-3604.
- [53] Rabideau B. D. and Ismail A. E. (2015), "Mechanisms of hydrogen bond formation between ionic liquids and cellulose and the influence of water content," *Physical chemistry chemical physics*, 17, 5767-5775.
- [54] Lu X., Burell G., Separovic F., and Zhao C. (2012), "Electrochemistry of room temperature protic ionic liquids: A critical assessment for use as electrolytes in electrochemical applications," *The journal of physical chemistry*, 116 (30), 9160-9171.
- [55] Siraj N., Grampp G., Landgraf S. and Punyain K. (2012), "Cyclic voltammetric study of heterogeneous electron transfer rate constant of various organic compounds in ionic liquids: measurements at room temperature," *zeitschrift für physikalische chemie*.
- [56] Barrado E., Couto R. A. S.; Quinaz M. B., Lima J. L. F. C. And Castrillejo Y. (2014), "Electrochemical behaviour of ferrocene in the ionic liquid 1-ethyl-3-methylimidazolium tetrafluoroborate, EMIMBF₄, at 298 K," *Journal of electroanalytical chemistry*, 720-721, 139-146.
- [57] <https://www.electrochem.org/dl/ma/203/pdfs/2567.pdf>, Consulted at 04-06-2015.
- [58] Whyman R. (2001), "Applied Organometallic Chemistry and Catalysis," Oxford University Press, Oxford.
- [59] Smiley R. A., Jackson H. L. (2002), "Chemistry and the Chemical Industry," CRC Press.
- [60] Weissermel K. and Arpe H. –J. (1993), "Industrial Organic Chemistry," 2, VCH Press, Weinheim.
- [61] Bäckvall J.-E. (2004), "Modern Oxidation Methods," Wiley-VCH, Weinheim.
- [62] Sheldon R. A., Arends I. and Hanefeld U. (2007), "Green Chemistry and Catalysis," Wiley-VCH, Weinheim.
- [63] Chiusoli G. P. and Maitlis P. M. (2006), "Metal-catalysis in Industrial Organic Processes," Royal Society of Chemistry, Cambridge, ch. 2.
- [64] Wolf E. E. (ed.) (1992), "Methane Conversion by Oxidative Processes: Fundamental and Engineering Aspects," Van Nostrand Reinhold, New York.
- [65] Derouane E. G., Haber J., Lemos F., Ramôa Ribeiro F. and Guinet M. (Eds.) (1998), "Catalytic Activation and Functionalization of Light Alkanes" NATO ASI Series, 44, Kluwer Academic Publishers, Dordrecht, The Netherlands.
- [66] Schuchardt. U., Cardoso D., Sercheli R., Pereira R., da Cruz, R. S., Guerreiro M. C., Mandelli D., Spinacé E. V. and Pires, (2001), "Cyclohexane oxidation continues to be a challenge," *E. L. Applied Catalysis A: General*, 211, 1-17.

- [67] Pombeiro A. J. L. (Ed.) (2013), "Advances in Organometallic Chemistry and Catalysis: The Silver/Gold Jubilee International Conference on Organometallic Chemistry Celebratory Book," John Wiley & Sons, Inc., Hoboken, NJ, USA, Chapters 1, 2,3 and 22.
- [68] da Silva J. A. L., Fraústo da Silva J. J. R., A. Pombeiro A. J. L. (2011), "Oxovanadium Complexes in Catalytic Oxidations," *Coord. Chem. Rev.*, 255, 2232-2248;
- [69] L. M. D. R. S. Martins, A. J. L. Pombeiro (2014), "Tris(pyrazol-1yl)methane metal complexes for catalytic mild oxidative functionalizations of alkanes, alkenes and ketones," *Coord. Chem. Rev.*, 265, 74-88.
- [70] Martins L. M. D. R. S. , Peixoto de Almeida M., Carabineiro S. A. C., Figueiredo J. L. and Pombeiro A.J.L. (2013), "Heterogenisation of a C-Scorpionate FeII Complex on Carbon Materials for Cyclohexane Oxidation with Hydrogen Peroxide," *chemcatchem*, 5 (12), 3847-3856.
- [71] Karthikeyan P., Bhagat P. R. and Kumar S. S. (2012), "A novel, green 1-glycyl-3-methyl imidazolium chloride–copper(II) complex catalyzed CH oxidation of alkyl benzene and cyclohexane," *Chinese chemical letters*, 23 (6), 681-684.
- [72] Janying J., Hua Z., Xiangjing Z. and Yongqi H. (2008), "Oxidation of cyclohexane catalyzed by TS-1 in ionic liquid with Tert-butyl-hydroperoxide," *Chinese journal of chemical engineering*, 16 (3), 373-375.
- [74] Tian P., Liu Z., Wu Z., Xu. L and He Y. (2004), "Characterization of metal-containing molecular sieves and their catalytic properties in the selective oxidation of cyclohexane," *Catalysis today*, 93-95, 735-742.
- [75] Shul'pin G. B., Kirillova M. V., Shul'pina L. S., Pombeiro, A. J. L. Karslyan E. E. And Kozlov Y. N. (2013), "Mild oxidative alkane functionalization with peroxides in the presence of ferrocene," *Catalysis communications*, 31, 32-36.
- [76] Shul'pina L. S., Durova E. L., Kozlov Y. N., Kudinov A. R., Strelkova T. V. and Shul'pin G.B. (2013), "Oxidation of benzene with hydrogen peroxide catalyzed with ferrocene in the presence of pyrazine carboxylic acid," *Russian journal of physical chemistry A*, 87 (12), 1996-2000.
- [77] Li Z., Li G., Jiang L. Li J. Sun G., Xia C. And Li F. (2015), "Ionic liquids as precursors for efficient mesoporous iron-nitrogen-doped oxygen reduction electrocatalysts," *Angewandte chemie*, 127, 1514-1518.
- [78] Audin C., Daran J., Deydier É., Manoury E. And Poli R. (2010), "New ferrocenyl P,O ligand with polar substituents," *Comptes rendus chimie*, 13 (8-9), 890-899.
- [79] Neumann P. Dib H., Caminade A. M. And Hey-Hawkins E. (2015), "Redox control of a dendritic ferrocenyl-based homogenous catalyst," *Angewandte chemie*, 54 (1), 311-314.
- [80] Couling D. J., Bernot R. J., Docherty K. M., Dixon J. K. and Maggin E. J. (2006), "Assessing the factors responsible for ionic liquid toxicity to aquatic organisms via quantitative structure–property relationship modeling" *Green Chemistry*, 8, 82–90.

- [81] Pernak J., Kalewska J., Ksycinska H. and Cybulski J. (2001), "Synthesis anti-microbial activities of some pyridinium salts with alkoxymethyl hydrophobic group," *European journal of medicinal chemistry*, 36, 899.
- [82] Pernak J., Rogoza J. and Mirska I. (2001), "Synthesis and antimicrobial activities of new pyridinium and benzimidazolium chlorides," *European journal of medicinal chemistry*, 36, 313.
- [83] Pernak J. and Chwala P. E. (2001), "Synthesis and anti-microbial activities of choline-like quaternary ammonium chlorides," *European journal of medicinal chemistry*, 38, 1035.
- [84] Pernak J., Goc I. and Mirska I. (2004), "Anti-microbial activities of protic ionic liquids with lactate anion," *Green chemistry*, 6, 323-329.
- [85] Pernak J., Sobaszekiewicz K. and Mirska I. (2003), "Anti-microbial activities of ionic liquids," *Green Chemistry*, 5, 52-56.
- [86] Cho C.-W., Pham T. P. T., Jeon Y.-C., Vijayaraghavan K., Choe W.-S. And Yun Y.-S. (2007), "Toxicity of imidazolium salt with anion bromide to a phytoplankton *Selenastrum capricornutum*. Effect of alkyl-chain length," *Chemosphere*, 69 (6), 1003-1007.
- [87] Cho C. W., Jeon Y. C., Pham T. P., Vijayaraghavan K. and Yun Y. S. (2008), "The ecotoxicity of ionic liquids and traditional organic solvents on microalga *selenastrum capricornutum*," *Ecotoxicology and environmental safety*, 71 (1), 166-171.
- [88] Pang Y. L. and Abdullah A. Z. (2013), "Current status of textile industry wastewater management and research progress in Malaysia: A review," *Clean, soil, air and water*, 41 (8), 1-14.
- [89] Bokare A. D. , Chikate R. C., Rode C. V. and Paknikar K. M. (2008), "Iron-nickel bimetallic nanoparticles for reductive degradation of azo dye Orange G in aqueous solution," *Applied catalysis B: environmental*, (79 (3), 270-278.
- [90] Bhat R. V. and Mathur P. (1998), "Changing scenario of food colours in India," *Current science*, 74, 198-202.
- [91] Sharma K. P., Sharma K., Kumar S. Sharma S., Grover R., Soni P. Bhardwaj S.M., Chaturvedi R. K. and Sharma S. (2005), "Response of selected aquatic macrophytes towards textile dye wastewaters," *Indian journal of biotechnology*, 4, 538-545.
- [92] Mahmoud A. S., Ghaly A. E., and Brooks M. S. (2007), "Removal of dye from textile wastewater using plant oils under different pH and temperature conditions," *American Journal of Environmental Sciences*, 4 (3), 205-218.
- [93] Visser A.E., Swatoski R.P., and Rogers R.D. (200), "pH-Dependent partitioning in room temperature ionic liquids," *Green Chemistry*, 1-4.
- [94] Vijayaraghavan R., Vedaraman N., Surianarayanan M., and MacFarlane D.R. (2006), "Extraction and recovery of azo dyes in an ionic liquid," *Talanta*, 69, 1059-1062.

- [95] Ali M., Sarkar A., Pandey M.D., and Pandey S. (2006), "Efficient precipitation of dyes from dilute aqueous solutions of ionic liquids," *Analytical Sciences*, 22, 1051-1053.
- [96] Pei Y.C., Wang J.J., Xuan X.P., Fan J., and Fan M. (2007), "Factors affecting ionic liquids based removal of anionic dyes from water," *Environmental Science & Technology*, 41 (14), 5090-5095.
- [97] Li C., and Xin B. (2008), "Extraction and mechanisms of acid dyes into a room temperature ionic liquid," *2nd International Conference on Bioinformatics & Biomedical Engineering*, 3519-3522.
- [98] Fan J., Fan Y., Zhang S., and Wang J. (2011), "Extraction of azo dyes from aqueous solutions with room temperature ionic liquids," *Separation Science and Technology*, 46, 1172-1177.
- [99] Rydberg J., Choppin G. R., Musikas C. and Sekine T. (2004), "Solvation Extraction Principles and Practice, Revised and Expanded," CRC Press: Boca Raton.
- [100] Pei Y., Liu J., Yan Z., Li Z., Fan J. and Wang J. (2012), "Association of ionic liquids with cationic dyes in aqueous solution: A thermodynamic study," *Journal of chemical thermodynamics*, 47, 223-227.
- [101] Zhang S., Sun N., He X., Lu X., and Zhang, X. (2006), "Physical properties of ionic liquids: Database and evaluation," *Journal of Physical Chemical Reference Data*, 35 (5), 1475-1517.
- [102] O'Mahony A. M., Silvester D. S., Aldous L., Hardacre C. An Compton R. G. (2008), "Effect of Water on the Electrochemical Window and Potential Limits of Room-Temperature Ionic Liquids," *Journal of chemical engineering data*, 53 (12), 2884-2891.
- [103] Nowotny M., Pedersen L. N., Hanefeld U., and Maschmeyer T. (2002), "Increasing the ketone selectivity of the cobalt-catalyzed radical chain oxidation of cyclohexane," *Chemistry a European journal*, 8 (16), 3724-3731.
- [104] Pal N., Pramanik M., Bhaumik A. and Ali M. (2014), "Highly selective and direct oxidation of cyclohexane to cyclohexanone over vanadium exchanged NaY at room temperature under solvent-free conditions," *Journal of molecular catalysis A: chemical*, 392, 299-307.
- [105] Önal Y., Akmil-Basar C., Eren D., Sarıcl-Özdemir Ç. and Depci T. (2006), "Adsorption kinetics of malachite green onto activated carbon prepared from Tunçbilek lignite," *Journal of hazardous materials*, 128, 150-157.
- [106] Muthuraman G., Teng T. T. and Tan S. H. (2012), "Liquid-liquid extraction of Cibacron Red FN-R by TBAB as an extractant," *Desalination*, 284, 135-141.
- [107] Osma J. F., Saravia V., Toca-Herrera J. L., Couto S. R. (2007), "Sunflower seed shells: a novel and effective low-cost adsorbent for the removal of the diazo dye Reactive Black 5 from aqueous solutions," *Journal of hazardous materials*, 147, 900-905.
- [108] Oplawski S. (2014), "Extraction of indicator dyes into imidazolium-based ionic liquids," *theses and dissertations*, paper 477.
- [109] Garvey. S.L. and Dietz, M.L. (2013), "Ionic liquid anion effects in the extraction of metal ions by macrocyclic polyethers," *Separation and Purification Technology*, 123, 145-152.

[110] Tisinger P. T. and Heineman W. R. (1983), "Cyclic voltammetry," Journal of chemical education, 60, 702-706.

[111] Mabott G. A. (1983), "An introduction to cyclic voltammetry," Journal of chemical education, 60, 698-702.

[112] Brett C. M. A. (2005), "Electrochemistry principle, methods and applications," Oxford university press, London.

[113] Bard A.J. and Faulkner L.R. (2001), "Electrochemical Methods: Fundamentals and applications," John Wiley & sons, New York.

[114] Experiment 5. Cyclic voltammetry Retrieved from www.chemistry.msu.edu., consulted 05-04-2015

ANNEX

Annex 1

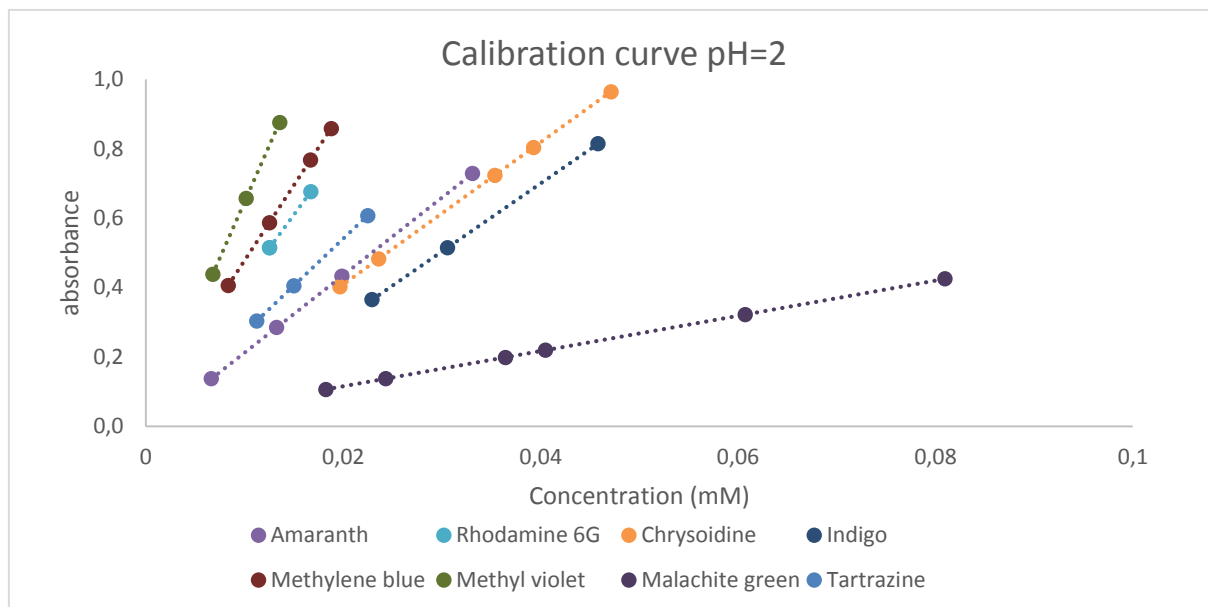


Figure A1 Calibration curve of absorbance vs concentration respectively Amaranth, Rhodamine 6G, Chrysoidine, Indigo Tartrazine, Malachite green, Methyl violet and Methylene blue at pH=2

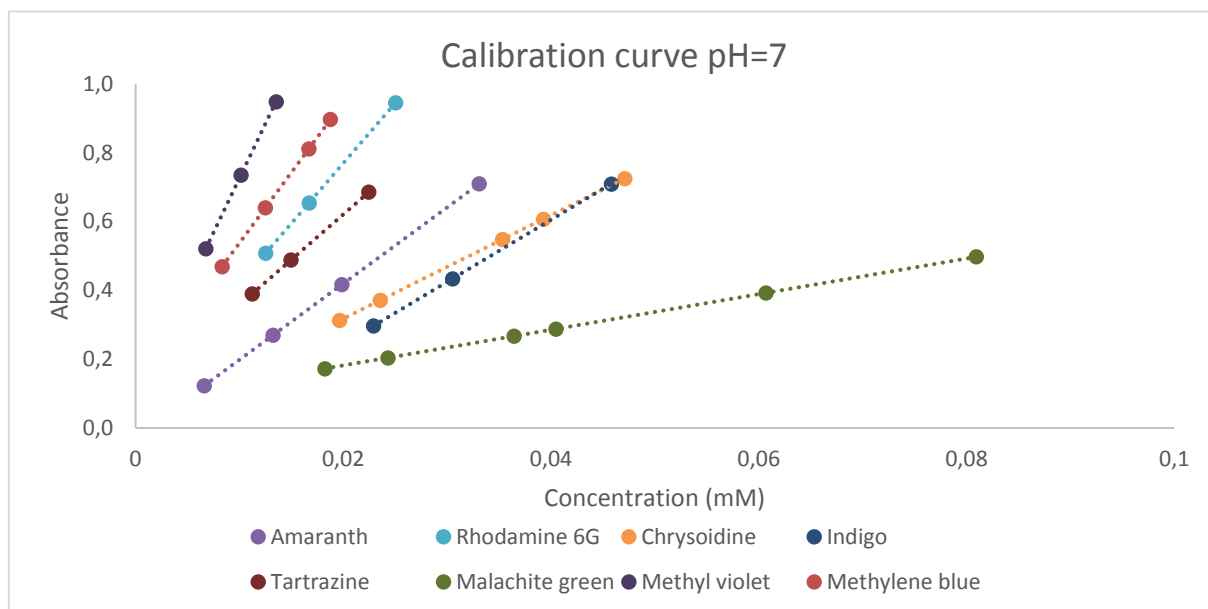


Figure A2 Calibration curve of absorbance vs concentration respectively Amaranth, Rhodamine 6G, Chrysoidine, Indigo Tartrazine, Malachite green, Methyl violet and Methylene blue at pH=7

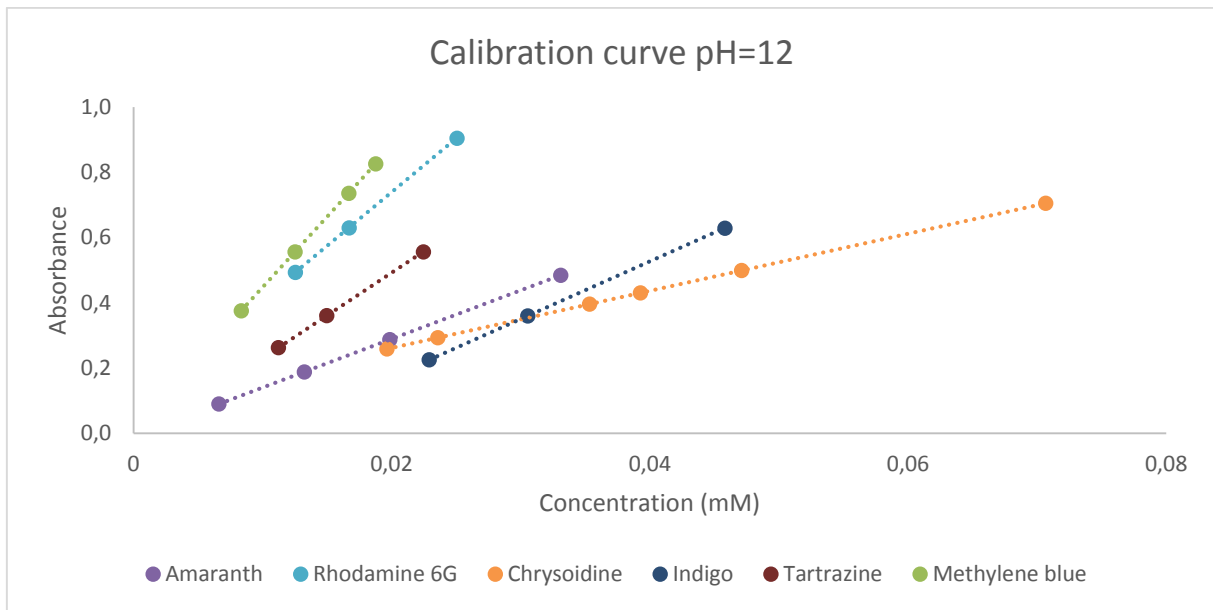


Figure A3 Calibration curve of absorbance vs concentration of respectively Amaranth, Rhodamine 6G, Chrysoidine, Indigo Tartrazine, and Methylene blue at pH =12

Annex 2

Annex 2.1

Table A1 Distribution ration of several pigments, namely Amaranth, Chrysoidine, Indigo and Tartrazine in IL105.

Amaranth		Chrysoidine	
C _{initial} (mM)	D	C _{initial} (mM)	D
0.00602	0.86553	0.00788	104.1702
0.01198	3.16818	0.01958	68.1166
0.01420	3.03921	0.03928	40.5294
0.02366	2.65108	0.05012	35.0169
Indigo		Tartrazine	
C _{initial} (mM)	D	C _{initial} (mM)	D
0.01028	0.4974	0.00772	2.8531
0.01693	4.0983	0.01578	3.0111
0.02623	4.1677	0.02173	2.7186
0.03470	3.0269		
0.03979	4.1433		

Annex 2.2

Table A2 Distribution ratios at a pH of 2, 7 and 12 of respectively Amaranth, Rhodamine 6G, Chrysoidine, Indigo Tartrazine, Malachite green, Methyl violet and Methylene blue

Time pH value	Amaranth				Rhodamine 6G			
	0	5	10	30	0	5	10	30
2.0	0.79	1.11	1.20	1.21	0.00	0.01	0.02	0.05
7.0	0.07	0.11	0.17	0.17	0.58	0.81	0.89	0.90
12.0	0.41	0.94	1.19	1.50	1.88	1.92	2.26	4.66
Time pH value	Chrysoidine				Indigo			
	0	5	10	30	0	5	10	30
2.0	0.09	0.11	0.11	0.22	2.20	3.24	3.82	5.36
7.0	1.79	2.78	3.33	4.67	0.20	0.26	0.43	0.47
12.0	1.95	2.62	13.38	14.71	1.74	3.23	3.13	6.16
Time pH value	Tartrazine				Malachite green			
	0	5	10	30	0	5	10	30
2.0	1.04	1.49	1.70	2.08	0.64	1.48	2.13	2.96
7.0	1.64	3.11	4.20	6.18	0.01	0.14	0.21	0.21
12.0	0.18	1.00	1.66	2.46	/	/	/	/
Time pH value	Methyl violet				Methylene blue			
	0	5	10	30	0	5	10	30
2.0	0.37	0.27	0.27	0.35	0.05	0.13	0.10	0.11
7.0	0.35	0.20	0.06	0.11	0.14	0.11	0.08	0.08
12.0	/	/	/	/	0.14	0.35	0.46	0.82

Annex 2.3

Table A3 Extraction ratios at a pH of 2, 7 and 12 of respectively Amaranth, Rhodamine 6G, Chrysoidine, Indigo Tartrazine, Malachite green, Methyl violet and Methylene blue

Time pH value	Amaranth				Rhodamine 6G			
	0	5	10	30	0	5	10	30
2.0	8.4	11.5	12.3	12.3	0.0	0.1	0.0	0.5
7.0	0.8	1.3	1.8	1.8	5.2	7.1	7.7	7.9
12.0	4.7	10.0	12.4	15.1	16.0	16.3	18.6	31.6
Time pH value	Chrysoidine				Indigo			
	0	5	10	30	0	5	10	30
2.0	0.8	1.0	1.0	2.0	22.2	30.0	33.8	42.3
7.0	3.8	7.5	9.3	13.2	2.4	3.2	5.2	5.6
12.0	15.7	19.8	52.5	54.5	25.4	41.4	40.4	63.5
Time pH value	Tartrazine				Malachite green			
	0	5	10	30	0	5	10	30
2.0	10.4	14.2	15.9	18.8	5.4	11.7	15.8	20.5
7.0	12.0	20.0	24.8	31.7	0.1	1.5	2.2	2.2
12.0	2.0	10.5	16.2	22.4	/	/	/	/
Time pH value	Methyl violet				Methylene blue			
	0	5	10	30	0	5	10	30
2.0	3.4	2.5	2.5	3.2		1.5	1.0	1.0
7.0	1.9	1.1	0.3	0.1	1.5	1.1	0.9	0.9
12.0	/	/	/	/	1.5	3.7	4.8	8.2